NASA TECHNICAL NOTE

NASA TN D-3847

NASA TN D-3847

EFFECT OF SKEWED WING-TIP CONTROLS ON A VARIABLE-SWEEP WING-FUSELAGE CONFIGURATION

by Emma Jean Landrum and Josephine W. Grow

Langley Research Center
Langley Station, Hampton, Va.

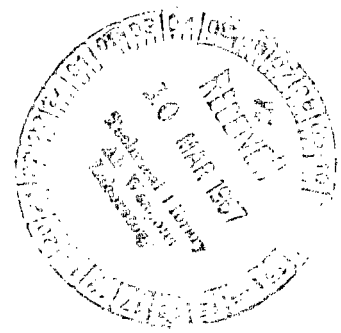

NATIONAL AERONAUTICS AND SPACE ADMINISTRATION • WASHINGTON, D. C. • MARCH 1967

NASA TN D-3847

EFFECT OF SKEWED WING-TIP CONTROLS ON A VARIABLE-SWEEP WING-FUSELAGE CONFIGURATION

By Emma Jean Landrum and Josephine W. Grow

Langley Research Center
Langley Station, Hampton, Va.

NATIONAL AERONAUTICS AND SPACE ADMINISTRATION

For sale by the Clearinghouse for Federal Scientific and Technical Information
Springfield, Virginia 22151 – Price $2.50

EFFECT OF SKEWED WING-TIP CONTROLS ON A VARIABLE-SWEEP WING-FUSELAGE CONFIGURATION

By Emma Jean Landrum and Josephine W. Grow
Langley Research Center

SUMMARY

Basic aerodynamic data are presented for Mach numbers from 0.50 to 1.20. Correlations obtained from these data are combined with correlations from previous tests to provide a summary of the complete investigation in the Mach number range from 0.50 to 4.62. For the complete investigation wing-sweep angle varied from 30° to 75° through an angle-of-attack range from -4° to 8°, a sideslip-angle range from -4° to 6°, and a control-deflection-angle range from 0° to 10°. Hinge-line angle relative to the wing leading edge varied from 75° to 115°. Reynolds number per foot (meter) varied from 1.44×10^6 (4.72×10^6) to 3×10^6 (9.84×10^6).

The increments in lift, rolling-moment, and pitching-moment coefficients due to control deflection correlate linearly on the basis of simple geometric parameters such as projected frontal control area and projected-frontal-control-area moment about a given axis. Deflection of the controls had little or no effect on the longitudinal and lateral stability characteristics. Yawing moment, in general, changed from favorable to adverse as the hinge-line angle relative to the wing leading edge varied from 115° to 75°.

Comparison of several controls with constant planform area showed that a control with the largest projected frontal area and moments was the most effective. However, this control also produced more drag and more adverse yawing moment than the other controls.

INTRODUCTION

The lateral control of a variable-wing-sweep configuration presents many problems to the designers of supersonic aircraft because of the difficulty in maintaining effectiveness throughout a large wing-sweep-angle range. Wing-tip controls with skewed hinge lines have been suggested as a means of providing better control effectiveness throughout the range of wing-sweep angles anticipated.

The purpose of this investigation was to determine the effect of hinge-line location on the static longitudinal and lateral aerodynamic characteristics of a variable-sweep

wing-fuselage configuration with skewed wing-tip controls. Three wing-tip controls with different hinge-line locations were tested on the left wing only at wing-sweep angles from 30° to 75° through an angle-of-attack range from -4° to 8° and a sideslip-angle range from -4° to 6°. Hinge-line angles relative to the wing leading edge varied from 75° to 115°.

In this report, the results of tests in the Langley 8-foot transonic wind tunnel are presented for Mach numbers from 0.50 to 1.20. Results from tests in the Langley 4- by 4-foot supersonic pressure tunnel at Mach numbers 1.41 and 2.20 and in the Langley Unitary Plan wind tunnel at Mach numbers from 2.60 to 4.62 have been presented in references 1 and 2, respectively. The correlations from references 1 and 2 are combined with those from this report to provide a summary of the complete investigation in the Mach number range from 0.50 to 4.62.

SYMBOLS

All the results are referred to the body-axis system except the lift and drag coefficients which are referred to the stability-axis system. The coefficients are based on the wing area, the mean aerodynamic chord, and the span for an outboard-wing-panel sweep of 75°. The moment center is at a longitudinal location corresponding to 33.5 percent of the wing mean aerodynamic chord for the 75° swept wing (see fig. 1).

b	wing span, 18.22 inches (46.28 centimeters) for $\Lambda = 75^{\circ}$
c	wing local chord
$\bar{c}$	wing mean aerodynamic chord, 11.62 inches (29.51 centimeters) for $\Lambda = 75^{\circ}$
C_D	drag coefficient, Drag/qS
C_L	lift coefficient, Lift/qS
C_{L_α}	lift-curve slope, $\partial C_L/\partial\alpha$, per degree
C_{L_δ}	slope of lift with respect to control deflection, $\partial C_L/\partial\delta$, per degree
C_l	rolling-moment coefficient, Rolling moment/qSb
C_{l_β}	effective dihedral parameter, $\partial C_l/\partial\beta$, per degree

C_{l_δ}	slope of rolling moment with respect to control deflection, $\partial C_l / \partial \delta$, per degree
C_m	pitching-moment coefficient, Pitching moment/$qS\bar{c}$
$C_{m_{C_L}}$	slope of curve of pitching moment with respect to lift, $\partial C_m / \partial C_L$
C_{m_δ}	slope of pitching moment with respect to control deflection, $\partial C_m / \partial \delta$, per degree
C_n	yawing-moment coefficient, Yawing moment/qSb
C_{n_β}	directional stability parameter, $\partial C_n / \partial \beta$, per degree
C_Y	side-force coefficient, Side force/qS
C_{Y_β}	side-force parameter, $\partial C_Y / \partial \beta$, per degree
M	free-stream Mach number
$M_{F,X}$	projected-frontal-control-area moment about roll center, inches^3 (meters^3)
$M_{F,Y}$	projected-frontal-control-area moment about pitch center, inches^3 (meters^3)
q	free-stream dynamic pressure
S	wing area including body intercept, 187.4 inches^2 (1209.03 centimeters^2) at $\Lambda = 75^o$
S_c	control area, inches^2 (meters^2)
S_F	projected frontal control area, $S_c \sin \gamma \sin \delta$
α	angle of attack, degree
β	angle of sideslip, positive nose left, degree
γ	control-hinge-line angle relative to free-stream direction, positive when measured from free-stream direction inboard, degree

γ_{le}	control-hinge-line angle relative to wing leading edge, positive when measured from wing leading edge outboard, degree
ΔC_L	increment in lift coefficient due to control deflection
ΔC_l	increment in rolling-moment coefficient due to control deflection
ΔC_m	increment in pitching-moment coefficient due to control deflection
δ	control deflection measured perpendicular to control hinge line, positive when trailing edge is down, degree
Λ	wing-leading-edge sweep angle, degree

MODEL

Details of the variable-sweep wing-fuselage configuration used in the present Langley 8-foot transonic wind-tunnel tests and those reported in references 1 and 2 are shown in figure 1. The inboard wing panel had a fixed leading-edge sweep angle of 65°, a leading-edge radius of 0.0023c, and a streamwise thickness-chord ratio that varied from 0.021 at the root to 0.051 at the pivot point of the outboard wing panel. The movable outboard wing panel, at $\Lambda = 12°$, had a streamwise airfoil section composed of the upper half of an NACA 64_1A012 airfoil section with a modified leading-edge radius of 0.0074c.

General wing information is as follows:

	$\Lambda = 12°$		$\Lambda = 75°$	
Area	199.3 in^2	(1285.80 cm^2)	187.4 in^2	(1209.03 cm^2)
Mean aerodynamic chord	8.40 in.	(21.34 cm)	11.62 in.	(29.51 cm)
Span	35.11 in.	(89.18 cm)	18.22 in.	(46.28 cm)
Aspect ratio	6.18		1.77	
Thickness-chord ratio:				
Outboard panel	0.060		0.021	
Pivot	0.051		0.032	
Root	0.021		0.021	
Root chord	16.33 in.	(41.48 cm)	16.33 in.	(41.48 cm)
Tip chord	2.22 in.	(5.64 cm)		

Three wing-tip controls of varying size and hinge-line location (fig. 1(b)) were used in this investigation and are designated controls A, B, and C. Geometric details of the controls are as shown in the following table:

Control	Area		Hinge-line angle relative to wing leading edge, deg
	in^2	cm^2	
A	5.34	34.45	115
B	6.68	43.10	95
C	8.14	52.52	75

TRANSONIC WIND-TUNNEL DATA

Tests and Corrections

Tests were conducted in the Langley 8-foot transonic wind tunnel at Mach numbers 0.50, 0.80, 0.97, and 1.20 at Reynolds numbers per foot (meter) of 1.44×10^6 (4.72×10^6), 1.95×10^6 (6.40×10^6), 2.11×10^6 (6.92×10^6), and 2.18×10^6 (7.15×10^6), respectively, through an angle-of-attack range of approximately -4° to 8°, at sideslip angles of 0° and 5°.

Each control was tested at wing-sweep angles of 30°, 45°, and 75° at each Mach number. Hinge-line angle relative to the free-stream direction γ for each control is shown in figure 1(c) for $\Lambda = 75^\circ$. The variation of γ with Λ is given in the following table:

Control	γ for Λ of:		
	30°	45°	75°
A	5°	20°	50°
B	25°	40°	70°
C	45°	60°	90°

Force and moment measurements were made through the use of a sting-supported six-component strain-gage balance mounted within the model fuselage. The base pressure was measured by means of a static-pressure orifice located in the fuselage-base cavity, and the measured drag forces were adjusted to correspond to a base pressure equal to free-stream static pressure. The angles of attack were corrected for the deflection of the balance and the sting under load.

Boundary-layer transition was fixed by placing 1/16-inch-wide (0.159-cm) roughness strips of No. 60 carborundum grains 1/8 inch (0.318 cm) aft of the wing leading edge and 1/2 inch (1.27 cm) aft of the nose apex.

Aerodynamic Characteristics

The results of the Langley 8-foot transonic wind-tunnel tests at Mach numbers from 0.50 to 1.20 and the figures in which they are presented are as follows:

	Figure
Effect of control deflection on longitudinal aerodynamic characteristics, $\beta = 0^{\circ}$:	
$\Lambda = 30^{\circ}$, M = 0.50	2
$\Lambda = 45^{\circ}$, M = 0.50	3
$\Lambda = 75^{\circ}$, M = 0.50	4
$\Lambda = 30^{\circ}$, M = 0.80	5
$\Lambda = 45^{\circ}$, M = 0.80	6
$\Lambda = 75^{\circ}$, M = 0.80	7
$\Lambda = 30^{\circ}$, M = 0.97	8
$\Lambda = 45^{\circ}$, M = 0.97	9
$\Lambda = 75^{\circ}$, M = 0.97	10
$\Lambda = 30^{\circ}$, M = 1.20	11
$\Lambda = 45^{\circ}$, M = 1.20	12
$\Lambda = 75^{\circ}$, M = 1.20	13
Effect of control deflection on lateral aerodynamic characteristics, $\beta = 0^{\circ}$:	
$\Lambda = 30^{\circ}$, M = 0.50	14
$\Lambda = 45^{\circ}$, M = 0.50	15
$\Lambda = 75^{\circ}$, M = 0.50	16
$\Lambda = 30^{\circ}$, M = 0.80	17
$\Lambda = 45^{\circ}$, M = 0.80	18
$\Lambda = 75^{\circ}$, M = 0.80	19
$\Lambda = 30^{\circ}$, M = 0.97	20
$\Lambda = 45^{\circ}$, M = 0.97	21
$\Lambda = 75^{\circ}$, M = 0.97	22
$\Lambda = 30^{\circ}$, M = 1.20	23
$\Lambda = 45^{\circ}$, M = 1.20	24
$\Lambda = 75^{\circ}$, M = 1.20	25
Variation of static lateral stability derivatives with angle of attack	26

Control deflection produced reasonably linear increments in C_m and C_L and had no apparent effect on $C_{m_{C_L}}$ and C_{L_α}. (See figs. 2 to 13.) Each control was effective in producing an increment in C_l throughout the range of α, Λ, δ, and γ. (See figs. 14 to 25.) The effect of control deflection on the yawing moment is favorable for control A $\left(\gamma_{le} = 115^o\right)$ and unfavorable for control C $\left(\gamma_{le} = 75^o\right)$ throughout the range of Mach number and wing sweep (figs. 14 to 25). Control B produced a favorable increment in yawing moment at $\Lambda = 30^o$ and, generally, no change occurred at $\Lambda = 45^o$ and 75^o. These results are compatible with the results of references 1 and 2. The static lateral directional stability derivatives are shown in figure 26. Since previous results (refs. 1 and 2) showed no effect of hinge-line angle and control deflection, only $\delta = 0^o$ data are presented.

CONTROL EFFECTIVENESS

The effectiveness of a control is a measure of its ability to produce the forces and moments needed to control an aircraft in flight. It has been shown in reference 3 that the effectiveness of controls on a given wing planform at supersonic speeds can be correlated on the basis of simple geometric parameters such as control area and control-area moment. All the controls used in reference 3, although varying in planform and area, were deflected about hinge lines that were perpendicular to the free-stream direction ($\gamma = 90^o$). In reference 4, it was shown that the correlating parameters of reference 3 were first-order approximations of the projected frontal area of the controls $\left(S_F = S_c \sin \delta \sin \gamma\right)$.

Increments in lift, rolling-moment, and pitching-moment coefficients due to control deflection were shown in references 2 and 4 to be linear functions of projected frontal control area S_F, projected-frontal-control-area moment about the roll center $M_{F,X}$, and projected-frontal-control-area moment about the pitch center $M_{F,Y}$, respectively.

Correlations of ΔC_L, ΔC_l, and ΔC_m with S_F, $M_{F,X}$, and $M_{F,Y}$, respectively, are presented in figure 27 for Mach numbers from 0.50 to 1.20. Although more scatter in the data occurs at subsonic Mach numbers than at supersonic speeds (refs. 1 and 2), the data correlate very well. The effect of Mach number on the slopes of the correlation curves is shown in figure 28. Data for Mach numbers 1.41 to 4.62 were obtained from references 1 and 2.

In order to compare the effectiveness of each control, C_{L_δ}, C_{l_δ}, and C_{m_δ} were calculated from the correlations given in figure 28 for a control area equal to that of control C and for hinge-line angles relative to the wing leading edge that are equal to those of controls A (115^o), B (95^o), and C (75^o). These controls are designated A_1, B_1, and C,

respectively. Control-effectiveness parameters for $M = 0.5$ are presented in figure 29 as a function of wing-sweep angle. Only one Mach number is presented since the correlations are linear at each Mach number and vary only in magnitude. Control C is shown to be more effective throughout the wing-sweep-angle range. This might have been anticipated since this control has larger projected frontal areas and moments at each wing sweep. Although the effects of hinge-line angle on drag coefficient are not considered in this report, it should be pointed out that control C would also produce more drag when deflected. (See figs. 2 to 13.) In reference 4, the increment in drag at zero lift was shown to be a function of the square of the slope of the control deflection with respect to the free-stream direction and the drag due to lift was shown to be a function of the projected control area. Control C also produces an adverse yawing moment when deflected. (See figs. 14 to 25.)

The above comparison illustrates the usefulness of the correlations. Once correlation curves have been determined for a flight vehicle, the effectiveness of any control, regardless of planform or area, can be determined. If a particular level of effectiveness is needed $\left(\text{for example, } C_{l_\delta}\right)$ the control planform and area necessary to produce that level can be determined for the configuration and the effectiveness of that control can be also determined.

CONCLUDING REMARKS

An investigation has been made to determine the effect of hinge-line location on the aerodynamic and control characteristics of a variable-sweep wing-fuselage configuration with skewed wing-tip controls at Mach numbers from 0.50 to 4.62.

The increments in lift, rolling-moment, and pitching-moment coefficients due to control deflection correlate linearly on the basis of simple geometric parameters such as projected frontal control area and projected-frontal-control-area moment about a given axis.

Deflection of the controls had little or no effect on the longitudinal or lateral stability characteristics. Deflecting the controls, in general, caused the yawing moment to change from favorable to adverse as the hinge-line angle relative to the wing leading edge varied from 115° to 75°.

Comparison of the control effectiveness of controls with constant planform area showed that a control with the largest projected frontal area and moments was the most

effective throughout the wing-sweep range. Such a control, however, also produced more drag and more adverse yawing moment.

Langley Research Center,
National Aeronautics and Space Administration,
Langley Station, Hampton, Va., November 15, 1966,
126-13-02-04-23.

REFERENCES

1. Landrum, Emma Jean: Effect of Skewed Wing-Tip Controls on a Variable-Sweep Wing-Fuselage Configuration at Mach Numbers 1.41 and 2.20. NASA TM X-951, 1964.

2. Landrum, Emma Jean; and Babb, C. Donald: Effect of Skewed Wing-Tip Controls on a Variable-Sweep Wing-Fuselage Configuration at Mach Numbers From 2.60 to 4.62. NASA TM X-1031, 1964.

3. Lord, Douglas R.; and Czarnecki, K. R.: Recent Information on Flap and Tip Controls. NACA RM L53I17a, 1953.

4. Landrum, Emma Jean: Effect of Skewed Wing-Tip Controls on a Highly Swept Arrow Wing at Mach Number 2.03. NASA TN D-1867, 1964.

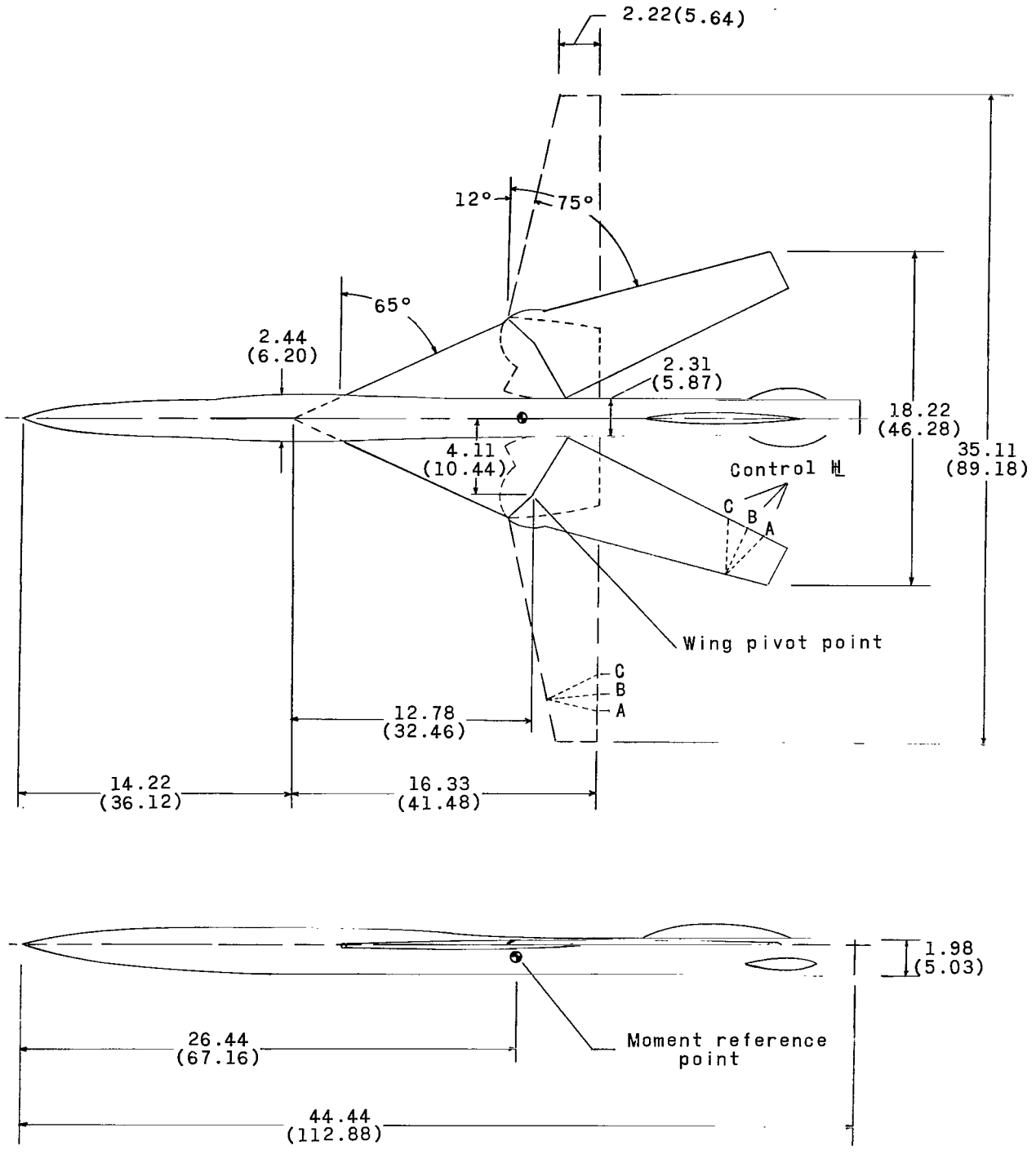

(a) Details of complete model.

Figure 1.- Model details. All dimensions are in inches. (Parenthetical dimensions are in centimeters.)

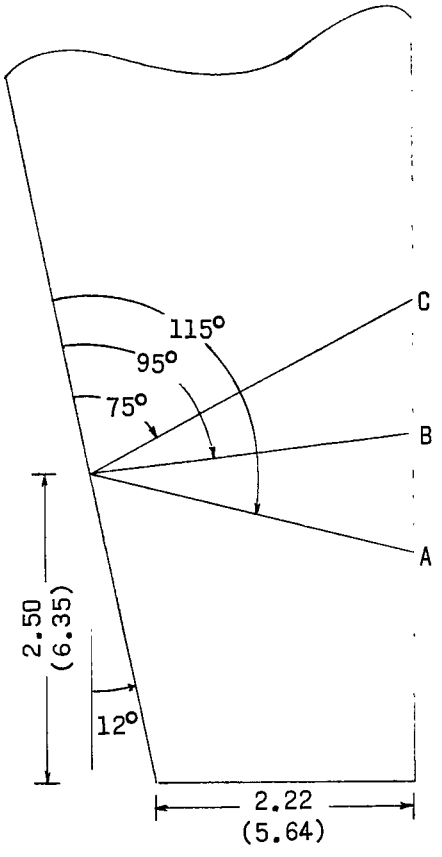

(b) Hinge-line orientation relative to wing leading edge.

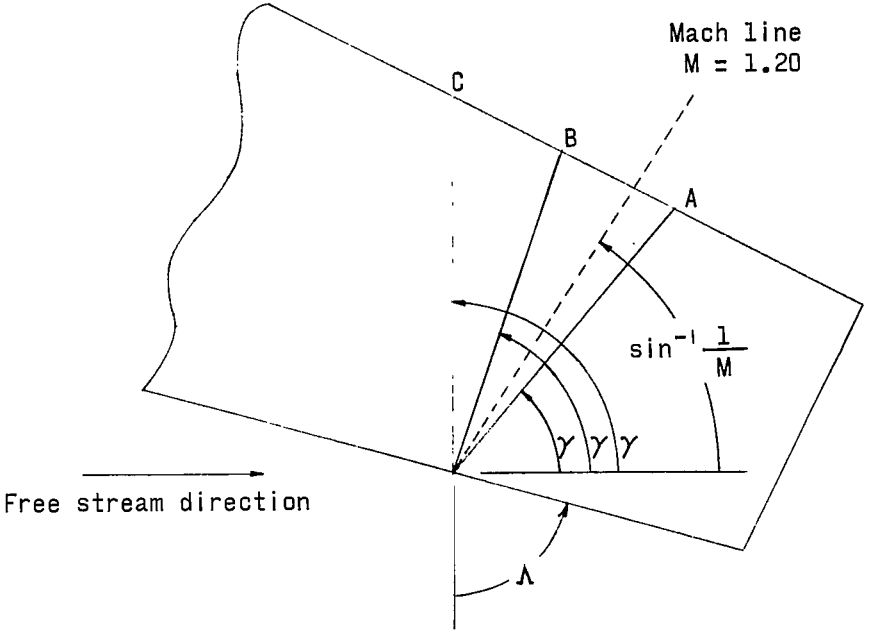

Control	Λ	γ
A	75°	50°
B	75°	70°
C	75°	90°

(c) Hinge-line orientation relative to free-stream direction. M = 1.20; Λ = 75°.

Figure 1.- Concluded.

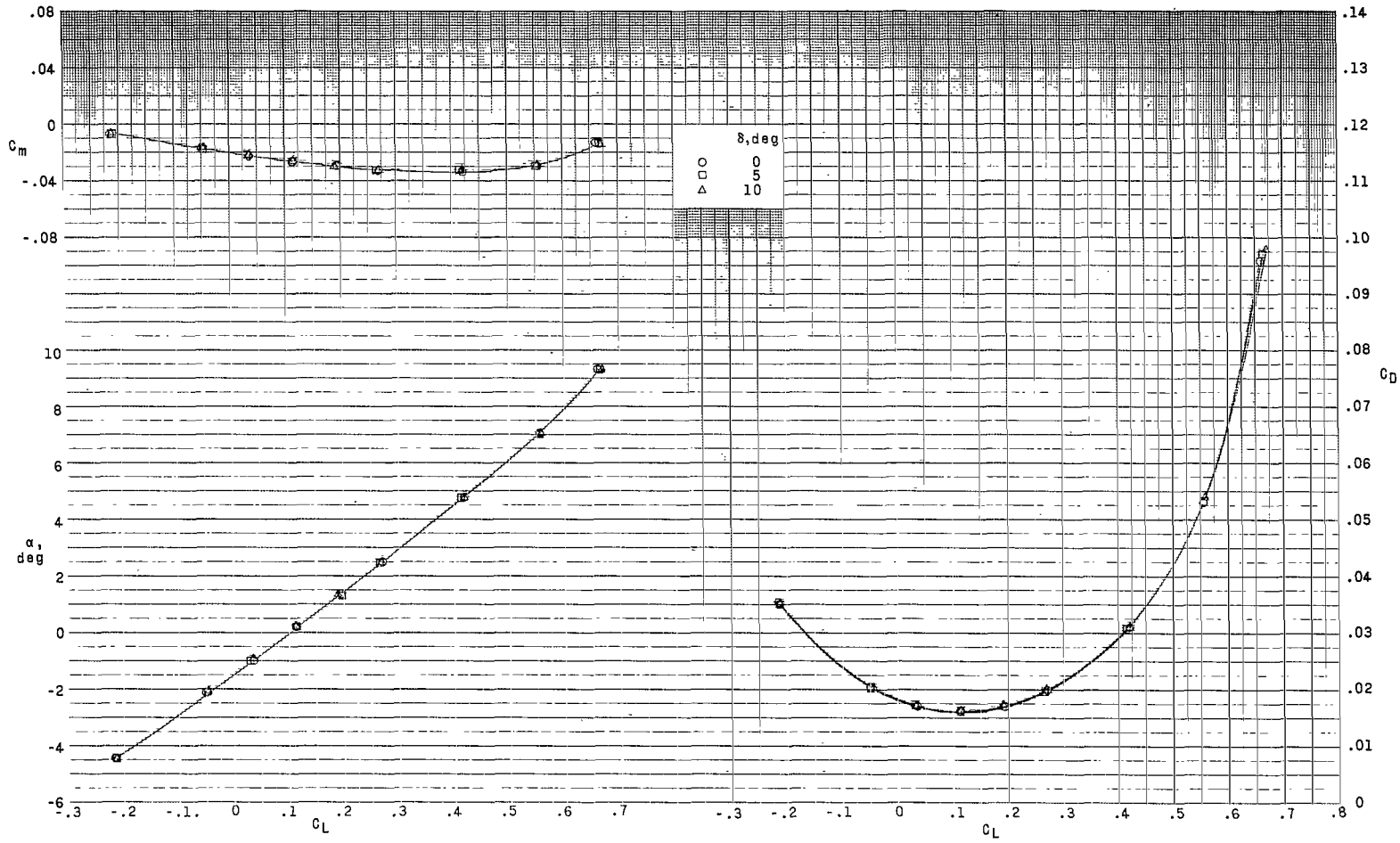

(a) Control A. $\gamma = 5^0$.

Figure 2.- Effect of control deflection on longitudinal aerodynamic characteristics. $\Lambda = 30^0$; $\beta = 0^0$; $M = 0.50$.

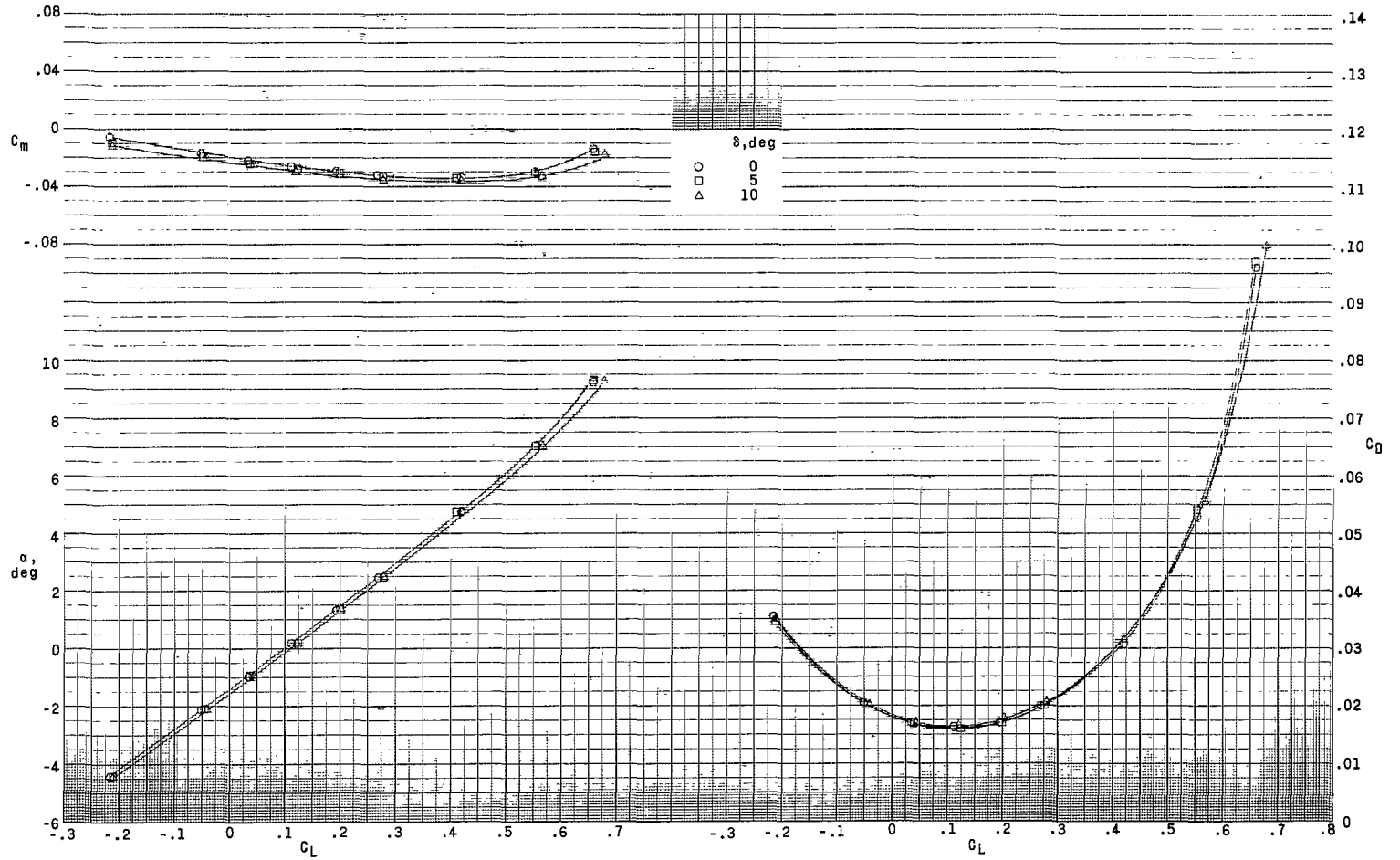

(b) Control B. $\gamma = 25^0$.

Figure 2.- Continued.

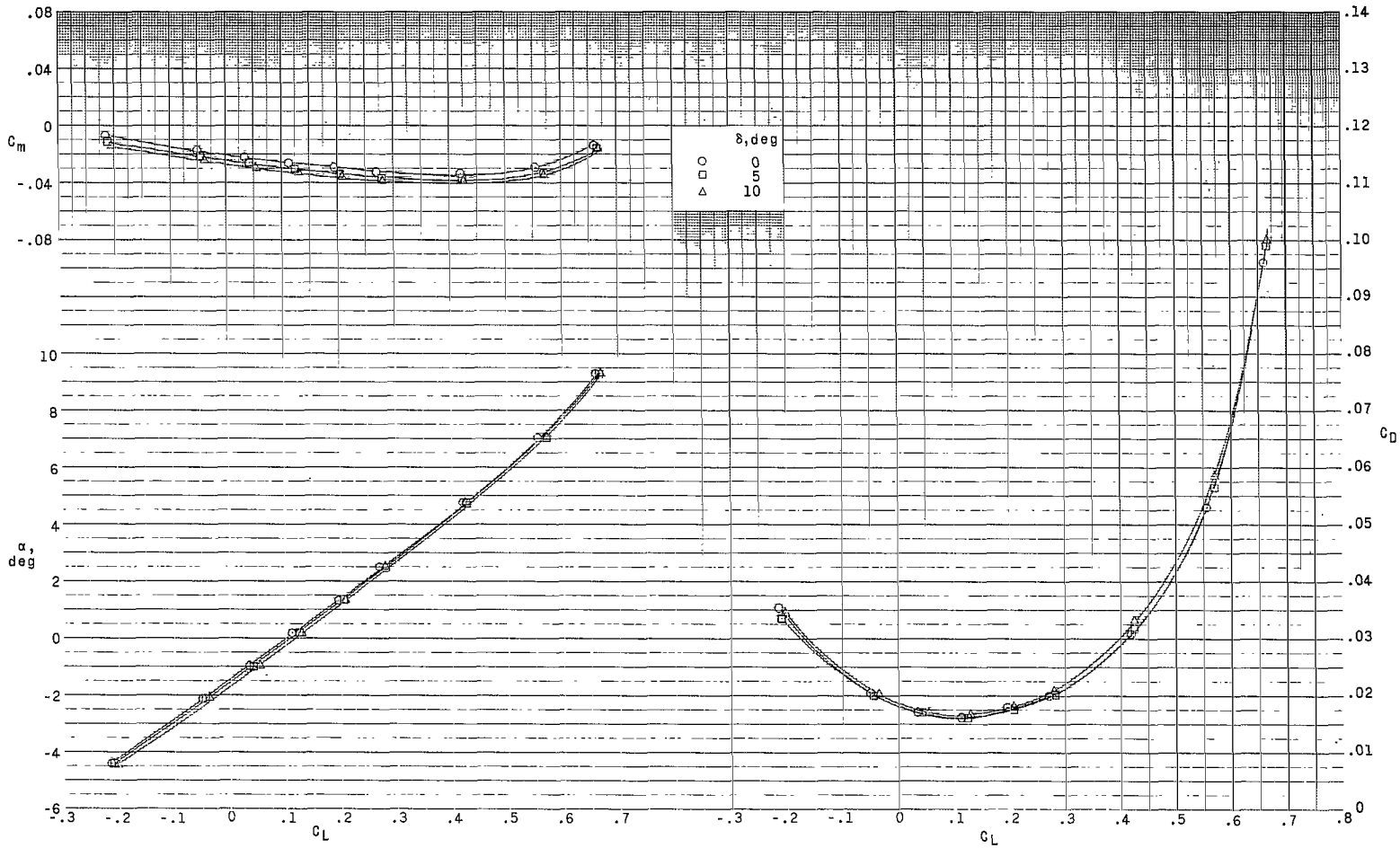

(c) Control C. $\gamma = 45^0$.

Figure 2.- Concluded.

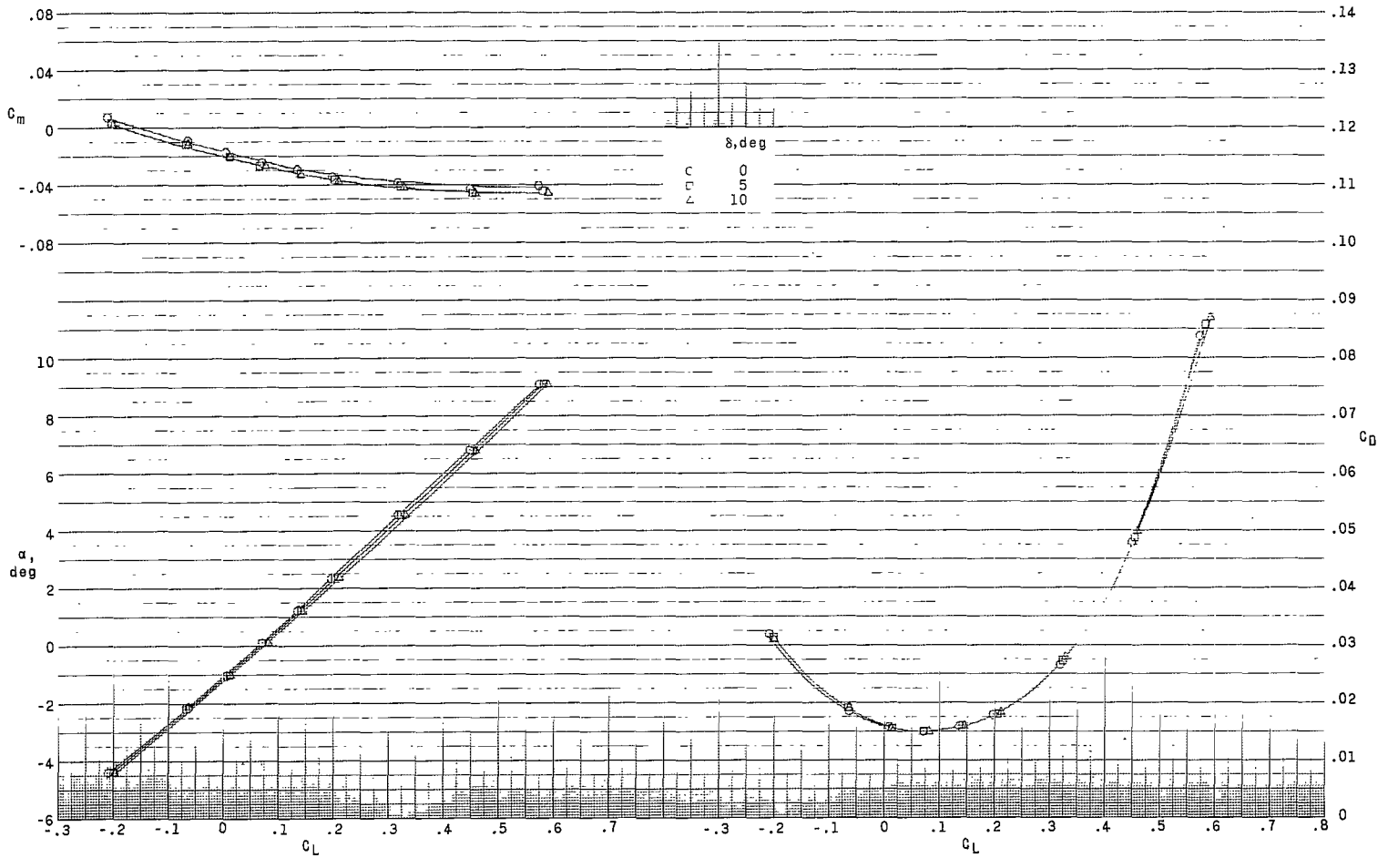

(a) Control A. $\gamma = 20^0$.

Figure 3.- Effect of control deflection on longitudinal aerodynamic characteristics. $\Lambda = 45^0$; $\beta = 0^0$; $M = 0.50$.

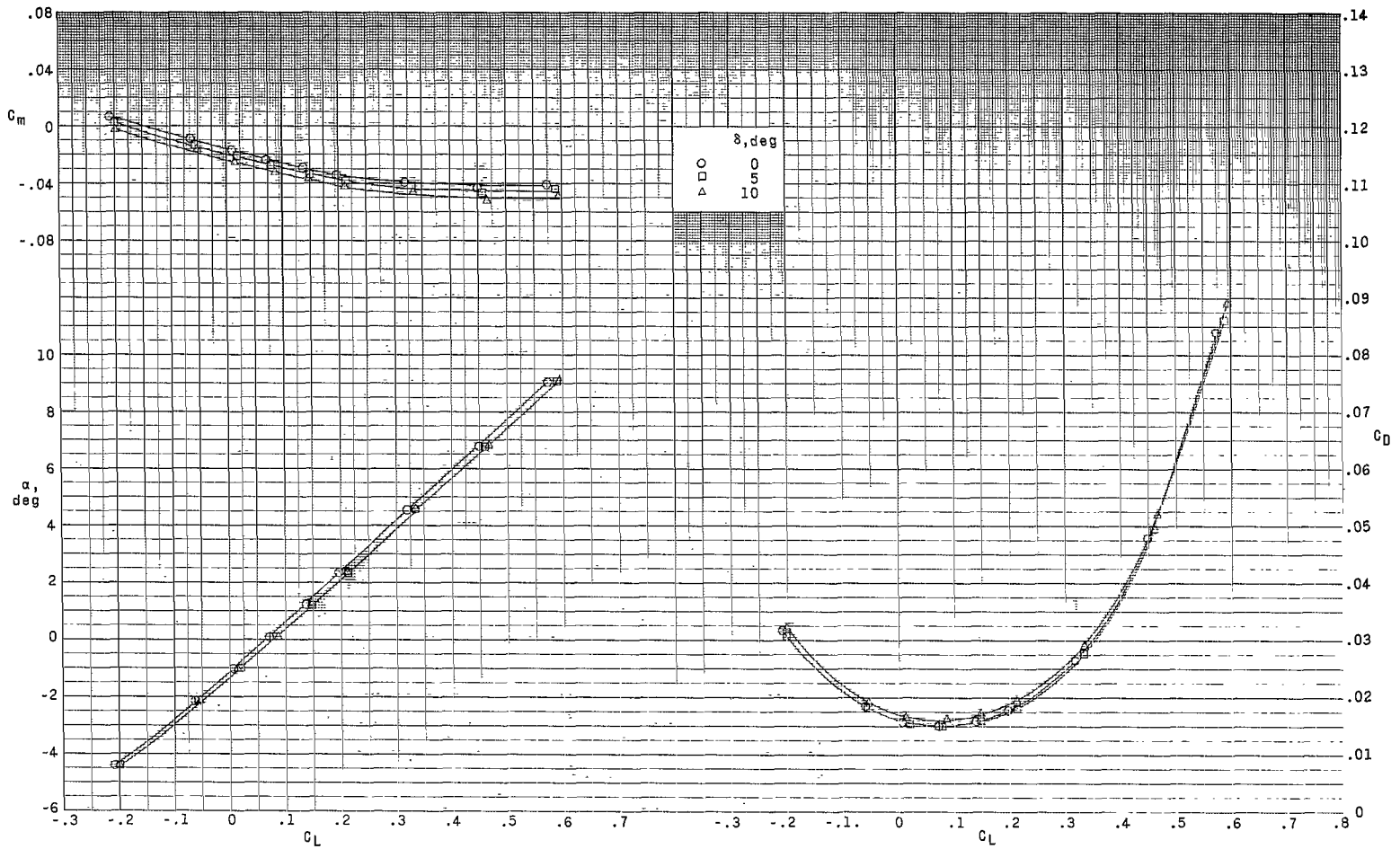

(b) Control B. $\gamma = 40^0$.

Figure 3.- Continued.

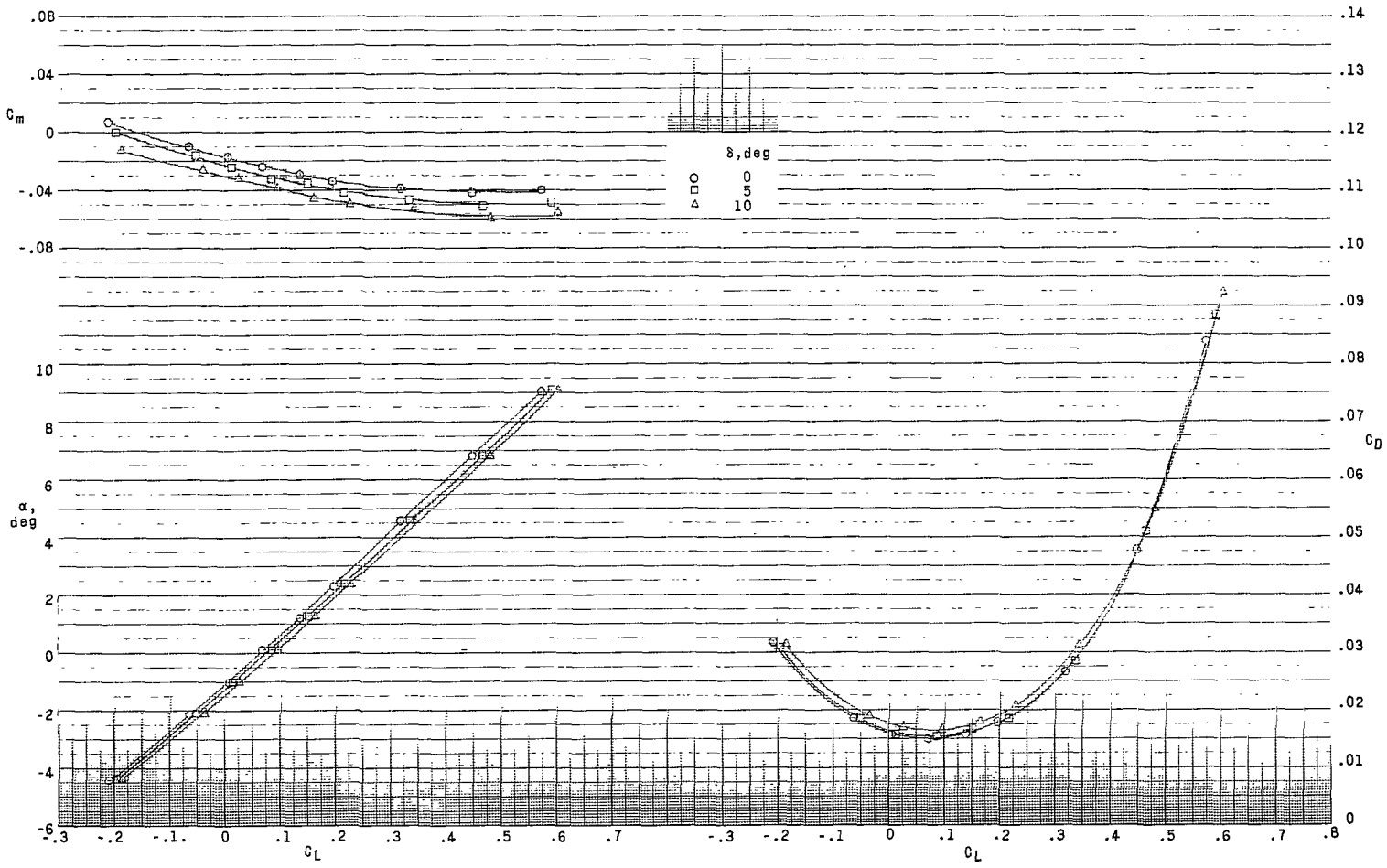

(c) Control C. $\gamma = 60^0$.

Figure 3.- Concluded.

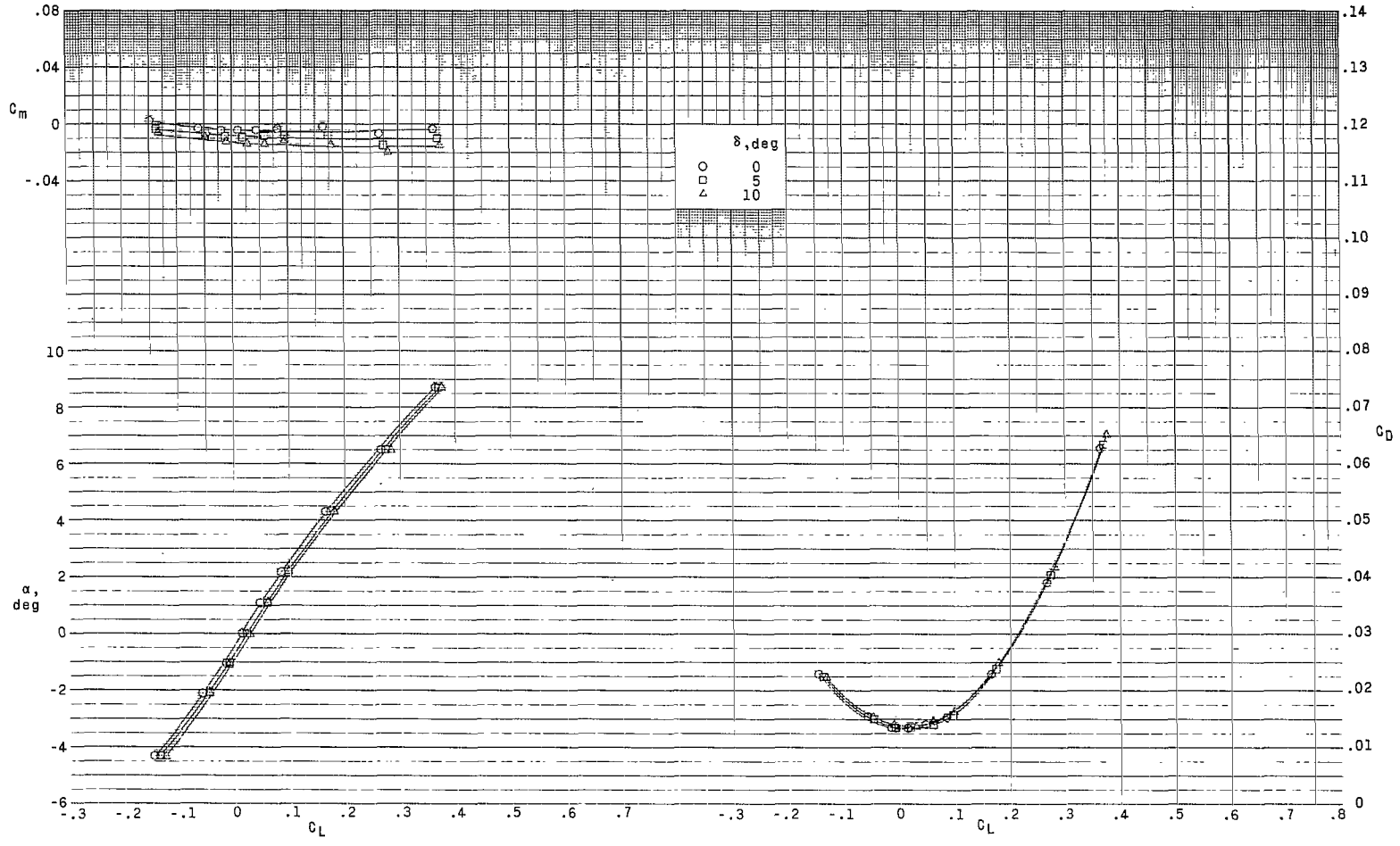

(a) Control A. $\gamma = 50^0$.

Figure 4.- Effect of control deflection on longitudinal aerodynamic characteristics. $\Lambda = 75^0$; $\beta = 0^0$; $M = 0.50$.

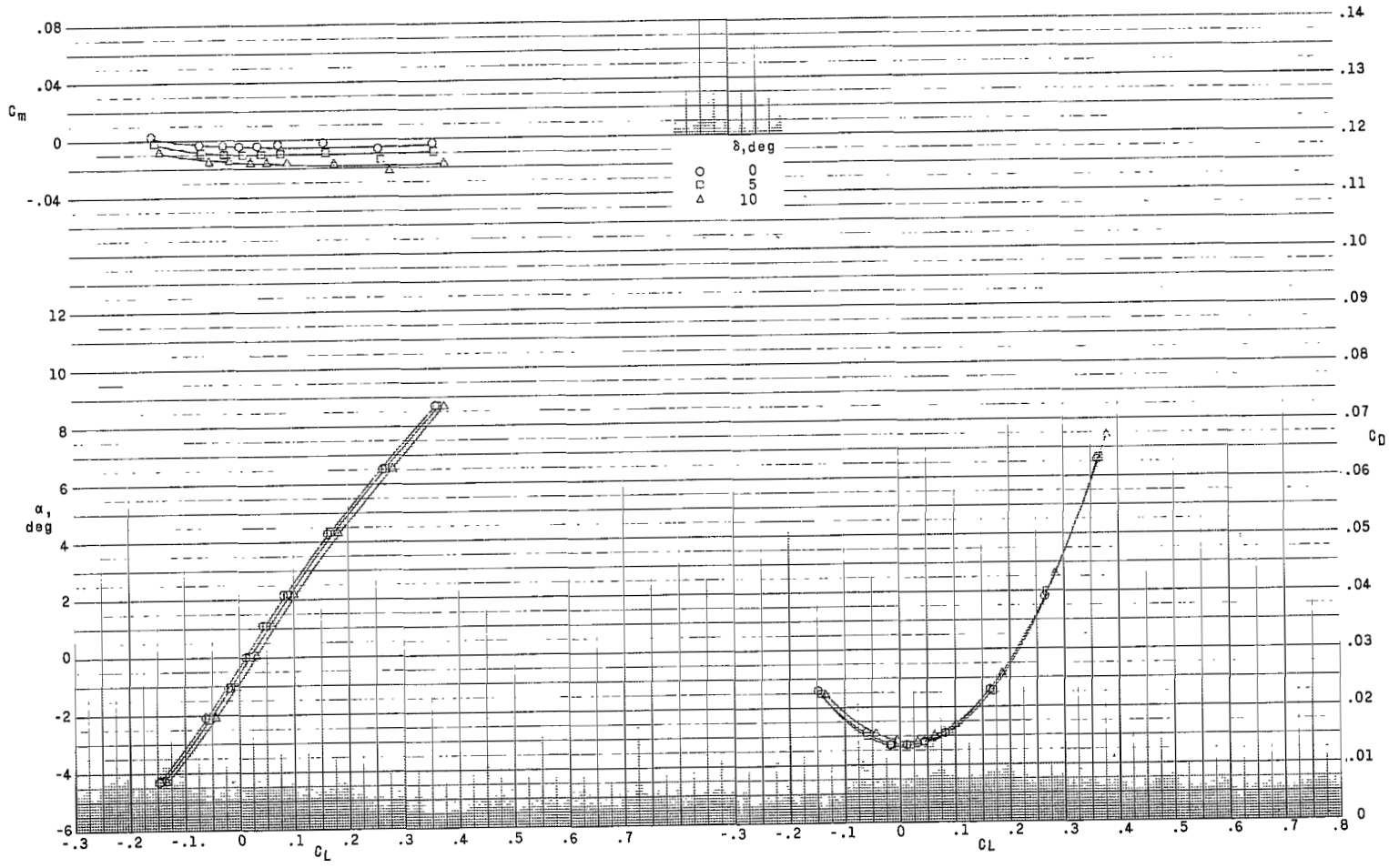

(b) Control B. $\gamma = 70^{o}$.

Figure 4.- Continued.

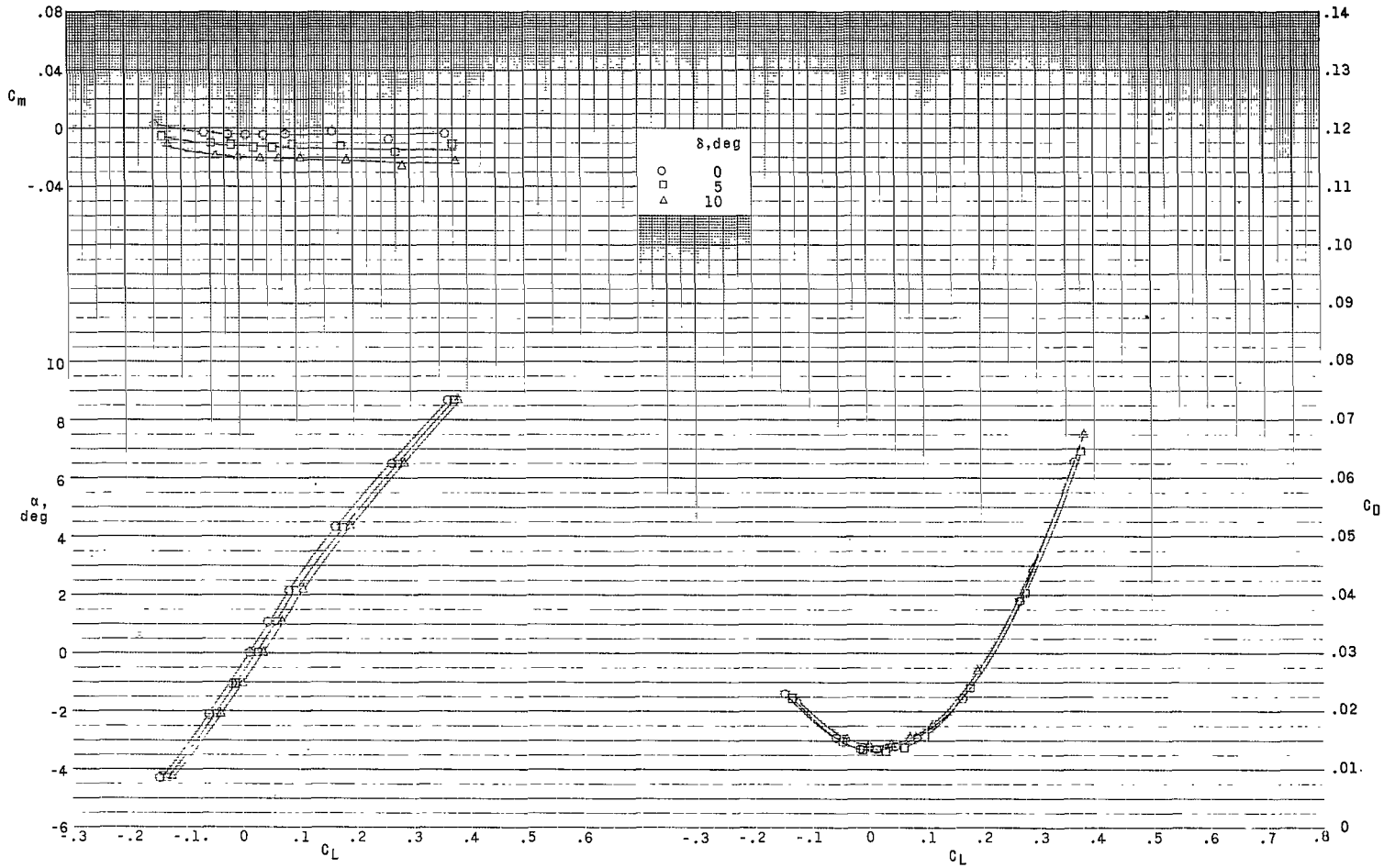

(c) Control C. $\gamma = 90^{\circ}$.

Figure 4.- Concluded.

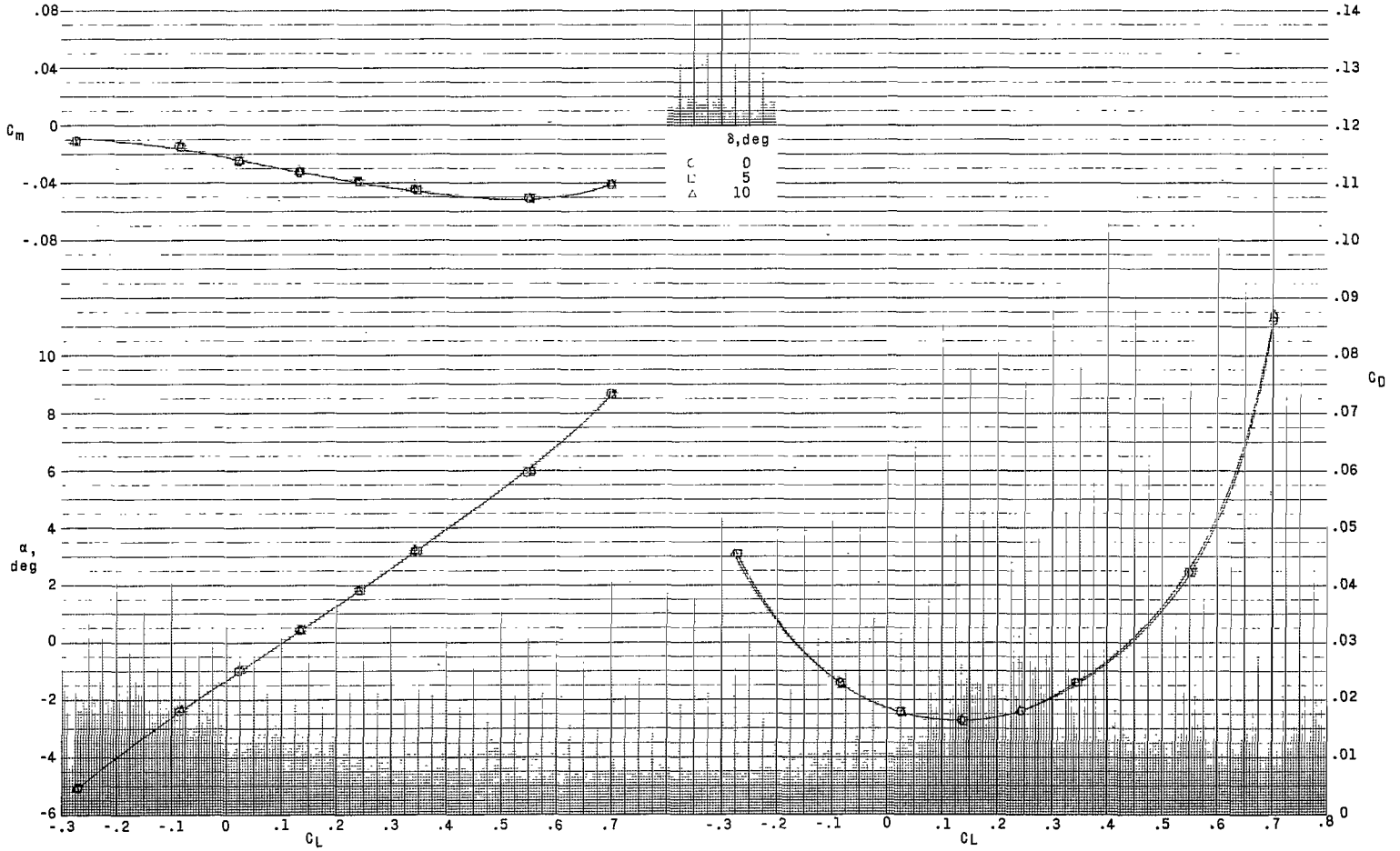

(a) Control A. $\gamma = 5^0$.

Figure 5.- Effect of control deflection on longitudinal aerodynamic characteristics. $\Lambda = 30^0$; $\beta = 0^0$; $M = 0.80$.

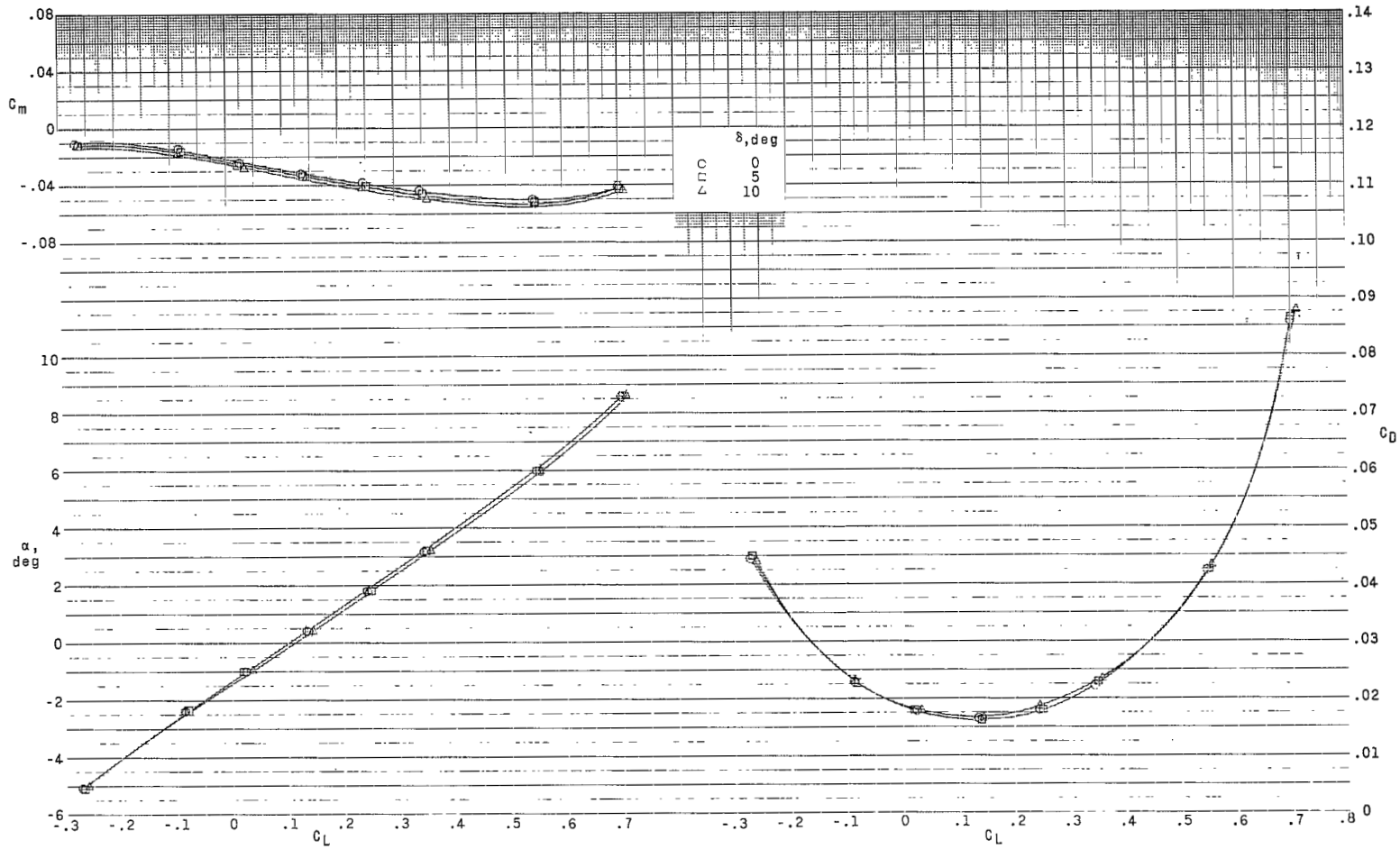

(b) Control B. $\gamma = 25^0$.

Figure 5.- Continued.

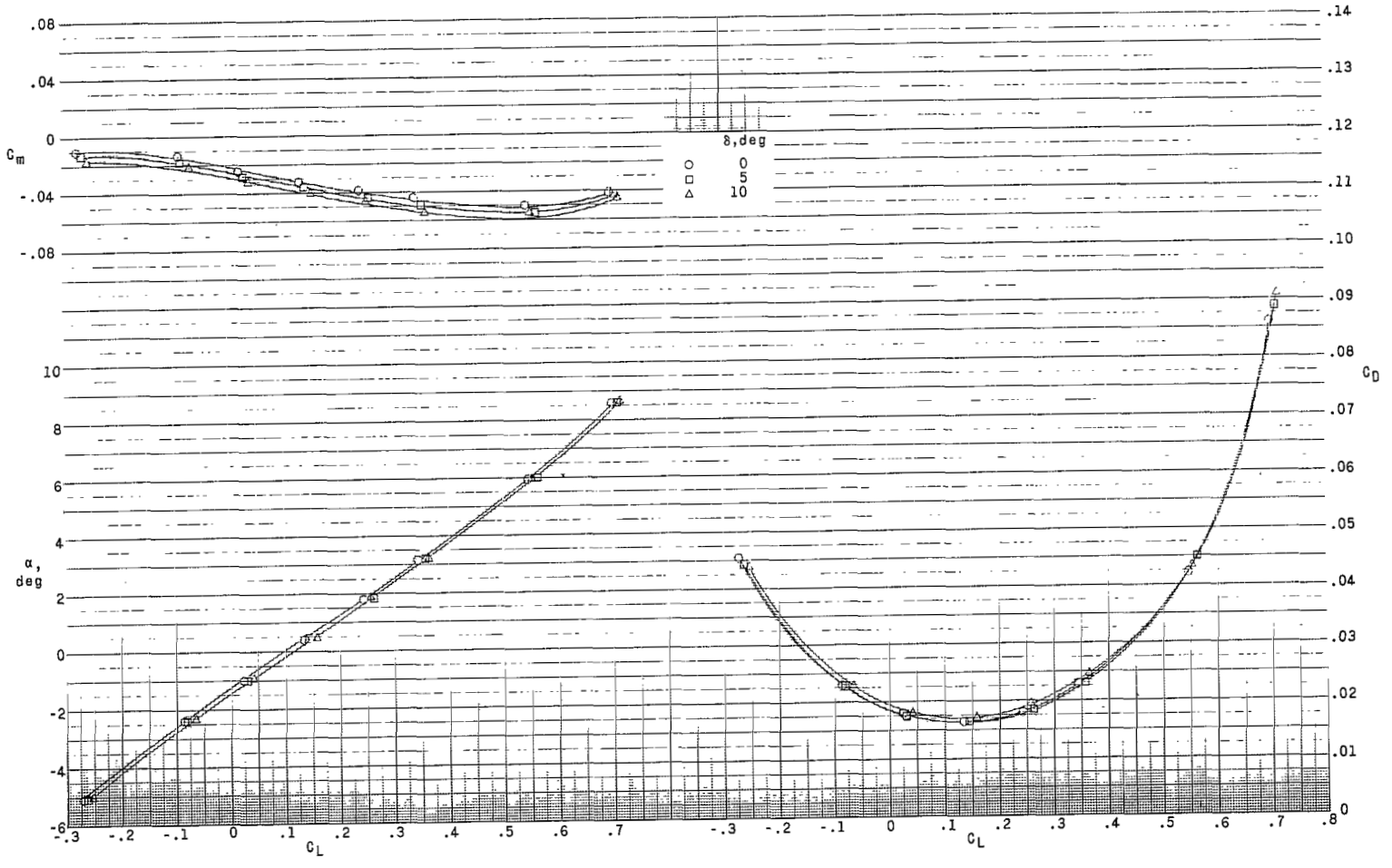

(c) Control C. $\gamma = 45^0$.

Figure 5.- Concluded.

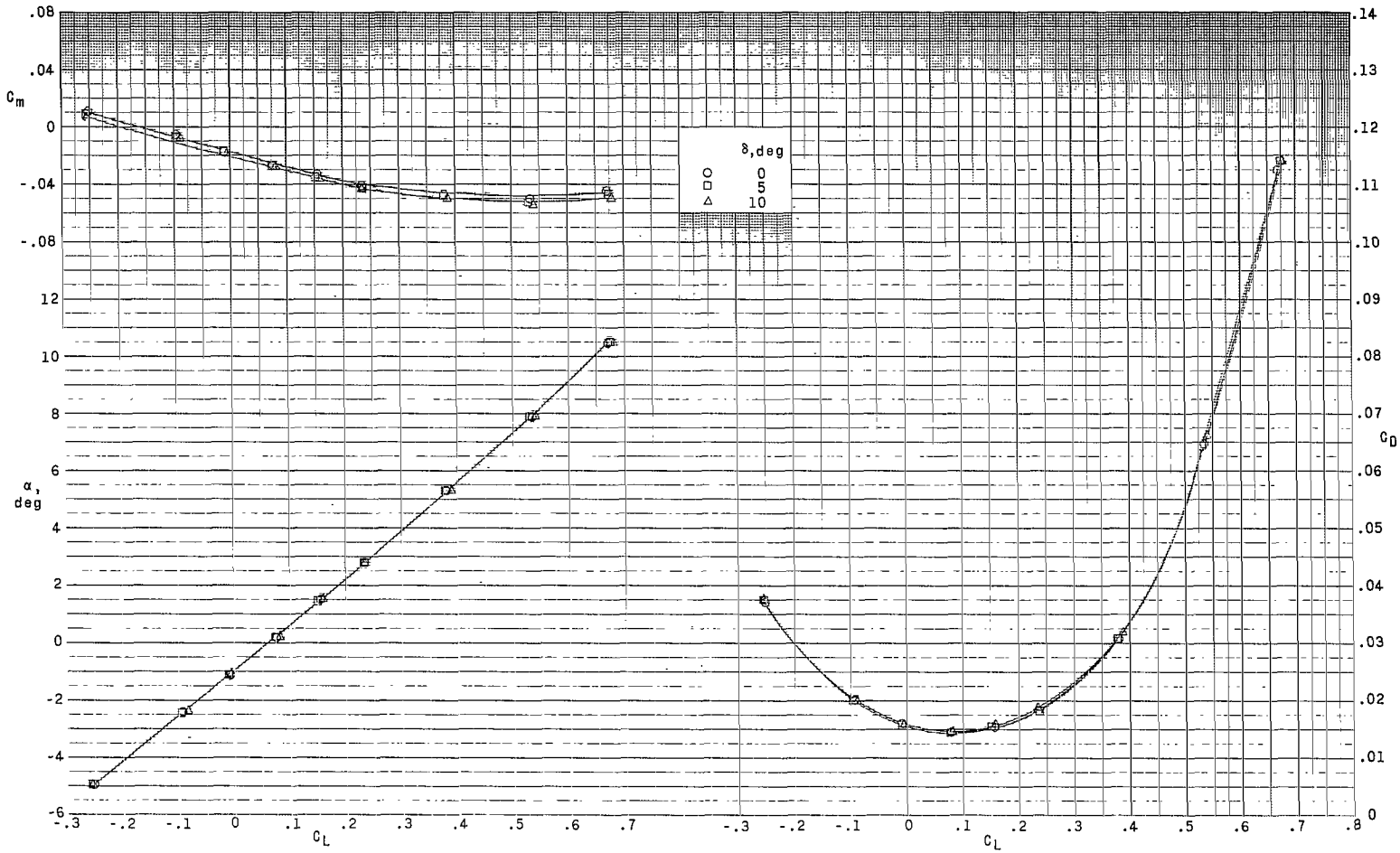

(a) Control A. $\gamma = 20^0$.

Figure 6.- Effect of control deflection on longitudinal aerodynamic characteristics. $\Lambda = 45^0$; $\beta = 0^0$; $M = 0.80$.

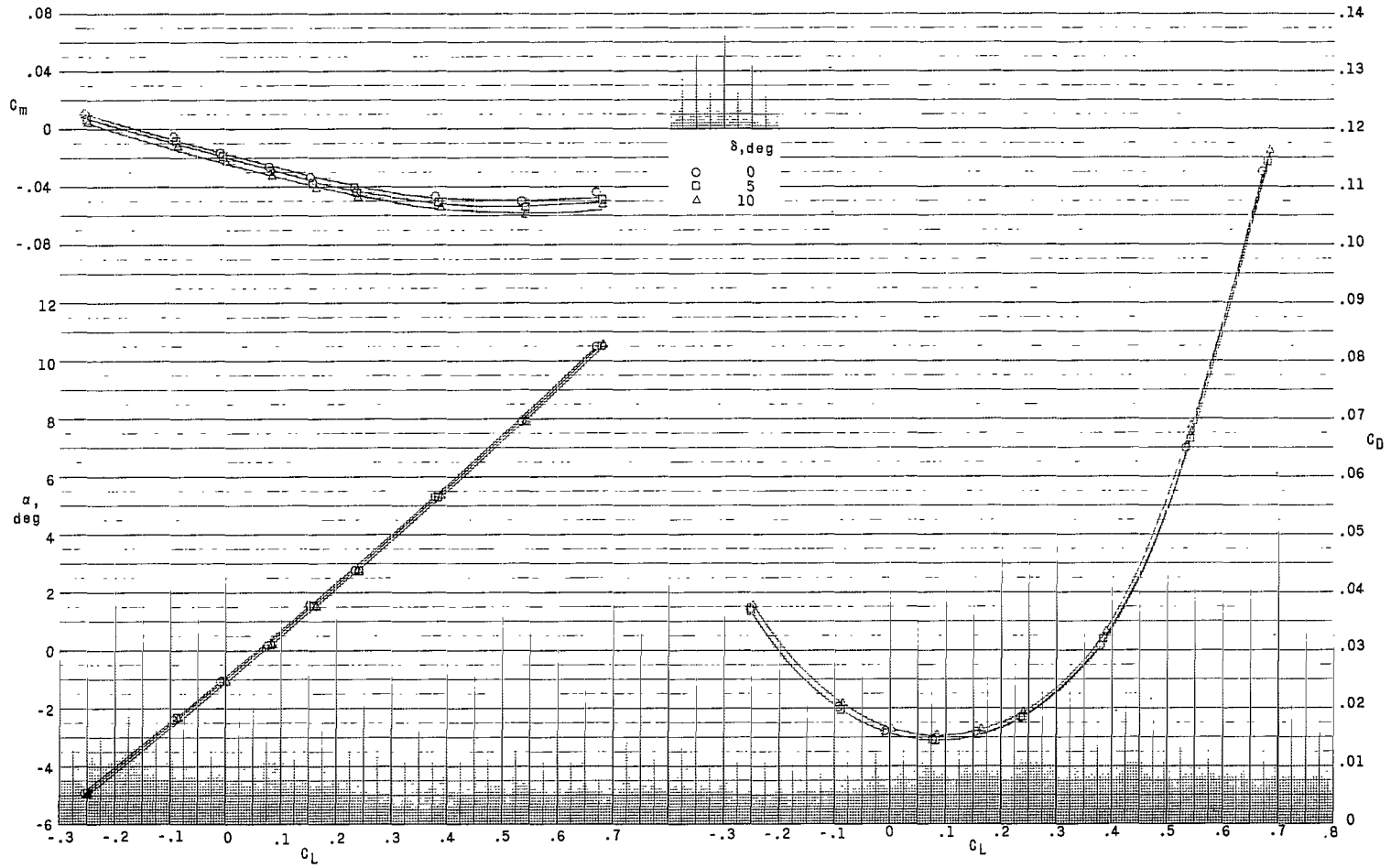

(b) Control B. $\gamma = 40^0$.

Figure 6.- Continued.

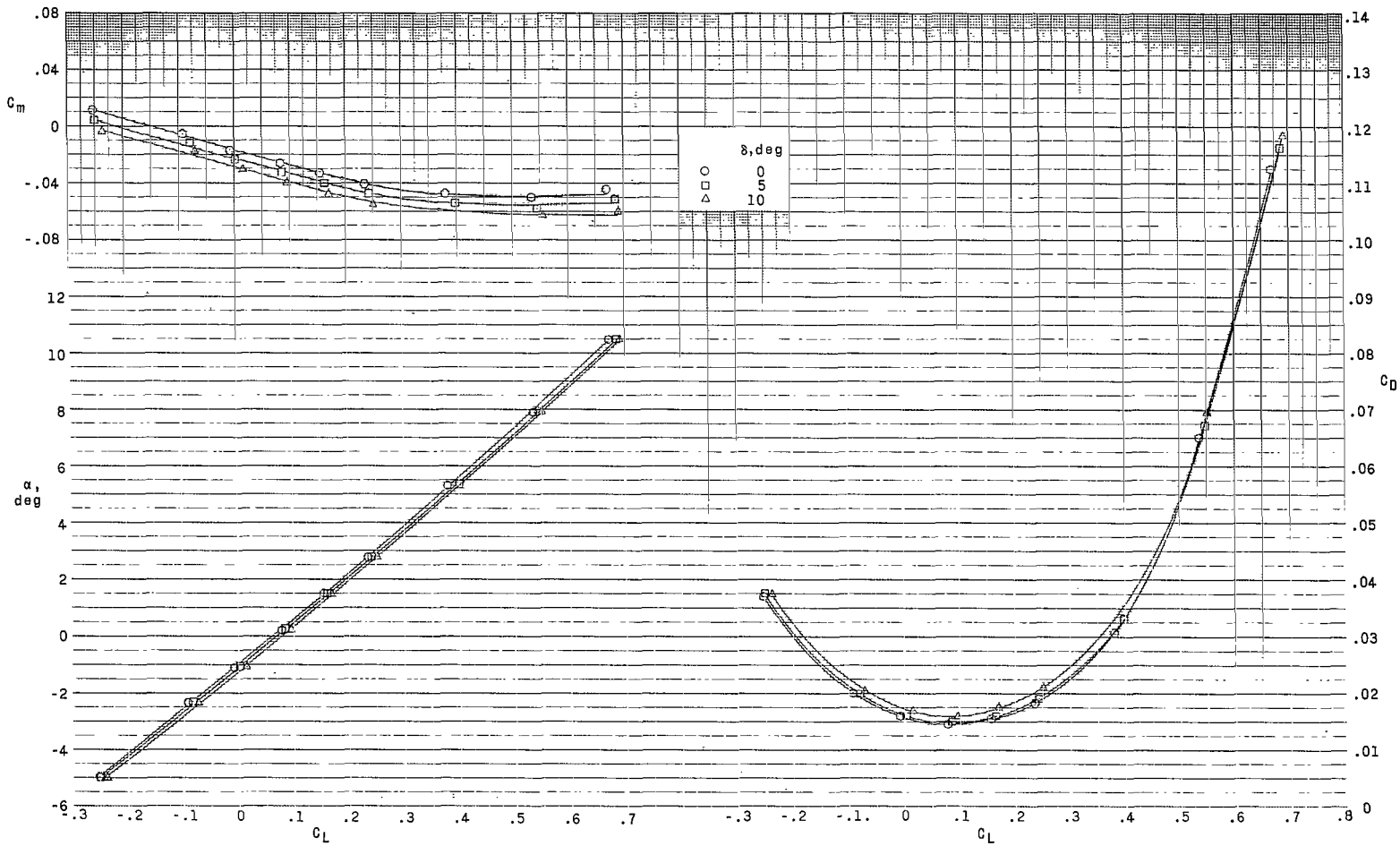

(c) Control C. $\gamma = 60^0$.

Figure 6.- Concluded.

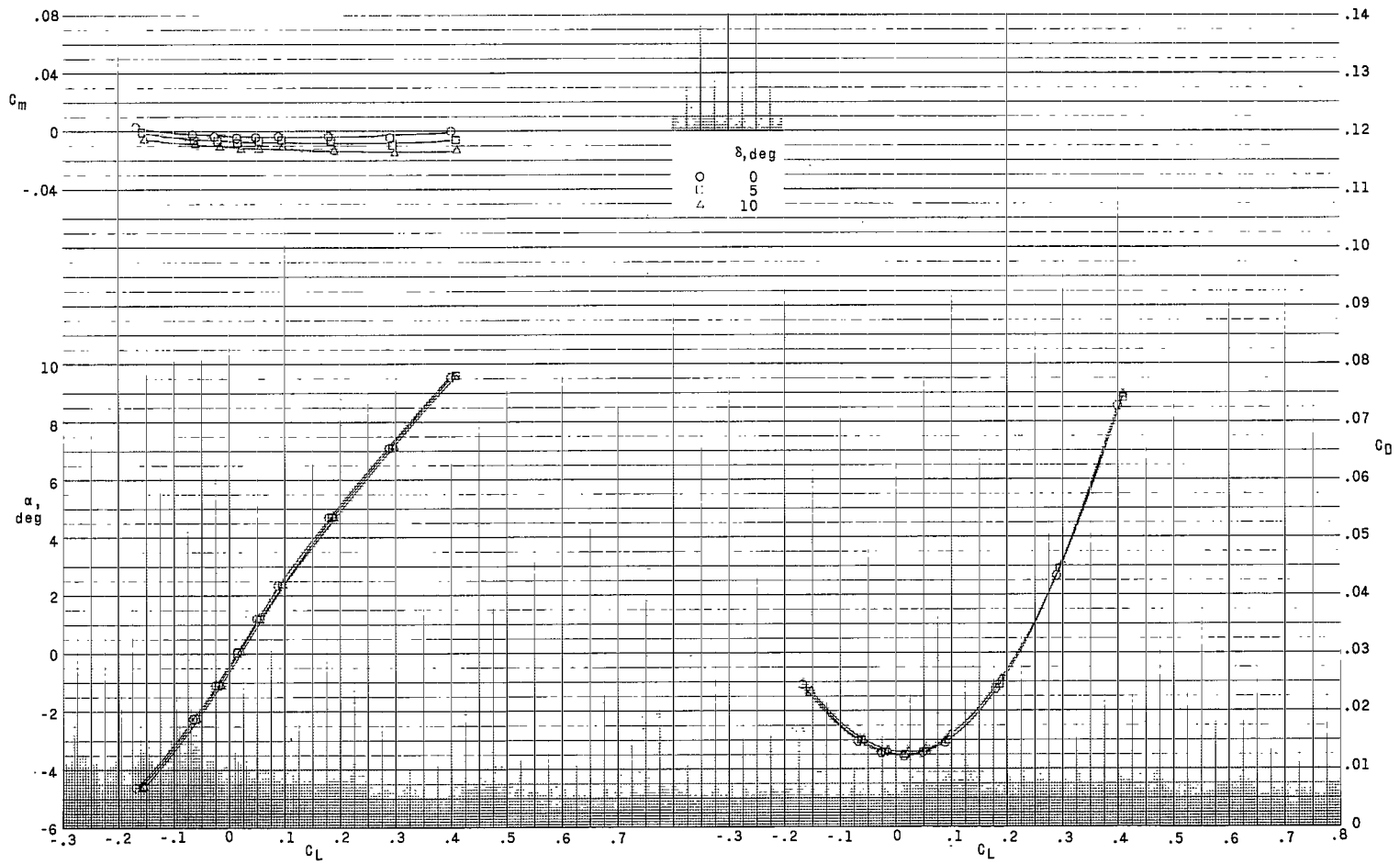

(a) Control A. $\gamma = 50^0$.

Figure 7.- Effect of control deflection on longitudinal aerodynamic characteristics. $\Lambda = 75^0$; $\beta = 0^0$; $M = 0.80$.

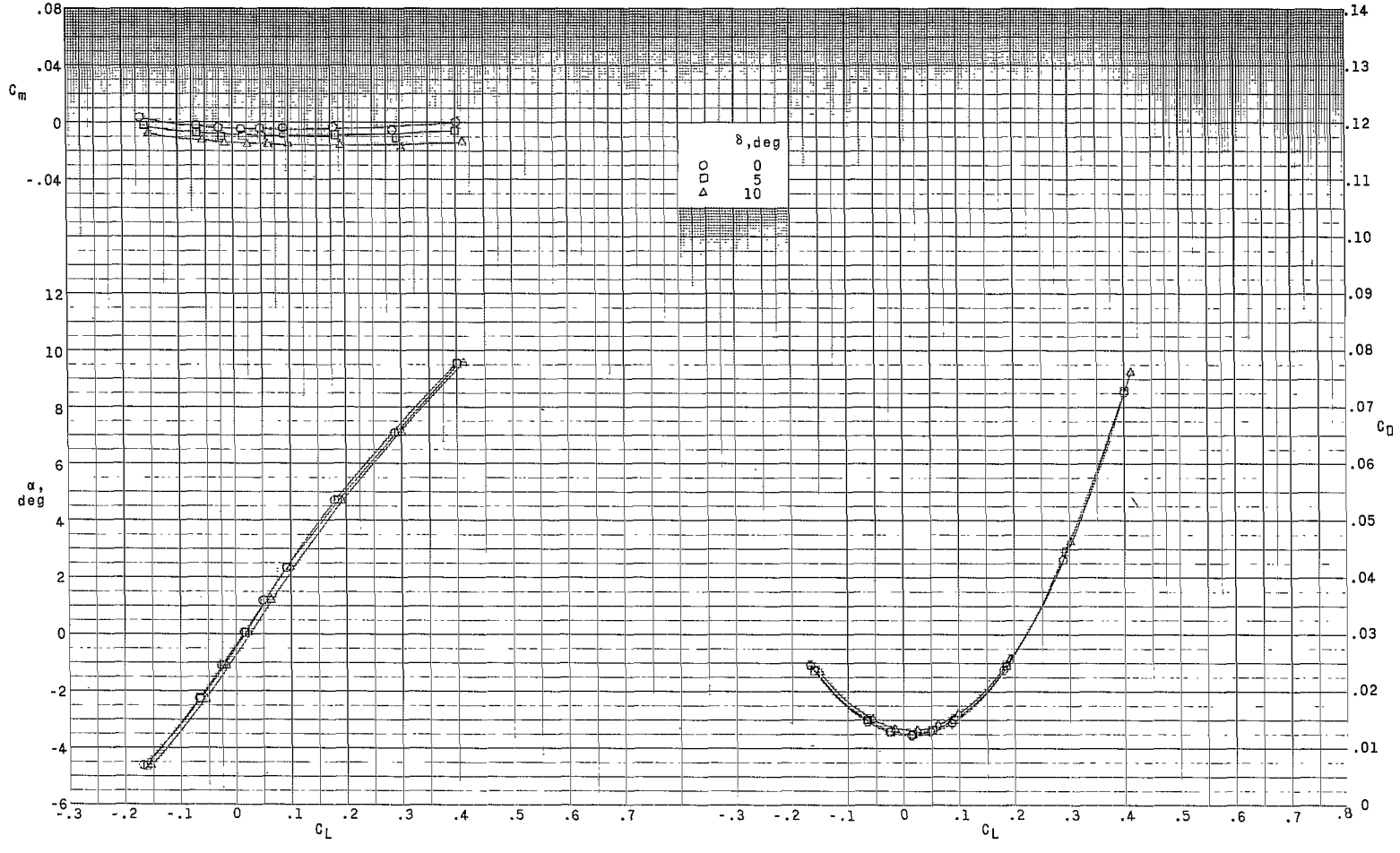

(b) Control B. $\gamma = 70^0$.

Figure 7.- Continued.

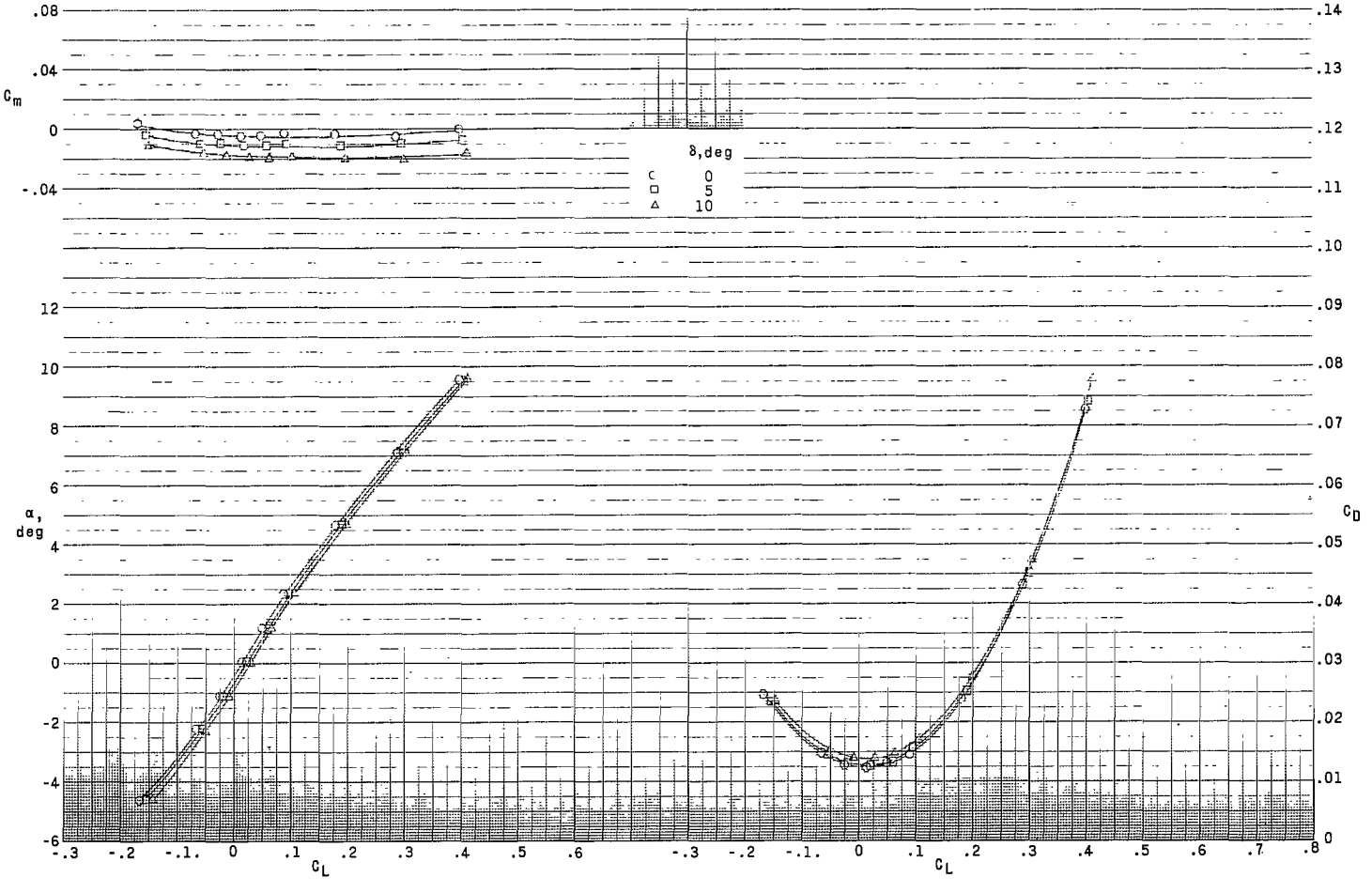

(c) Control C. $\gamma = 90^0$.

Figure 7.- Concluded.

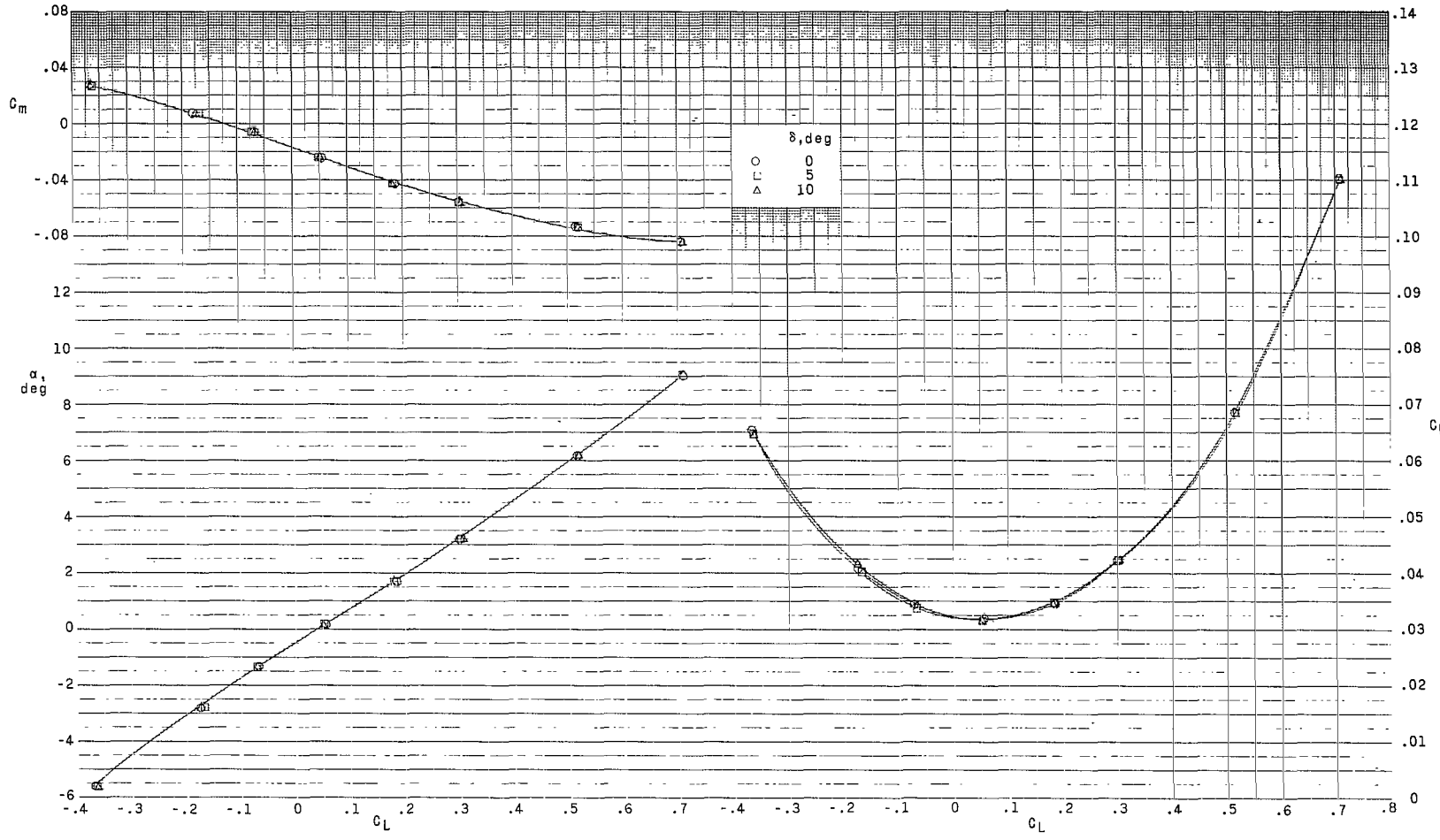

(a) Control A. $\gamma = 5^0$.

Figure 8.- Effect of control deflection on longitudinal aerodynamic characteristics. $\Lambda = 30^0$; $\beta = 0^0$; $M = 0.97$.

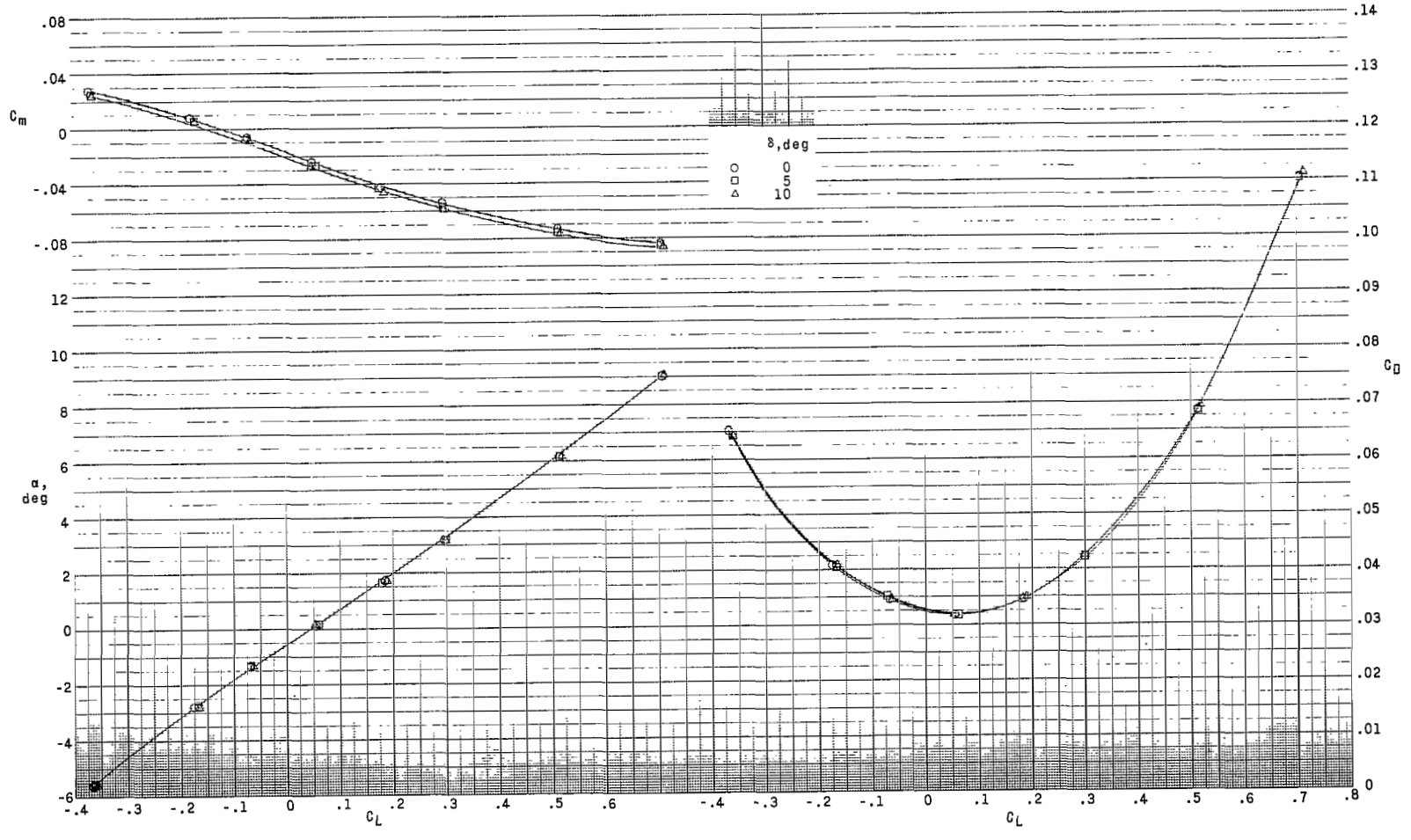

(b) Control B. $\gamma = 25^0$.

Figure 8.- Continued.

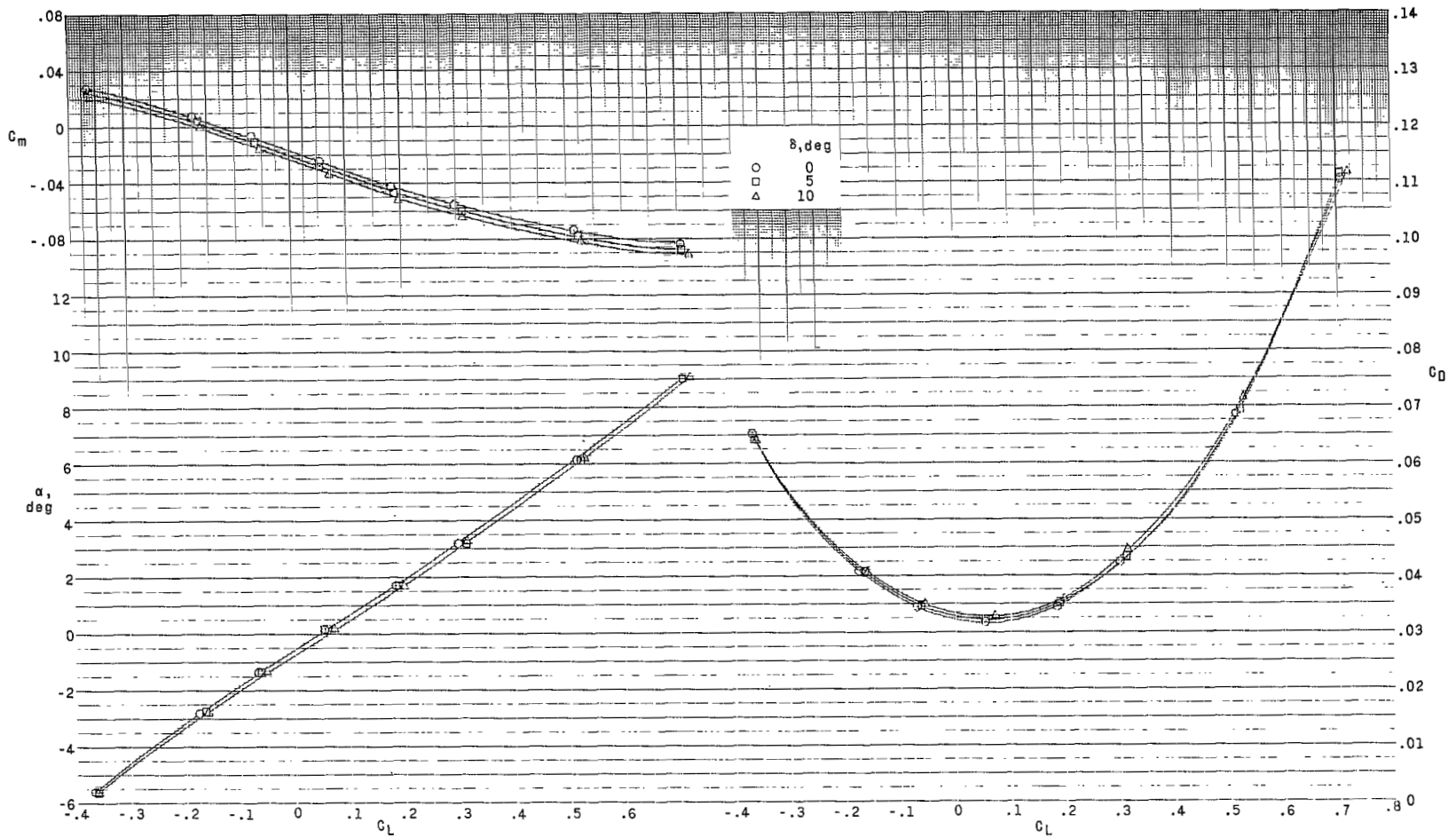

(c) Control C. $\gamma = 45^0$.

Figure 8.- Concluded.

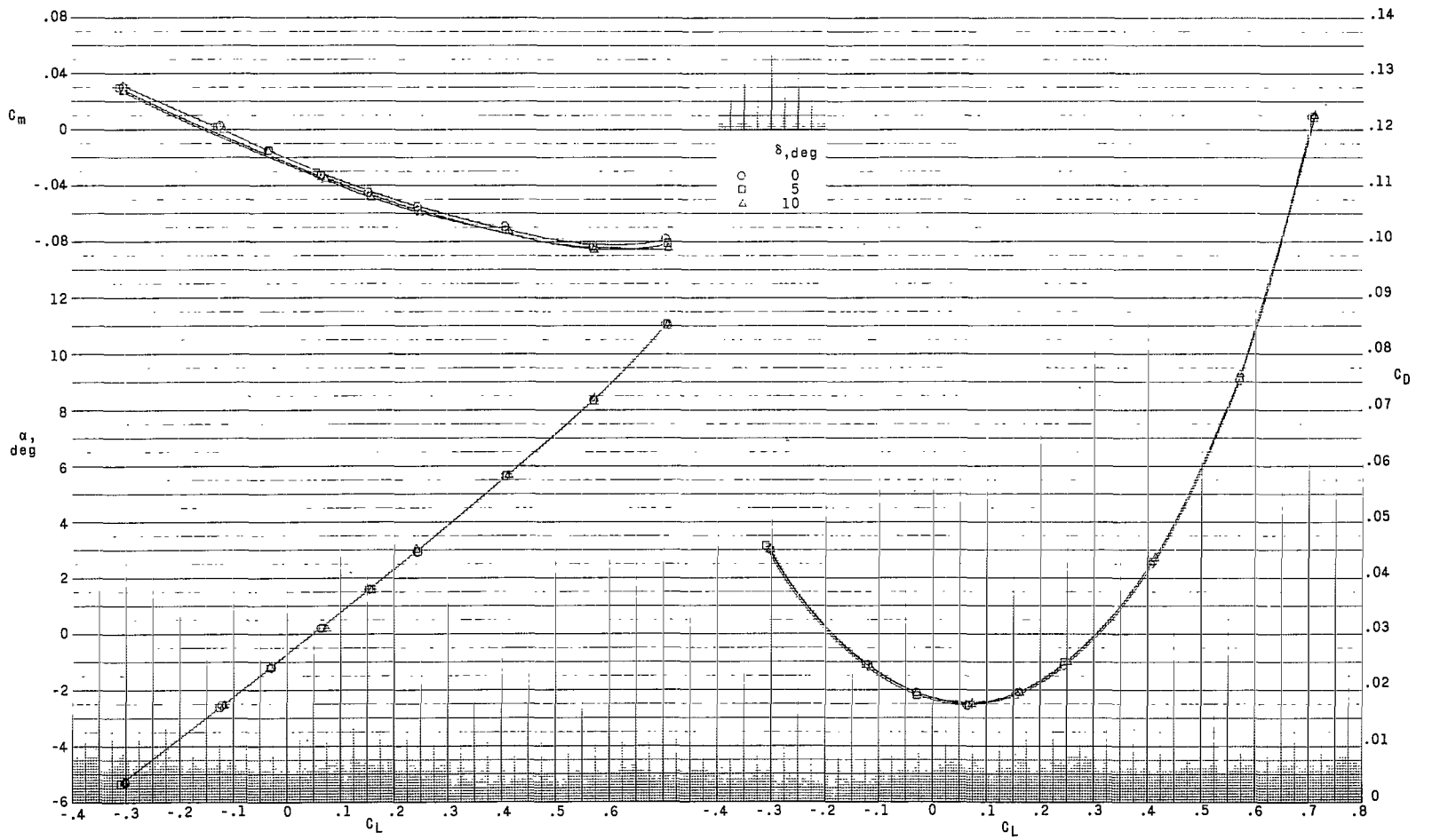

(a) Control A. $\gamma = 20^0$.

Figure 9.- Effect of control deflection on longitudinal aerodynamic characteristics. $\Lambda = 45^0$; $\beta = 0^0$; $M = 0.97$.

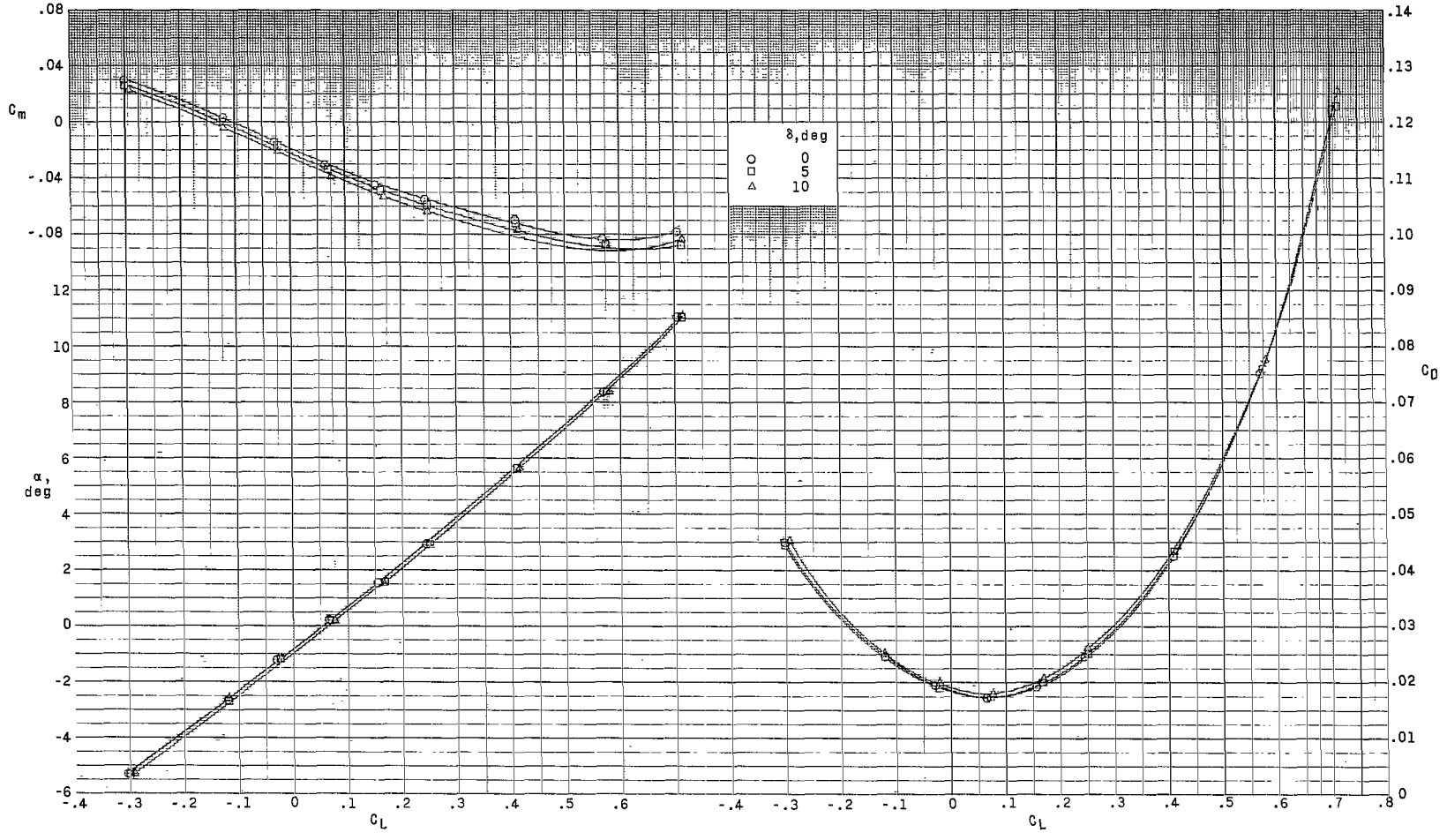

(b) Control B. $\gamma = 40^0$.

Figure 9.- Continued.

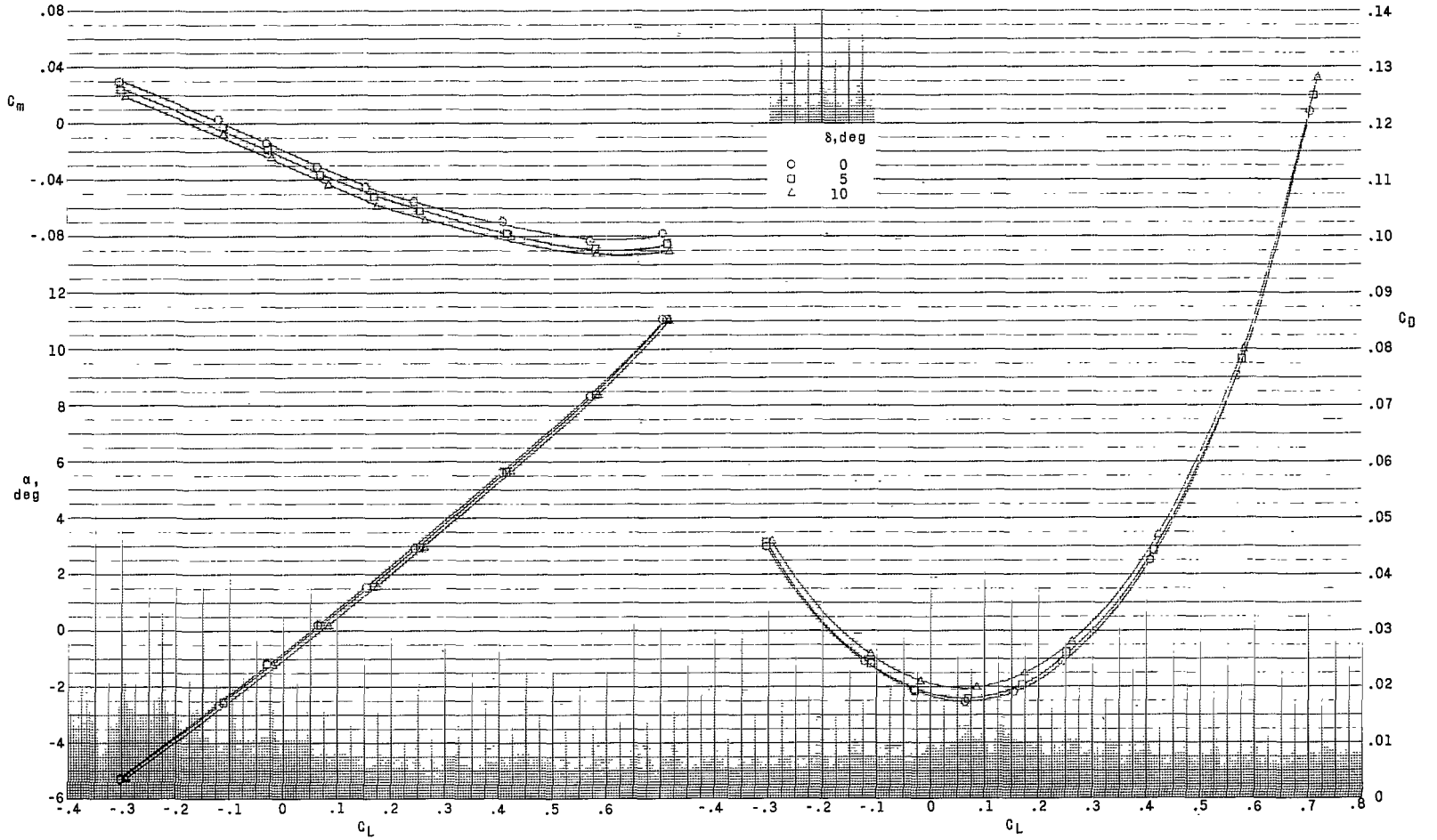

(c) Control C. $\gamma = 60^{\circ}$.

Figure 9.- Concluded.

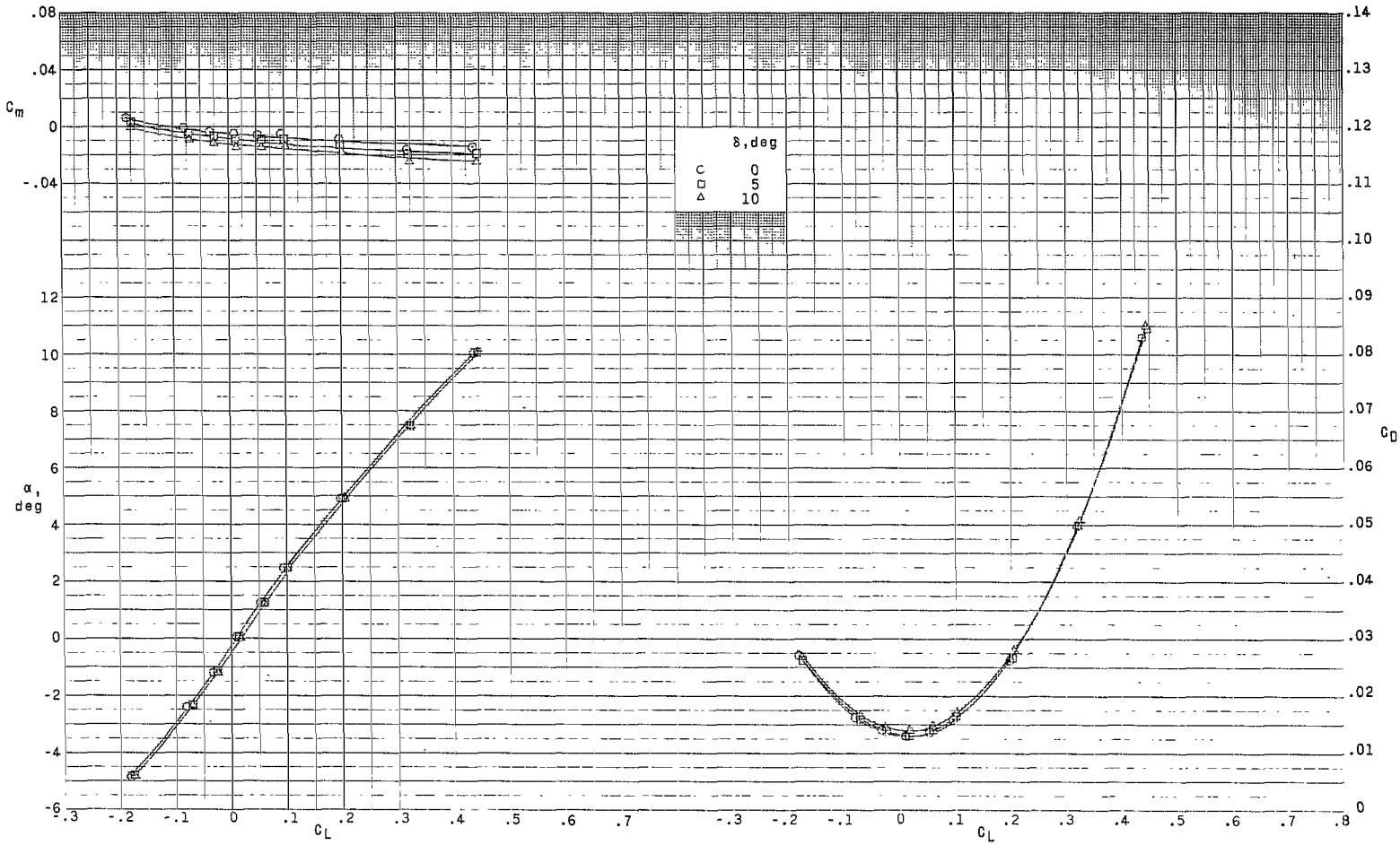

(a) Control A. $\gamma = 50^0$.

Figure 10.- Effect of control deflection on longitudinal aerodynamic characteristics. $\Lambda = 75^0$; $\beta = 0^0$; $M = 0.97$.

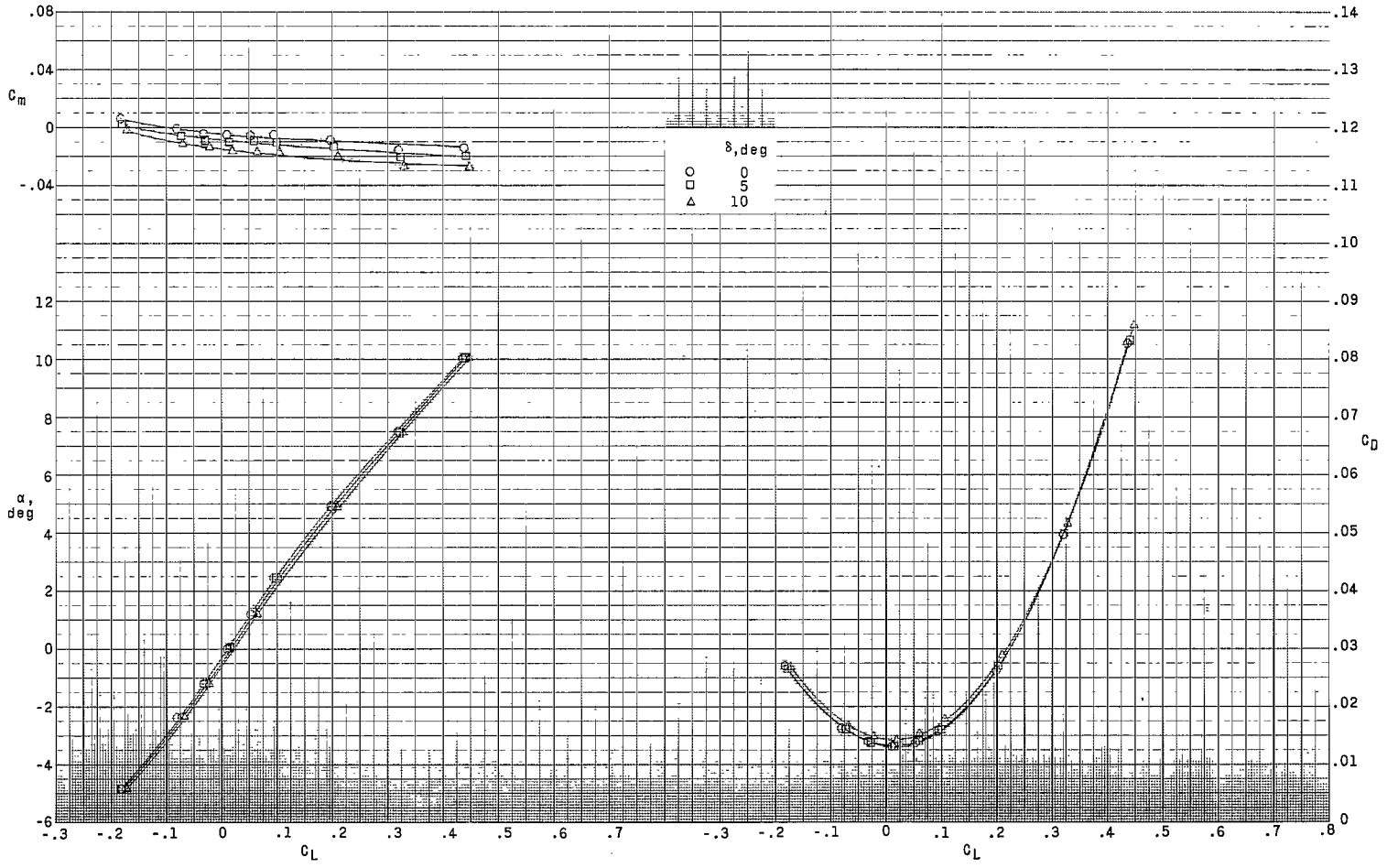

(b) Control B. $\gamma = 70^{0}$.

Figure 10.- Continued.

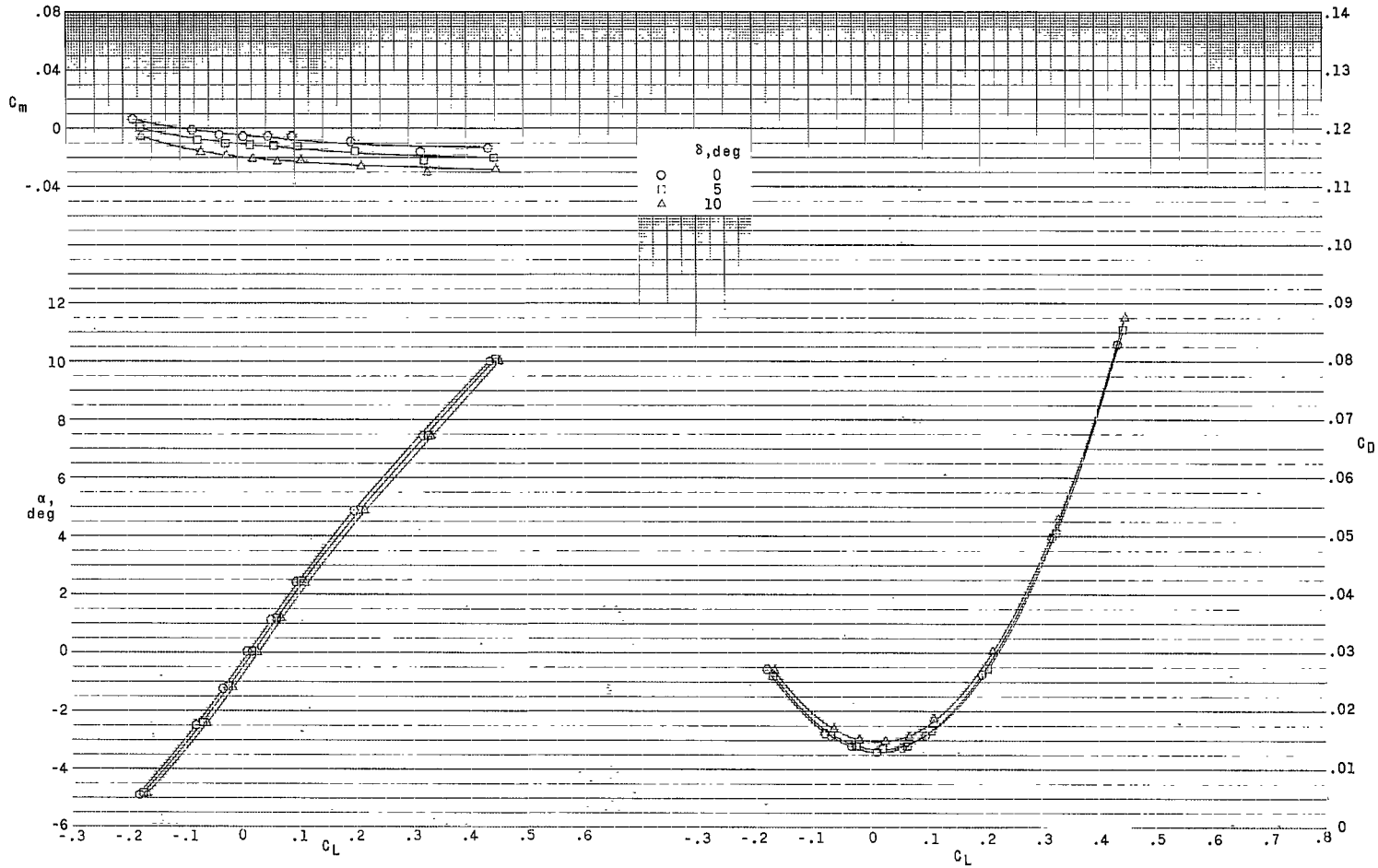

(c) Control C. $\gamma = 90^{o}$.

Figure 10.- Concluded.

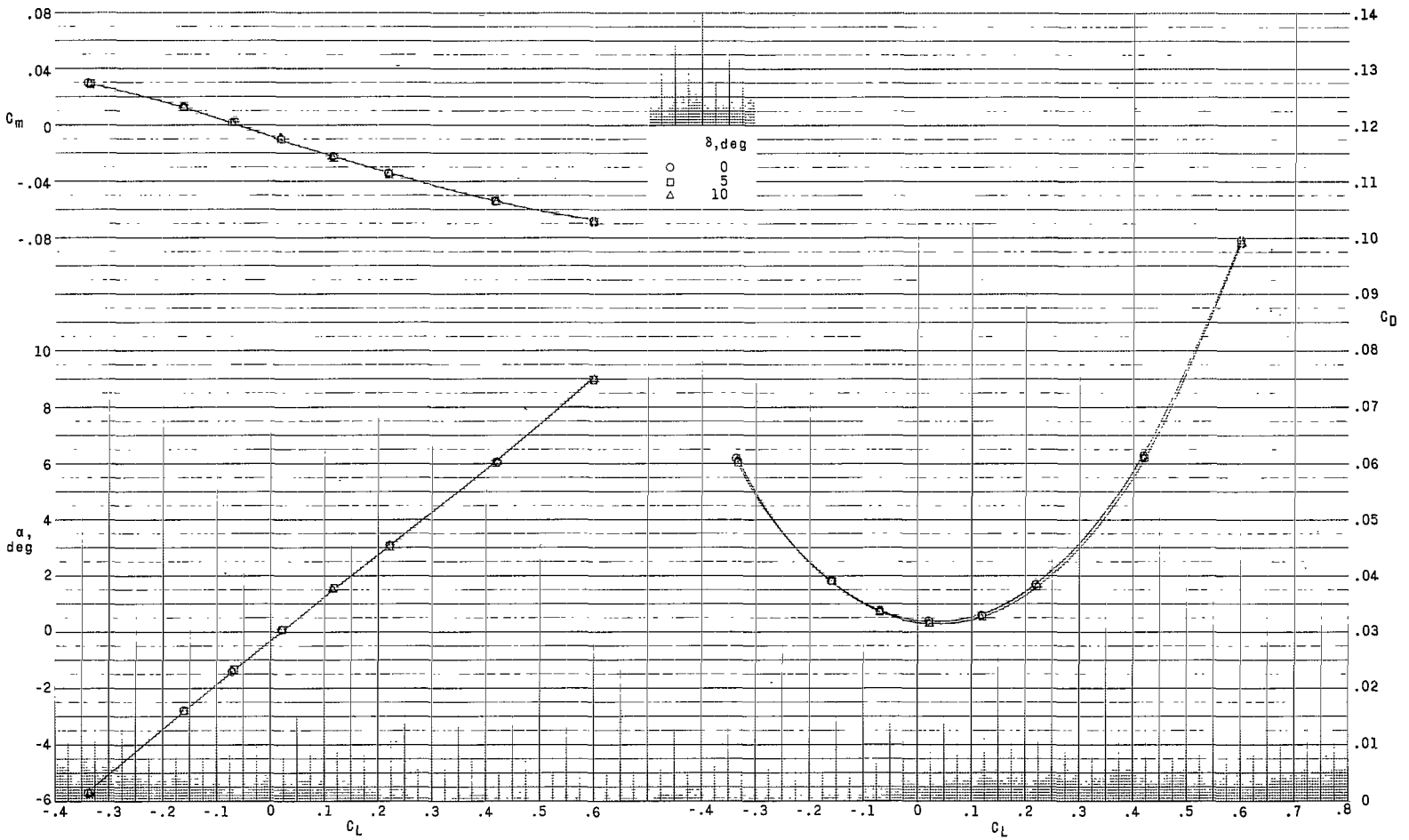

(a) Control A. $\gamma = 5^0$.

Figure 11.- Effect of control deflection on longitudinal aerodynamic characteristics. $\Lambda = 30^0$; $\beta = 0^0$; $M = 1.20$.

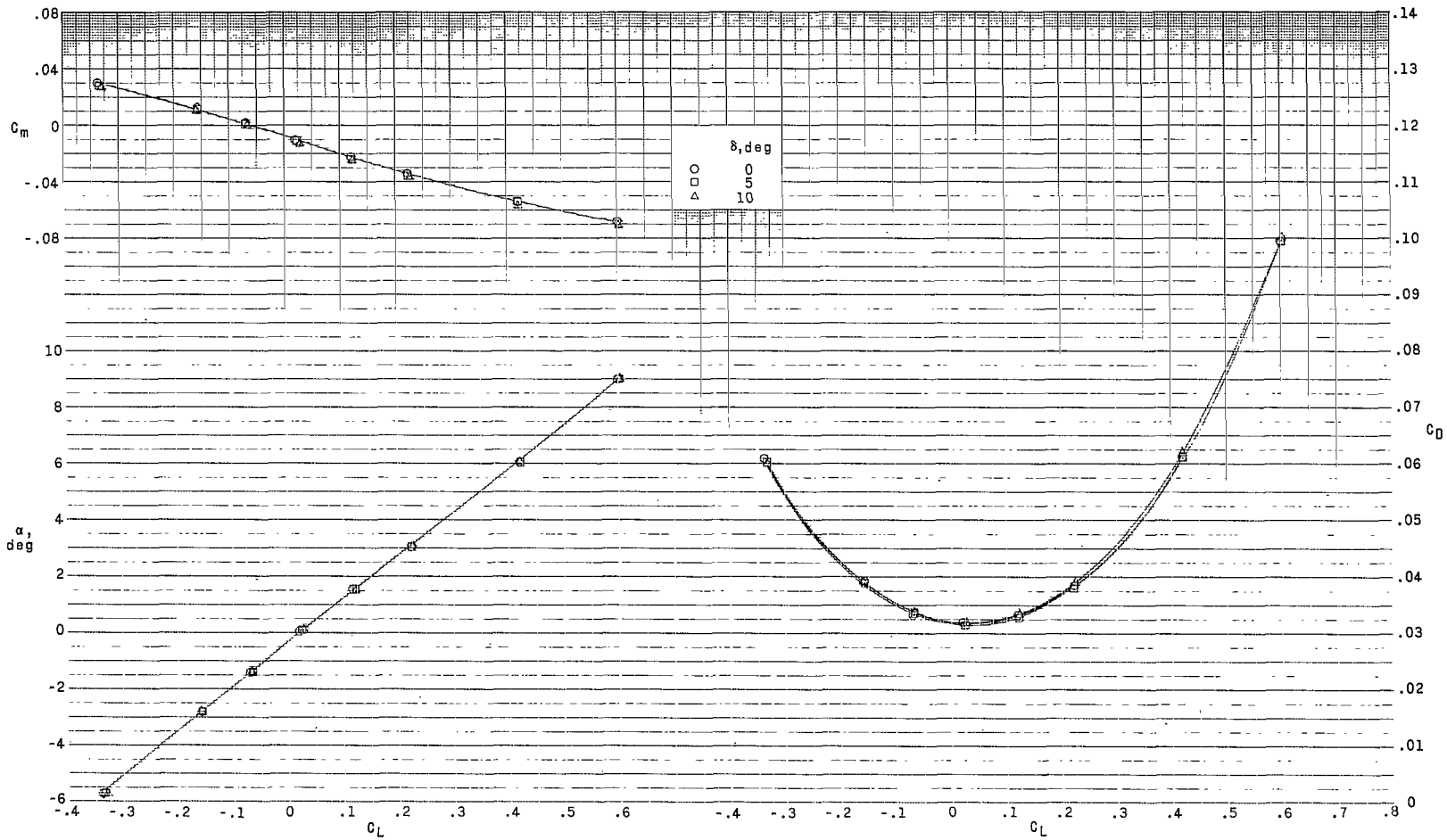

(b) Control B. $\gamma = 25^0$.

Figure 11.- Continued.

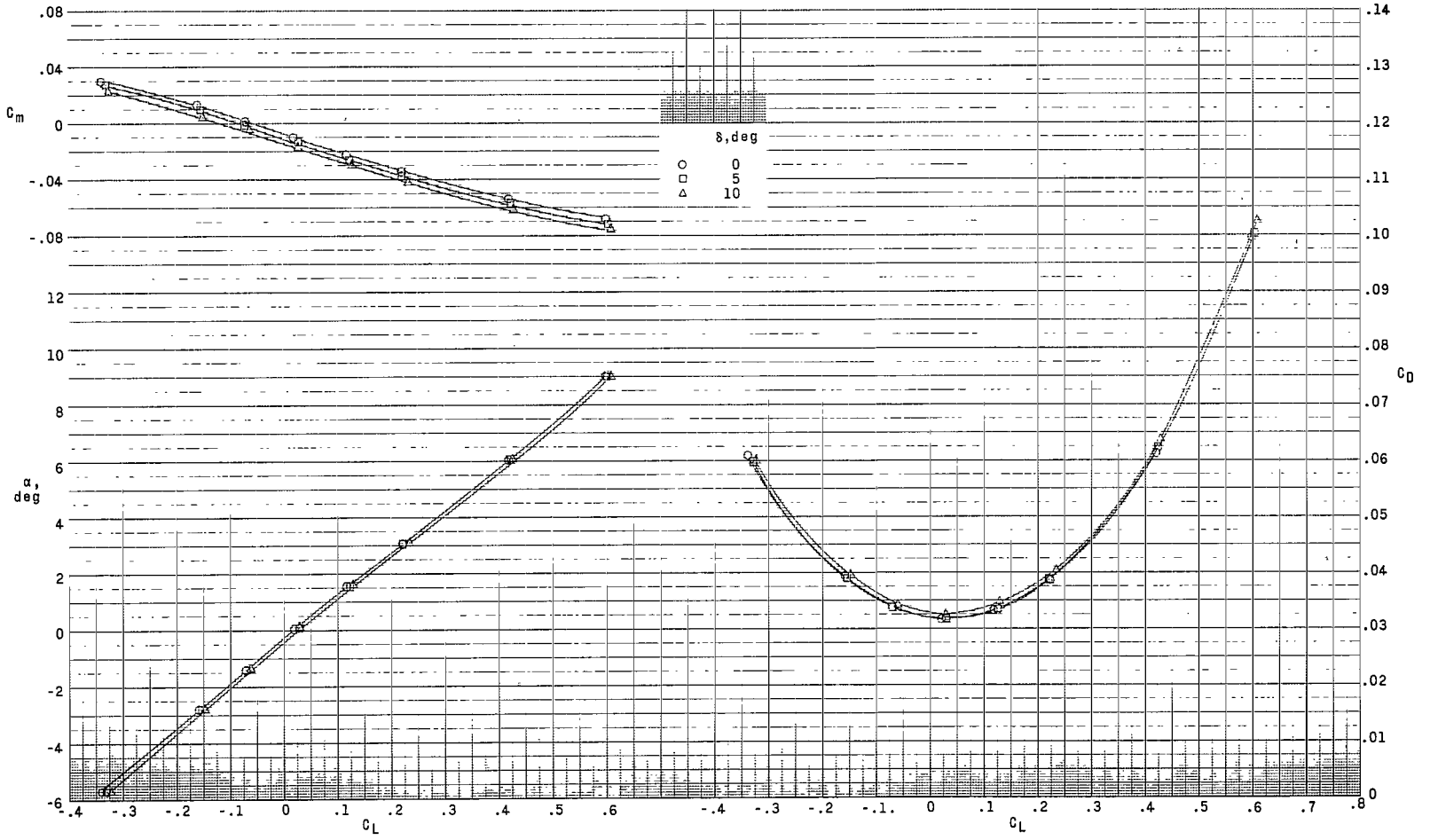

(c) Control C. $\gamma = 45^0$.

Figure 11.- Concluded.

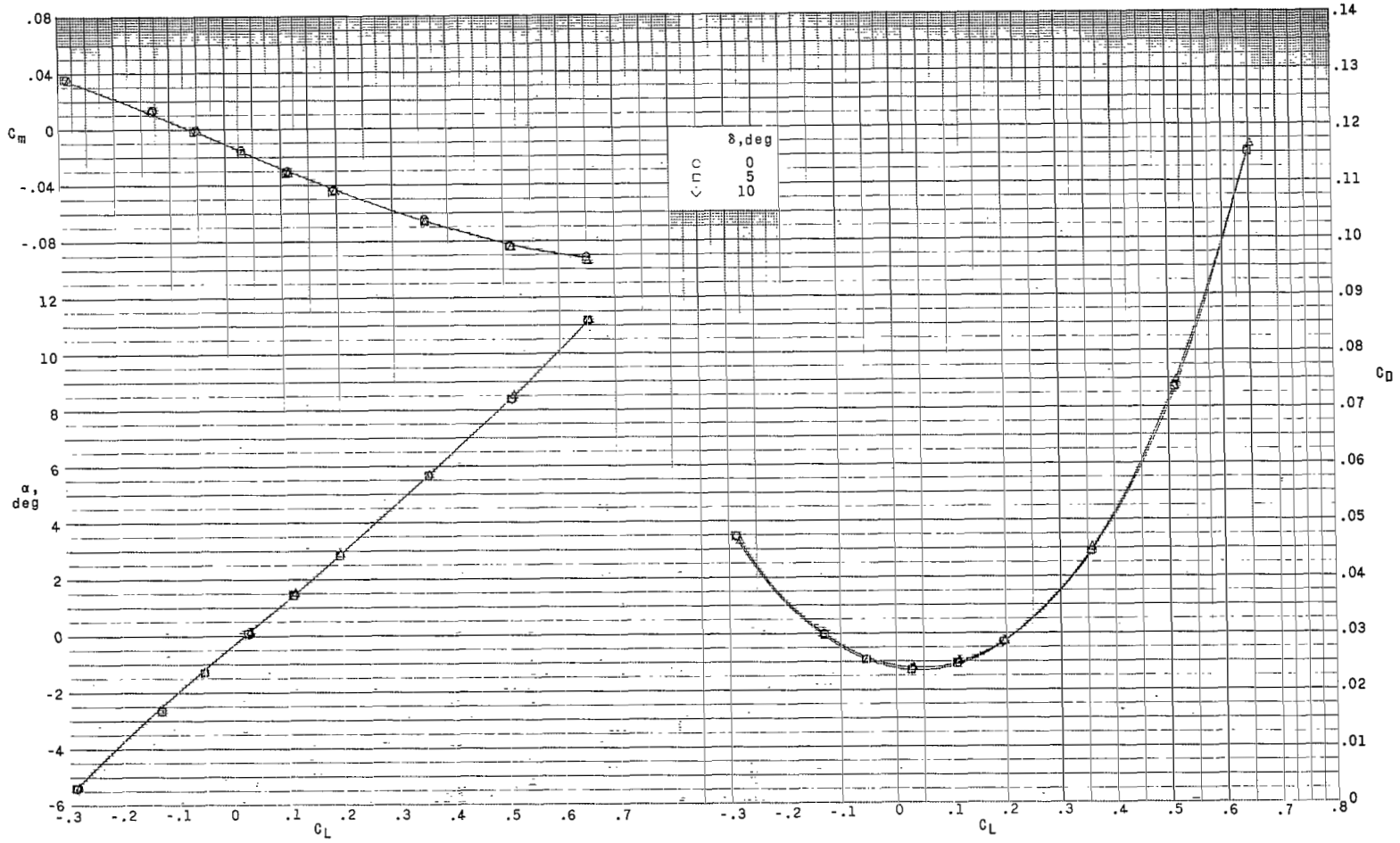

(a) Control A. $\gamma = 20^0$.

Figure 12.- Effect of control deflection on longitudinal aerodynamic characteristics. $\Lambda = 45^0$; $\beta = 0^0$; $M = 1.20$.

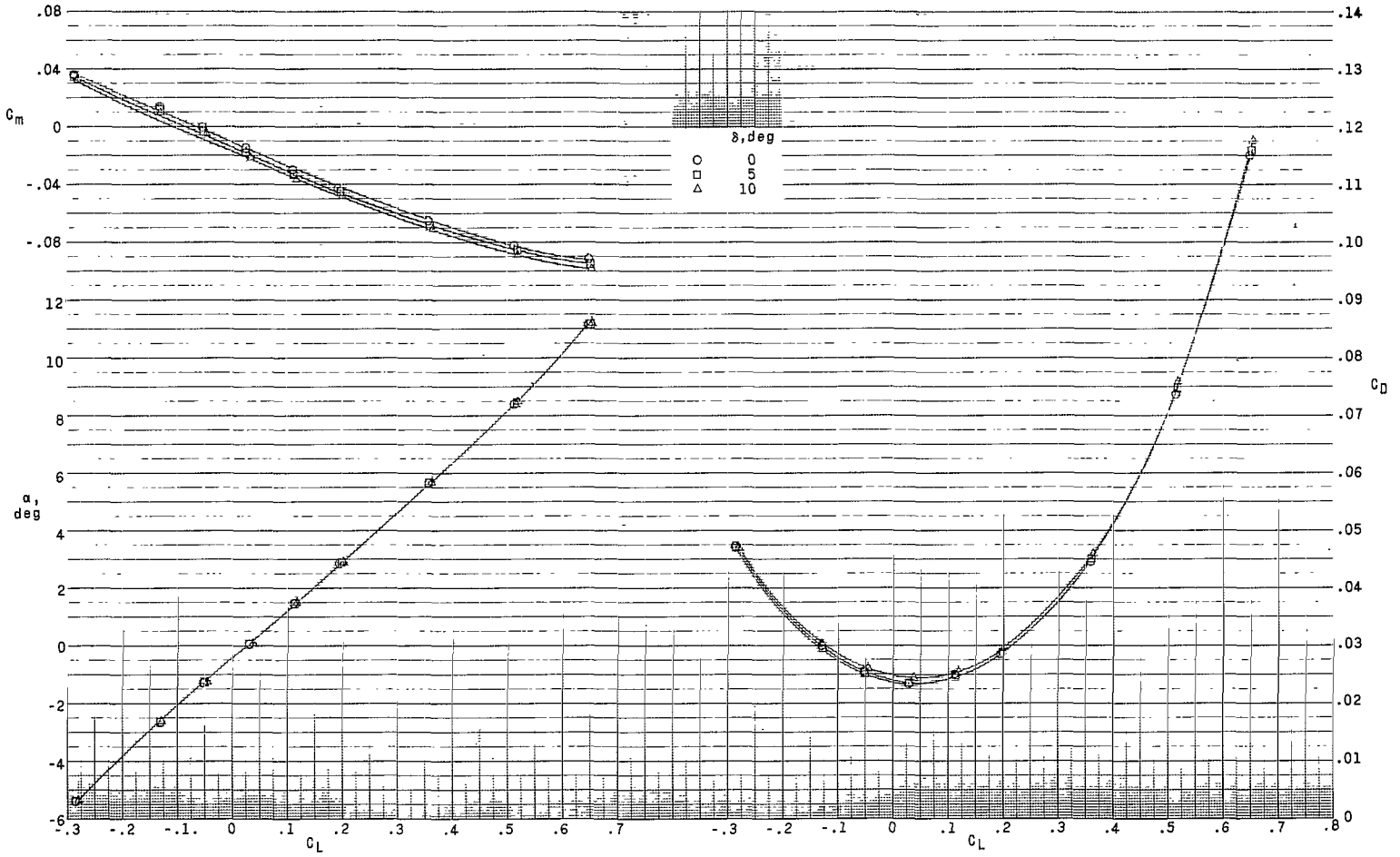

(b) Control B. $\gamma = 40^{\circ}$.

Figure 12.- Continued.

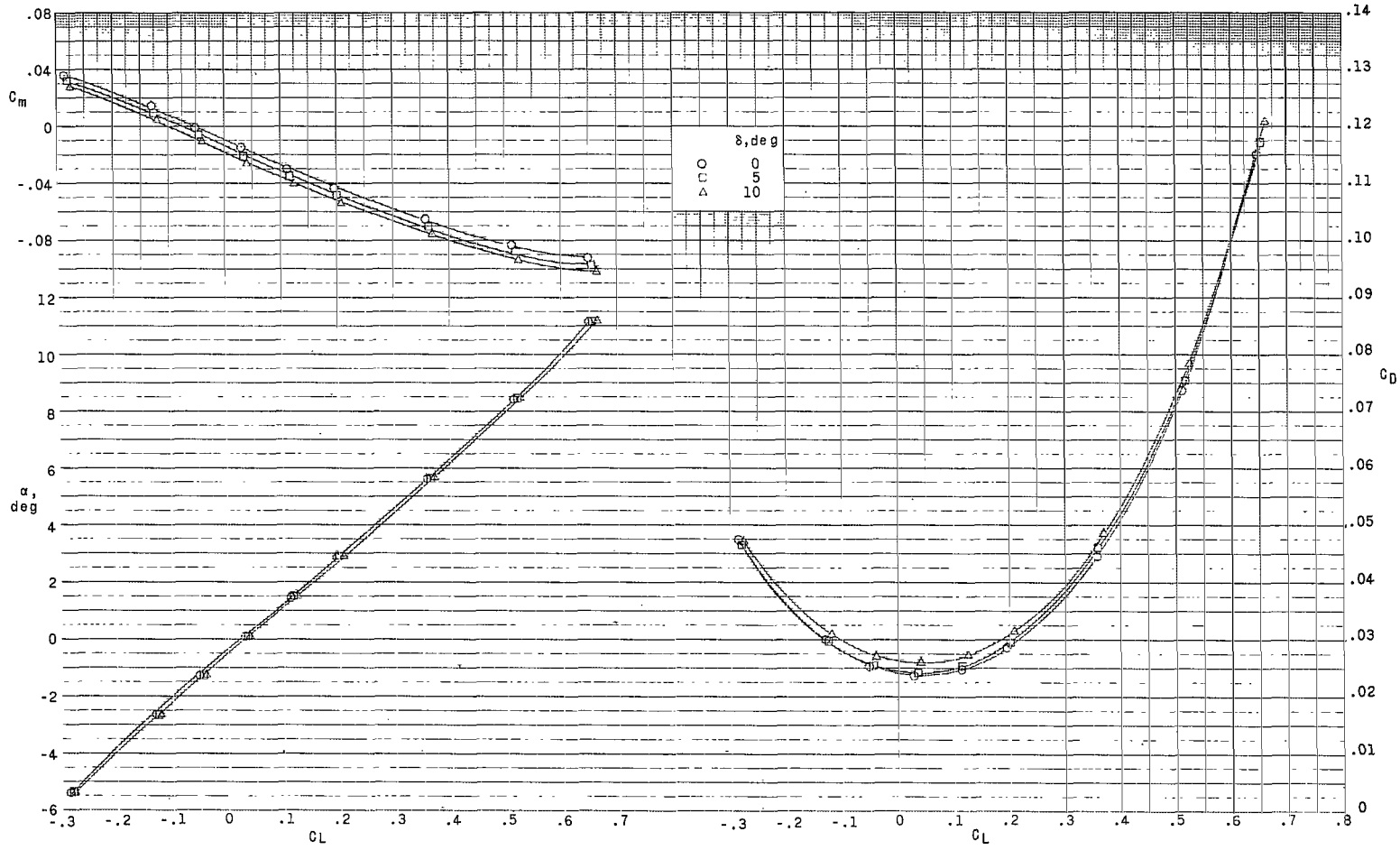

(c) Control C. $\gamma = 60^0$.

Figure 12.- Concluded.

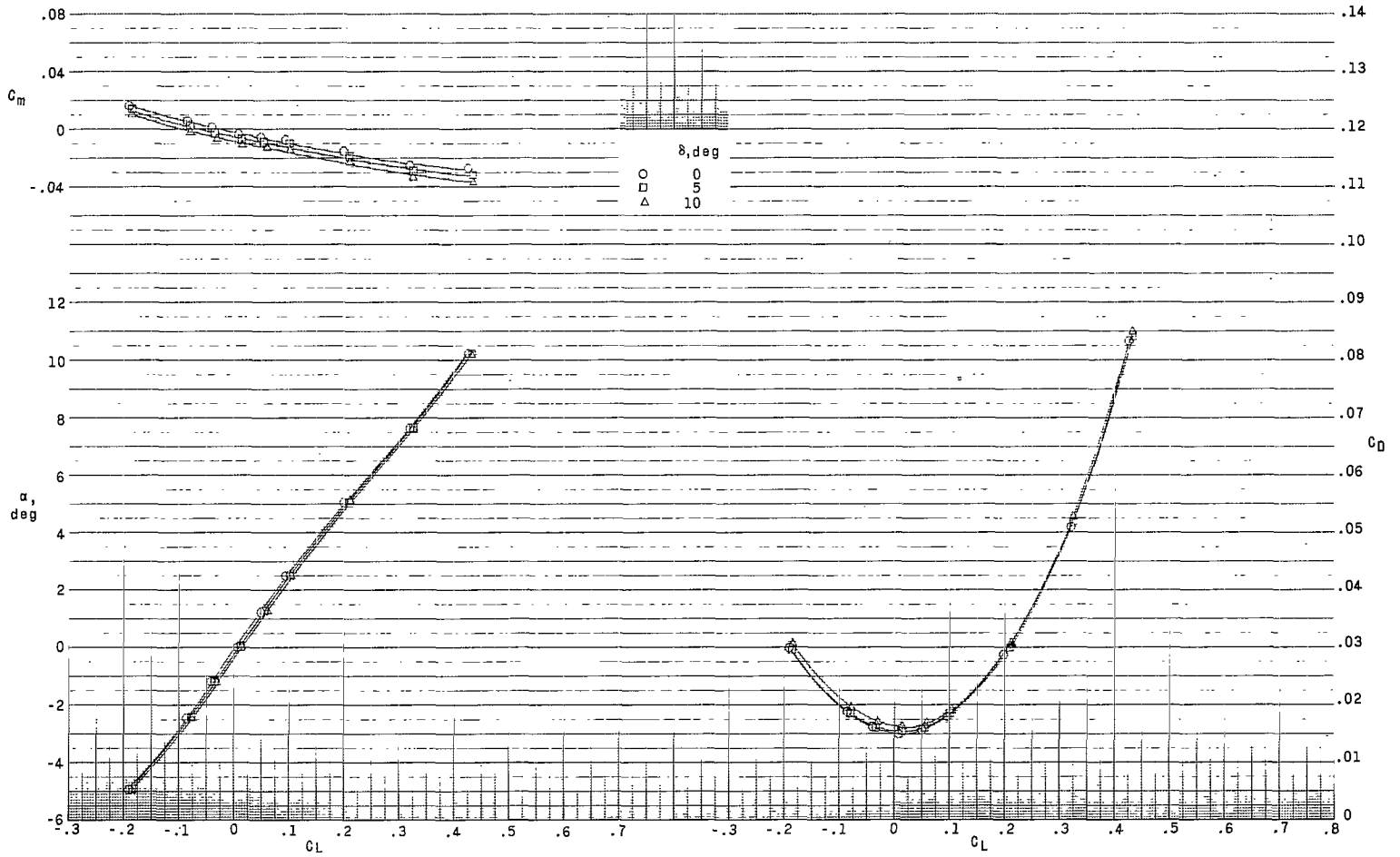

(a) Control A. $\gamma = 50^0$.

Figure 13.- Effect of control deflection on longitudinal aerodynamic characteristics. $\Lambda = 75^0$; $\beta = 0^0$; M = 1.20.

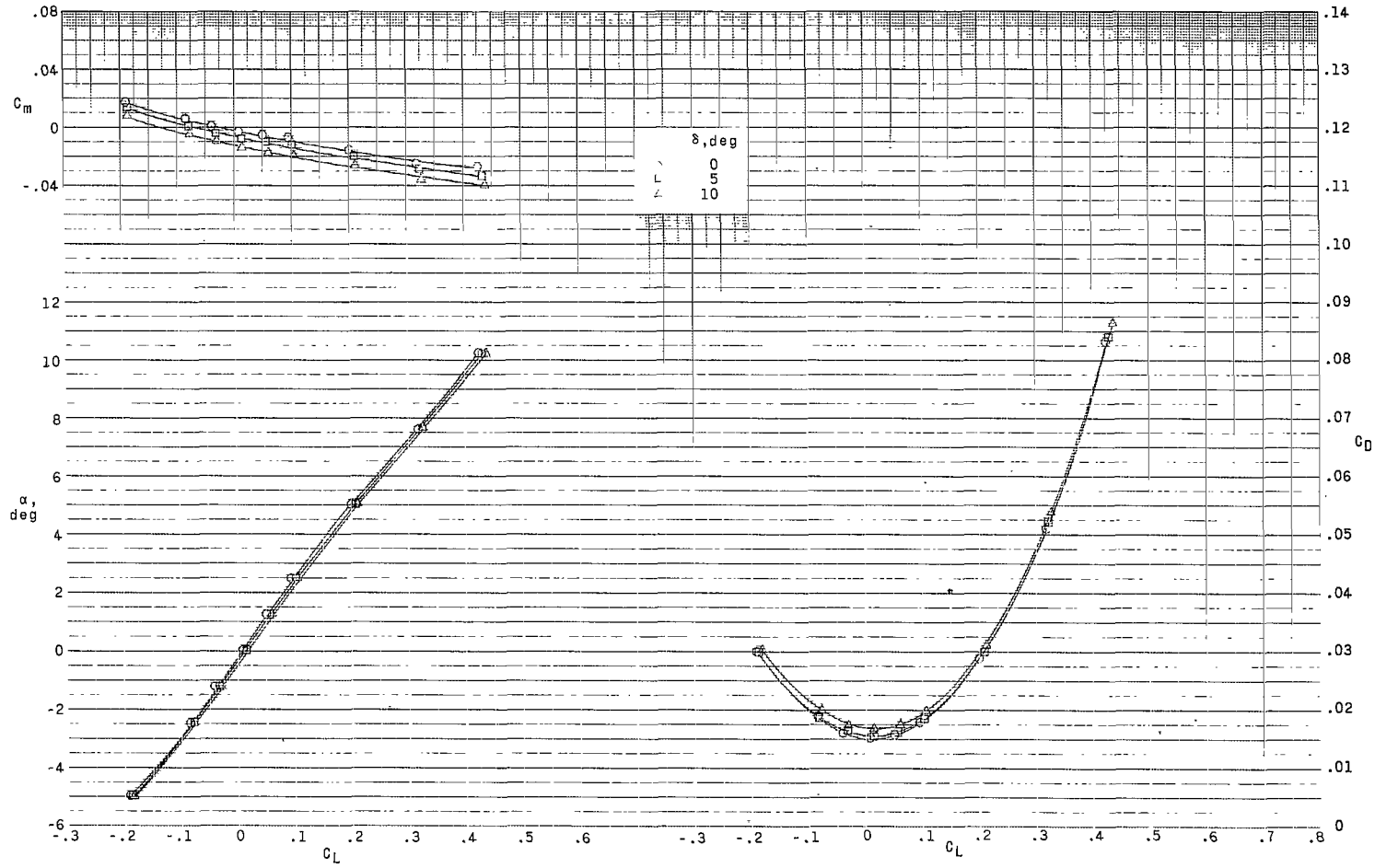

(b) Control B. $\gamma = 70^0$.

Figure 13.- Continued.

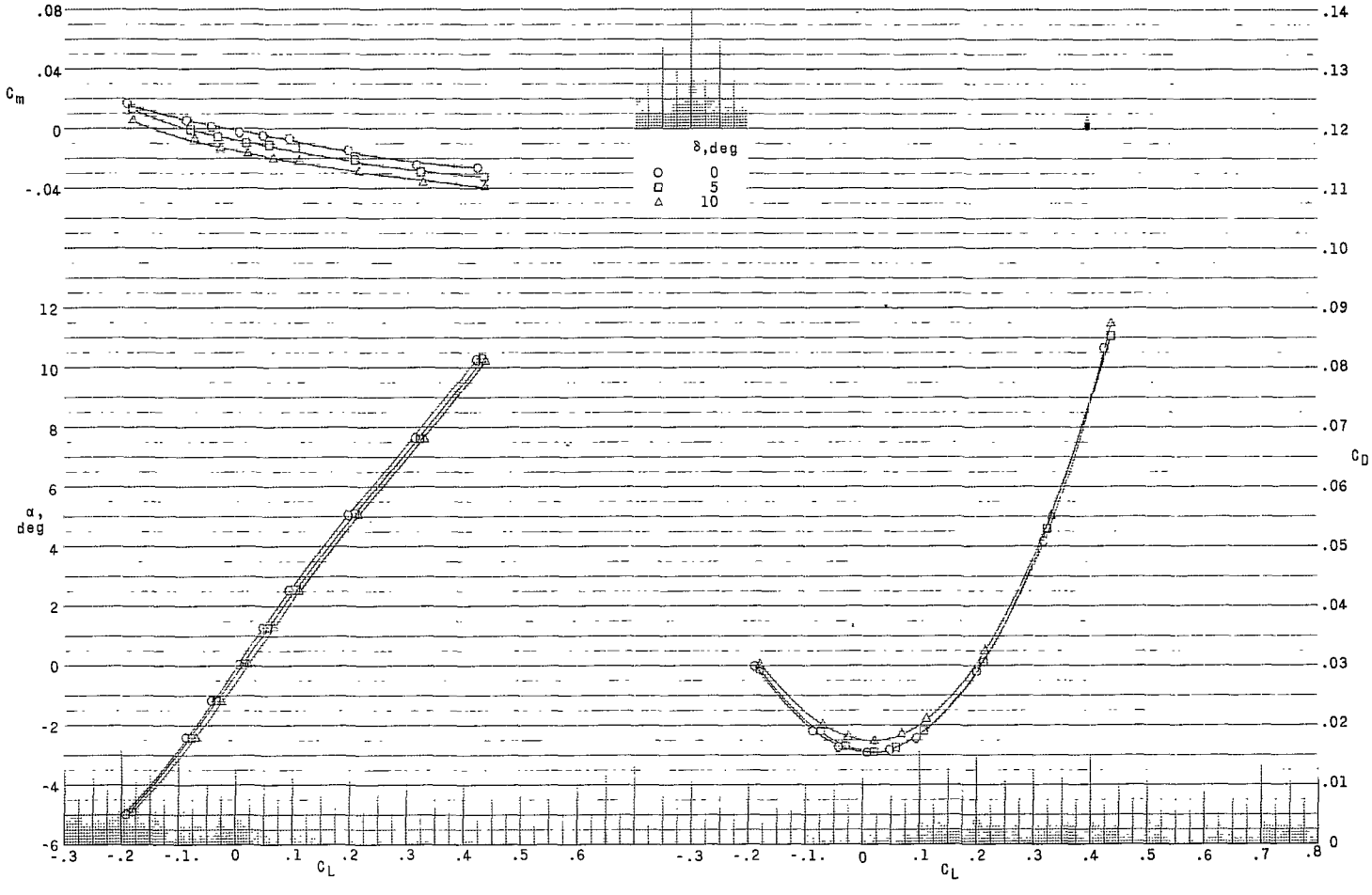

(c) Control C. $\gamma = 90^0$.

Figure 13.- Concluded.

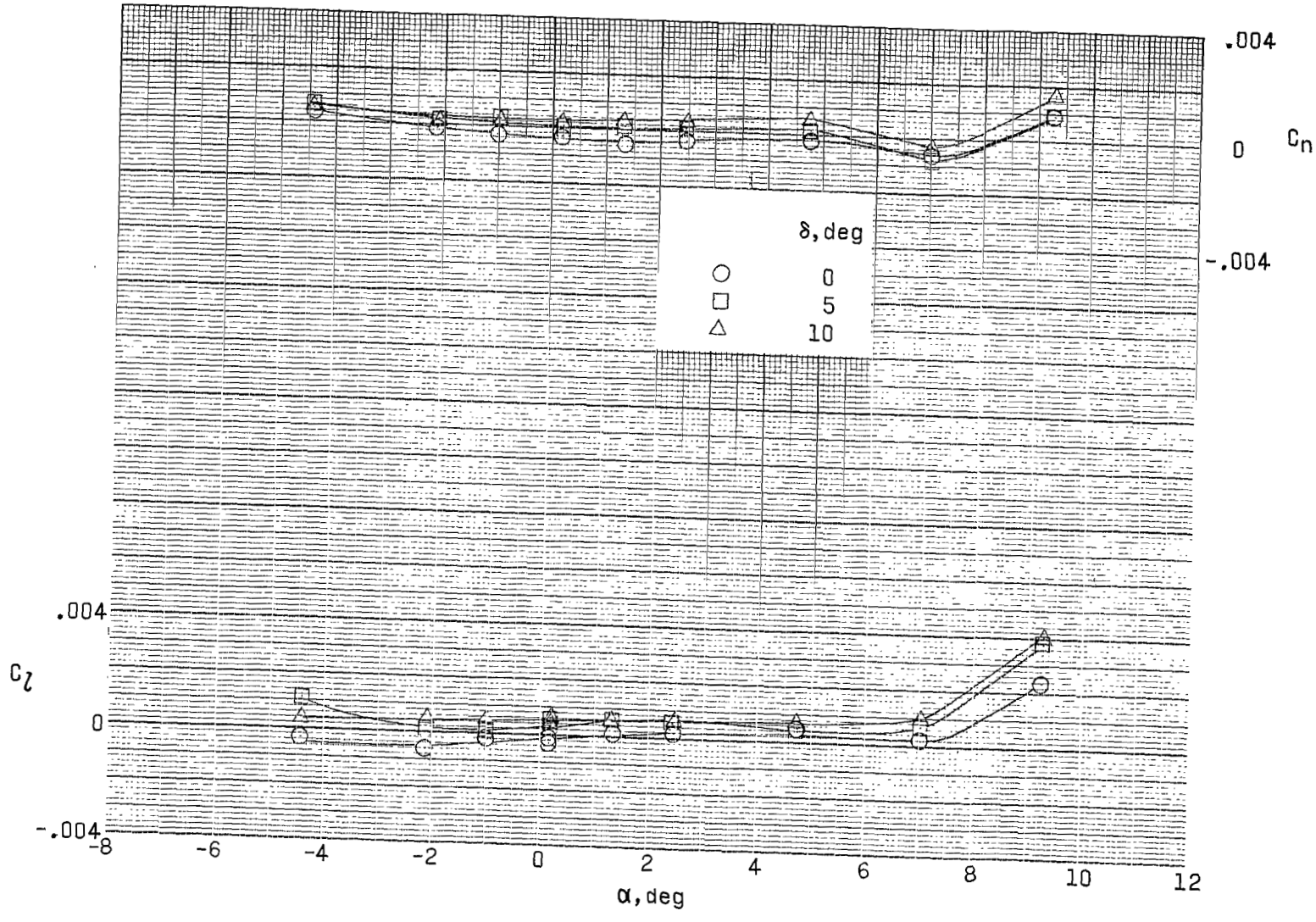

(a) Control A. $\gamma = 5^0$.

Figure 14.- Effect of control deflection on lateral aerodynamic characteristics. $\Lambda = 30^0$; $\beta = 0^0$; $M = 0.50$.

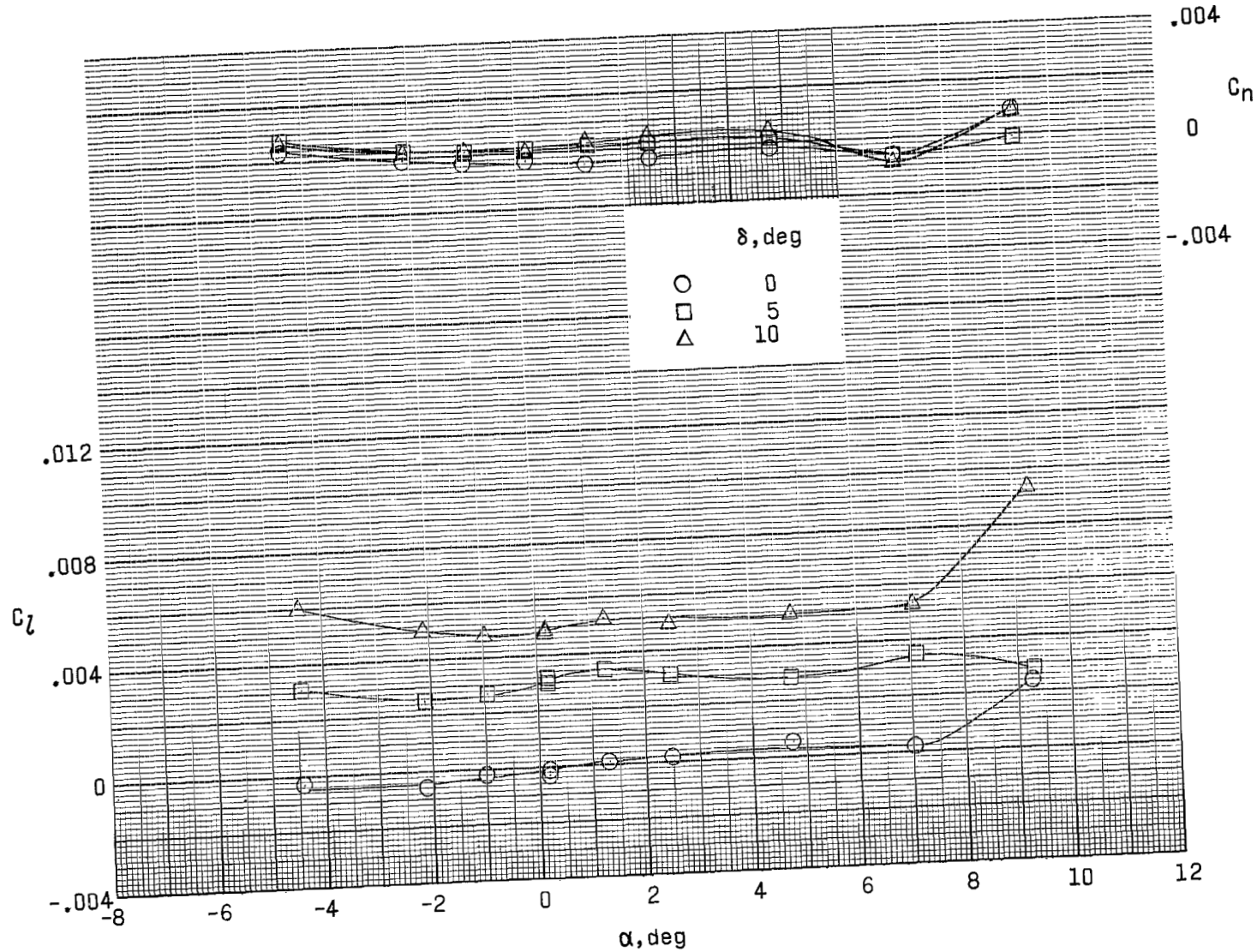

(b) Control B. $\gamma = 25^0$.

Figure 14.- Continued.

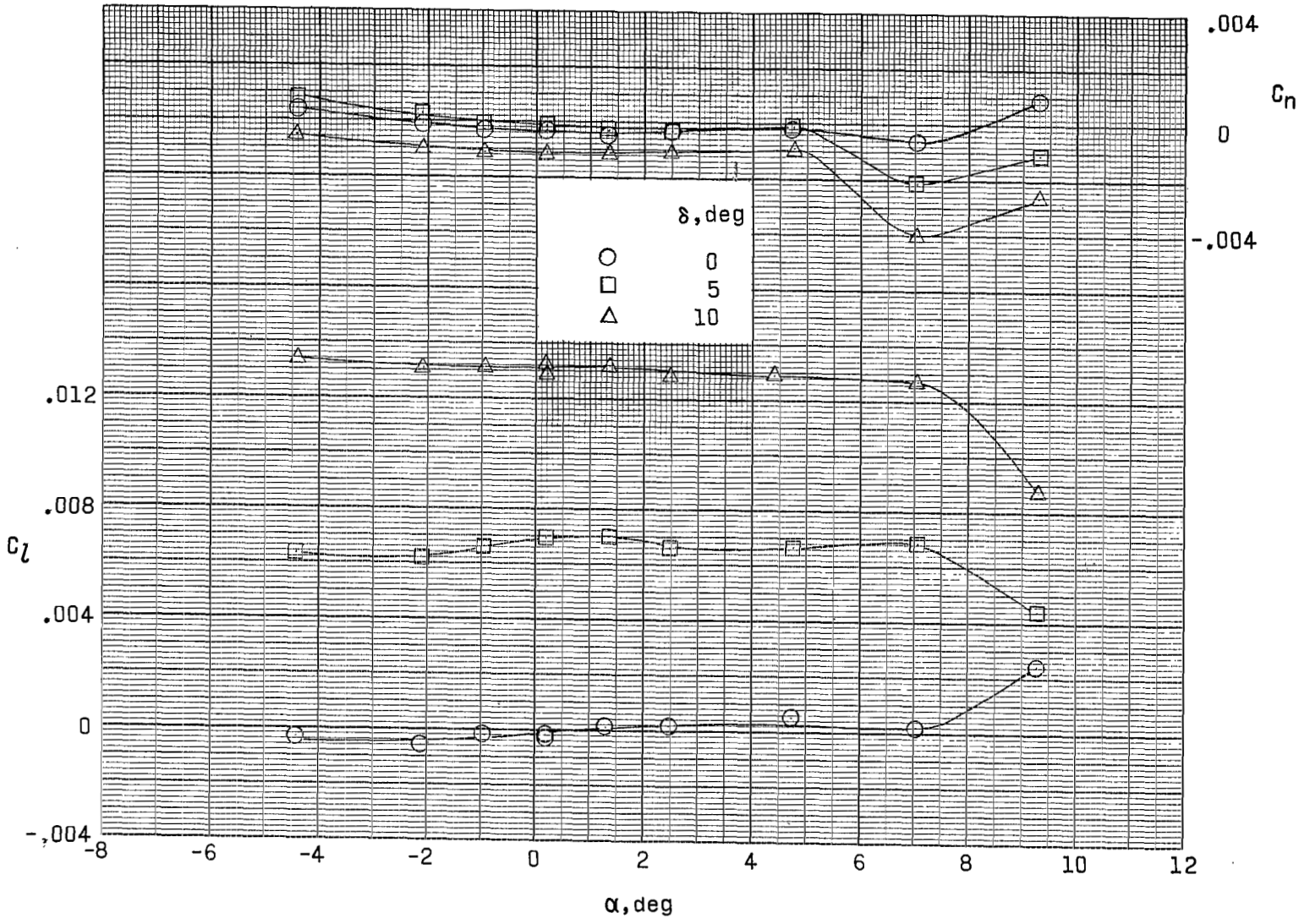

(c) Control C. $\gamma = 45^{0}$.

Figure 14.- Concluded.

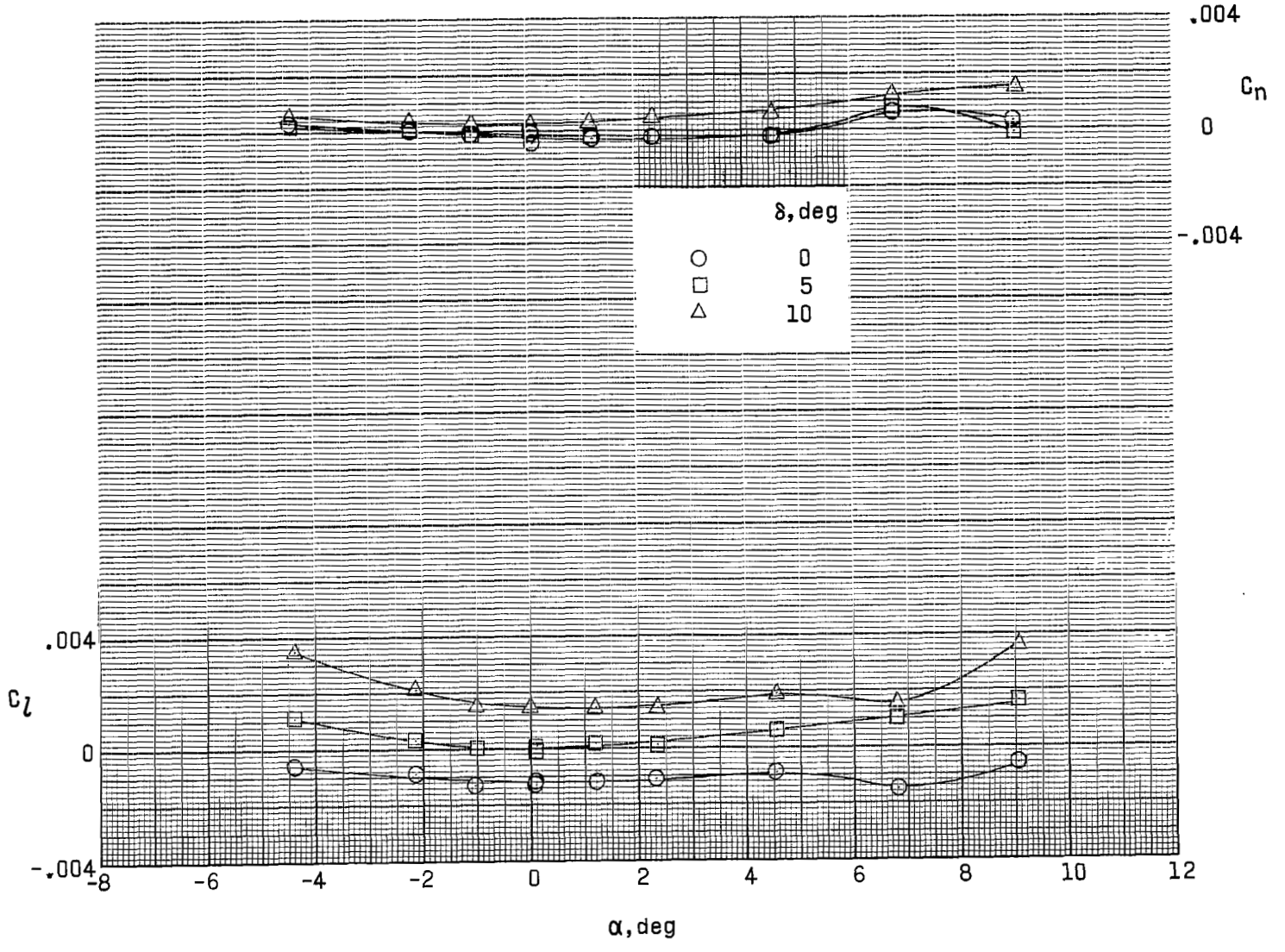

(a) Control A. $\gamma = 20^0$.

Figure 15.- Effect of control deflection on lateral aerodynamic characteristics. $\Lambda = 45^0$; $\beta = 0^0$; $M = 0.50$.

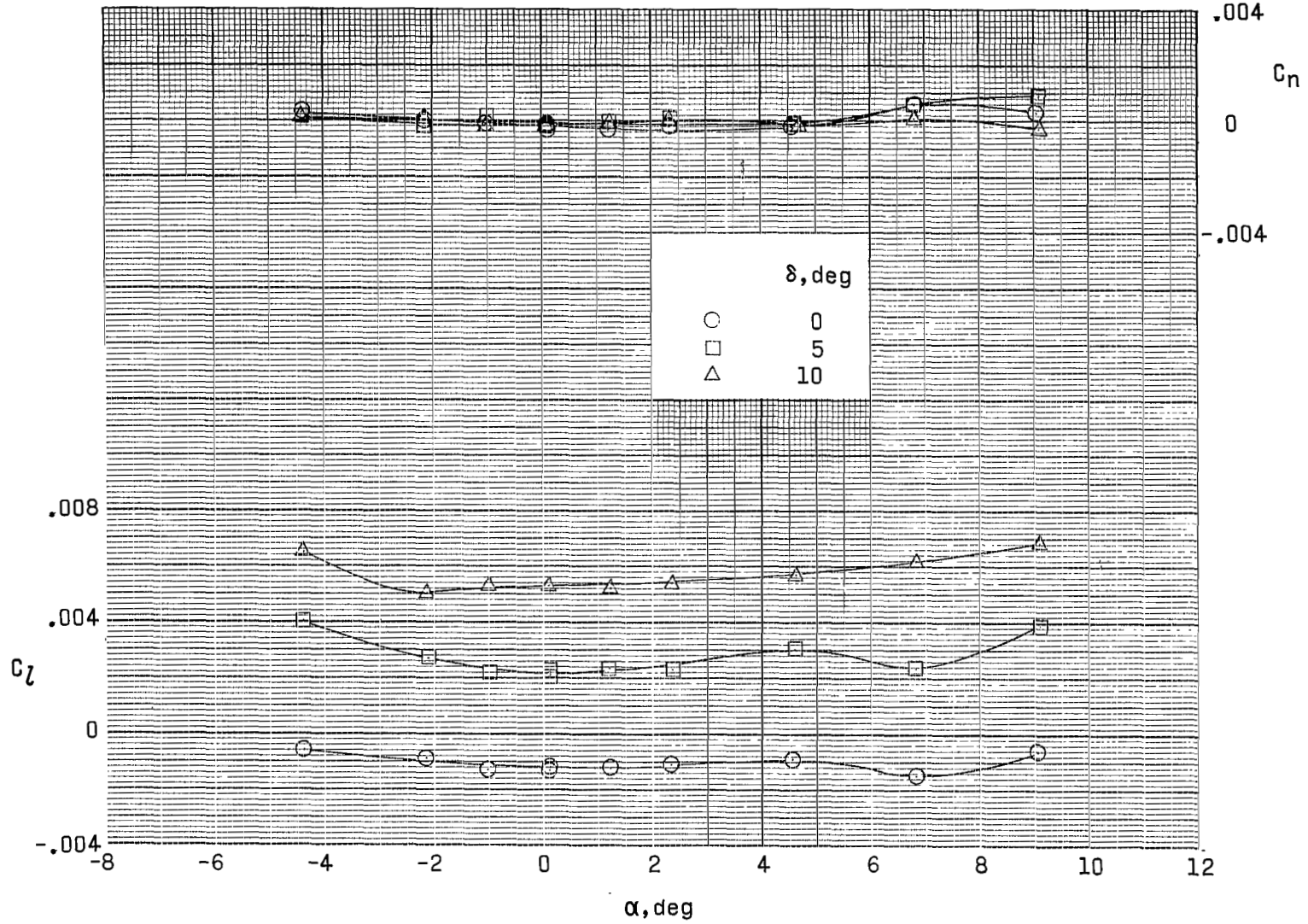

(b) Control B. $\gamma = 40^0$.

Figure 15.- Continued.

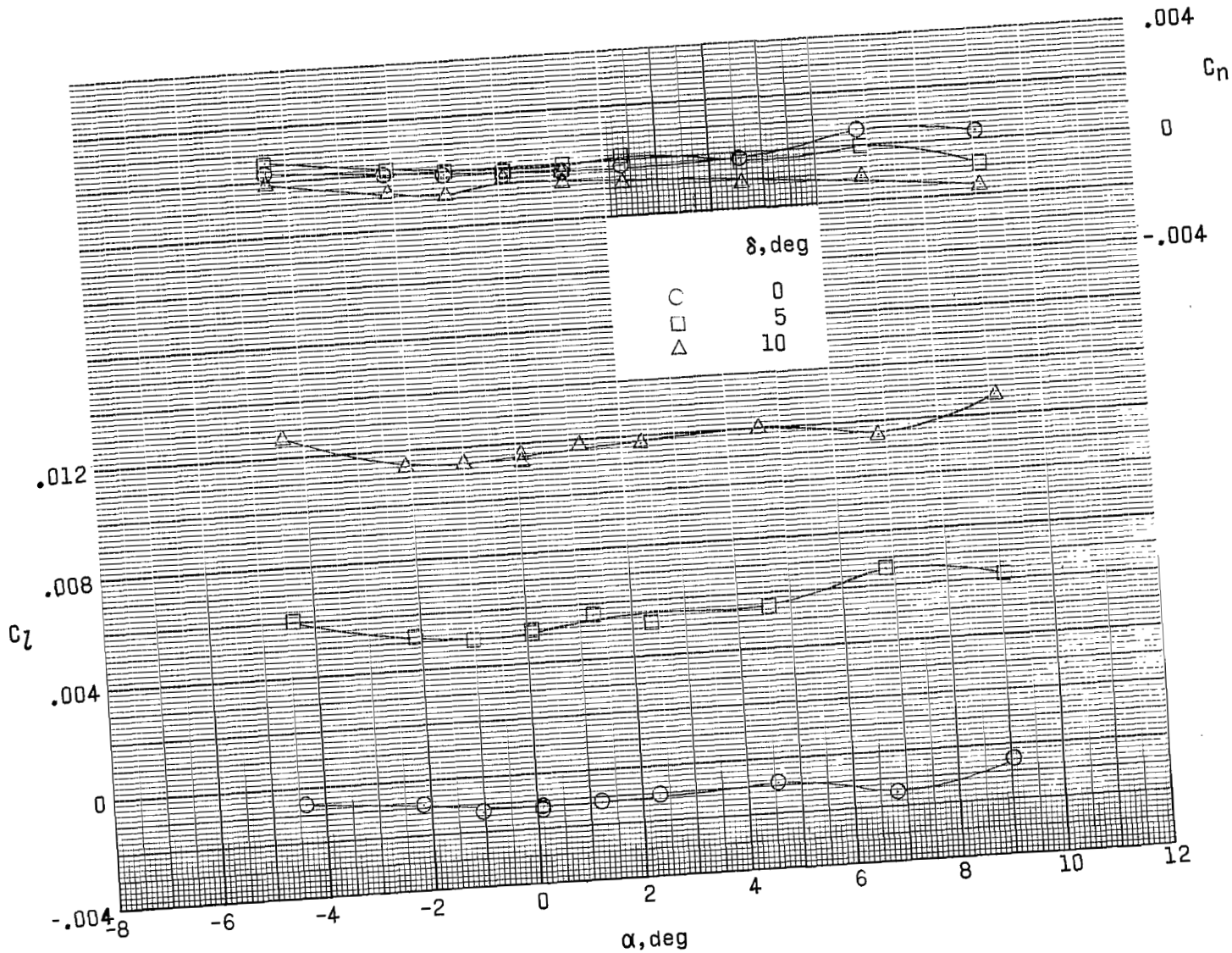

(c) Control C. $\gamma = 60^{o}$.

Figure 15.- Concluded.

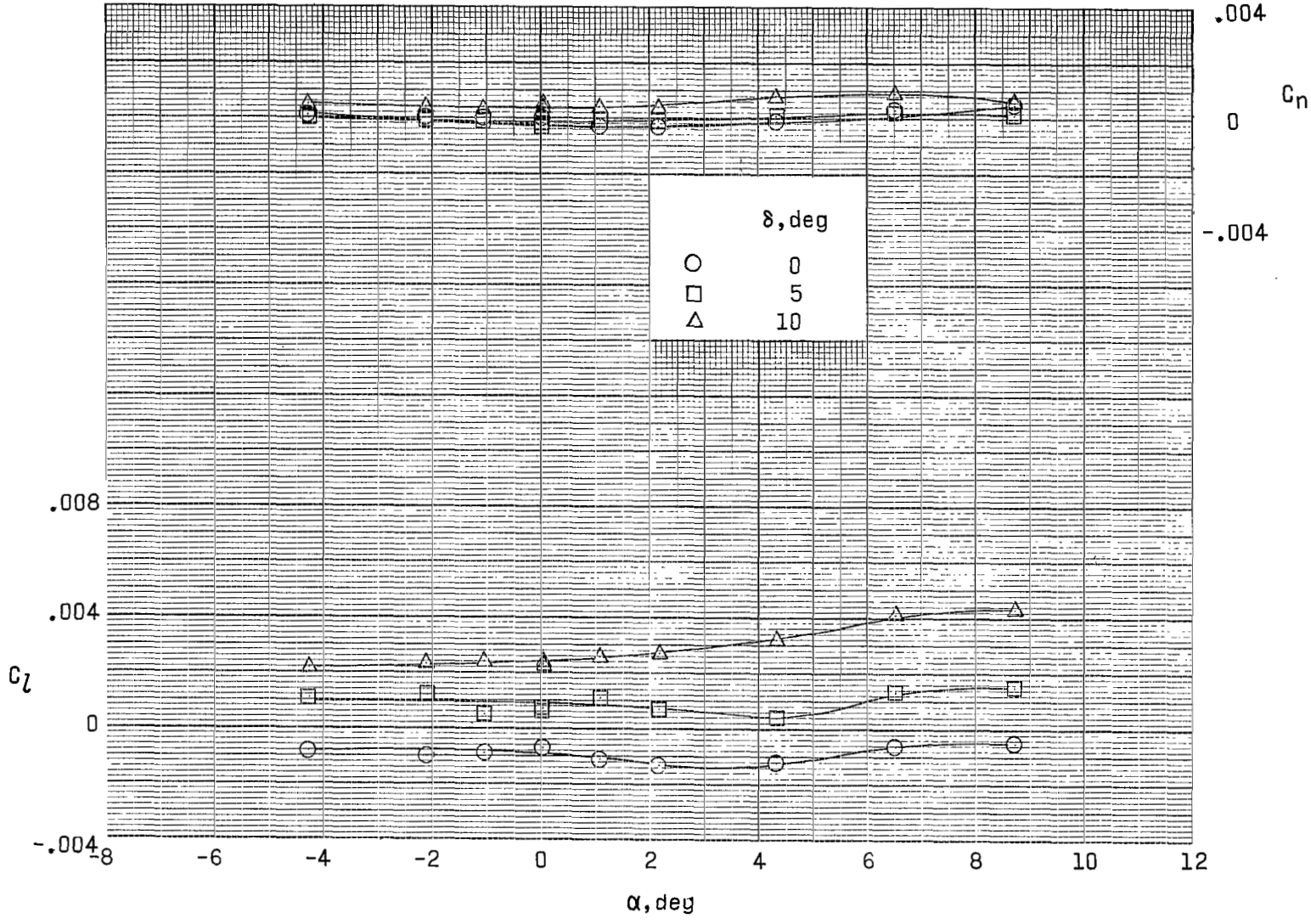

(a) Control A. $\gamma = 50^{0}$.

Figure 16.- Effect of control deflection on lateral aerodynamic characteristics. $\Lambda = 75^{0}$; $\beta = 0^{0}$; $M = 0.50$.

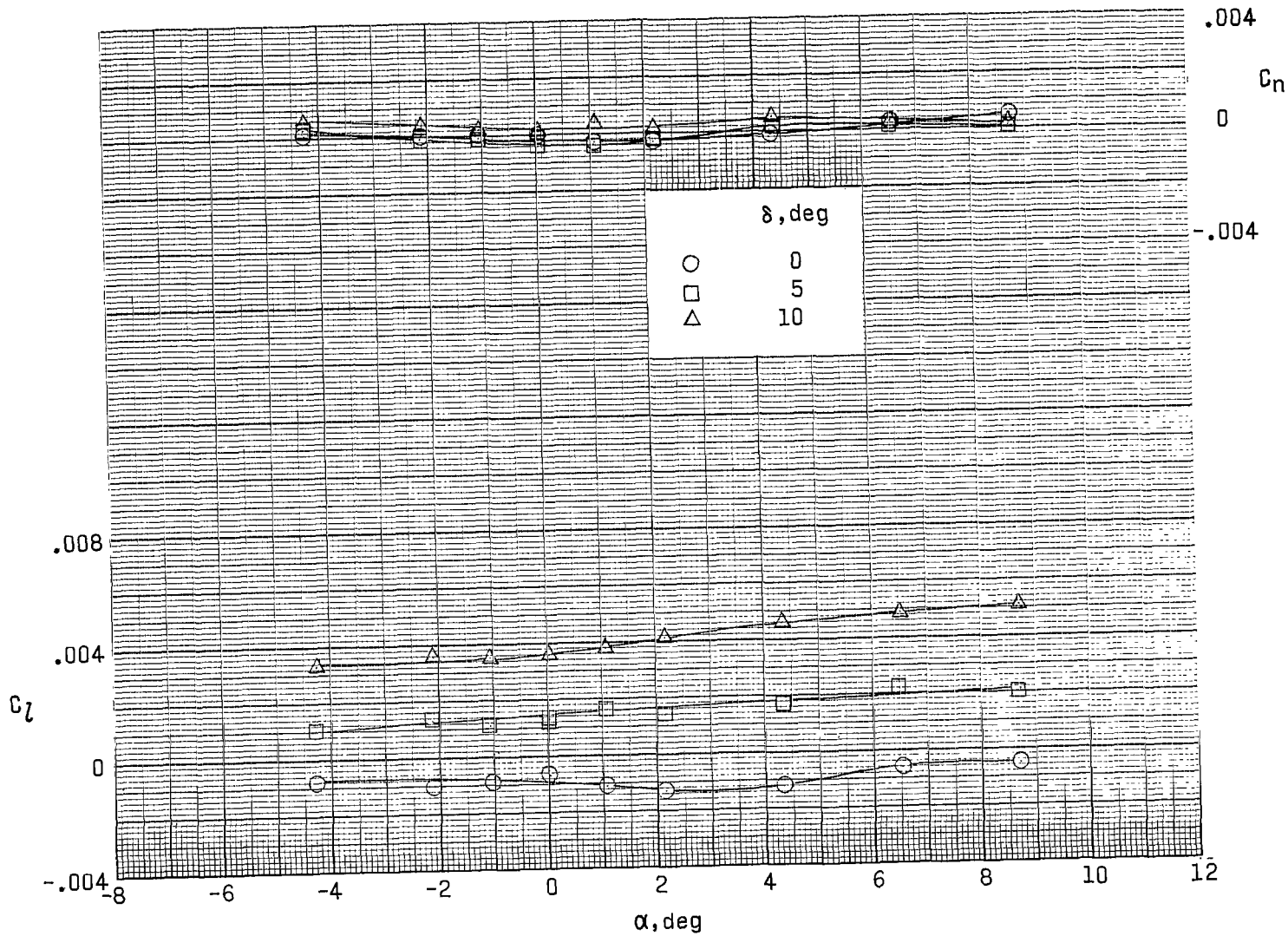

(b) Control B. $\gamma = 70^{0}$.

Figure 16.- Continued.

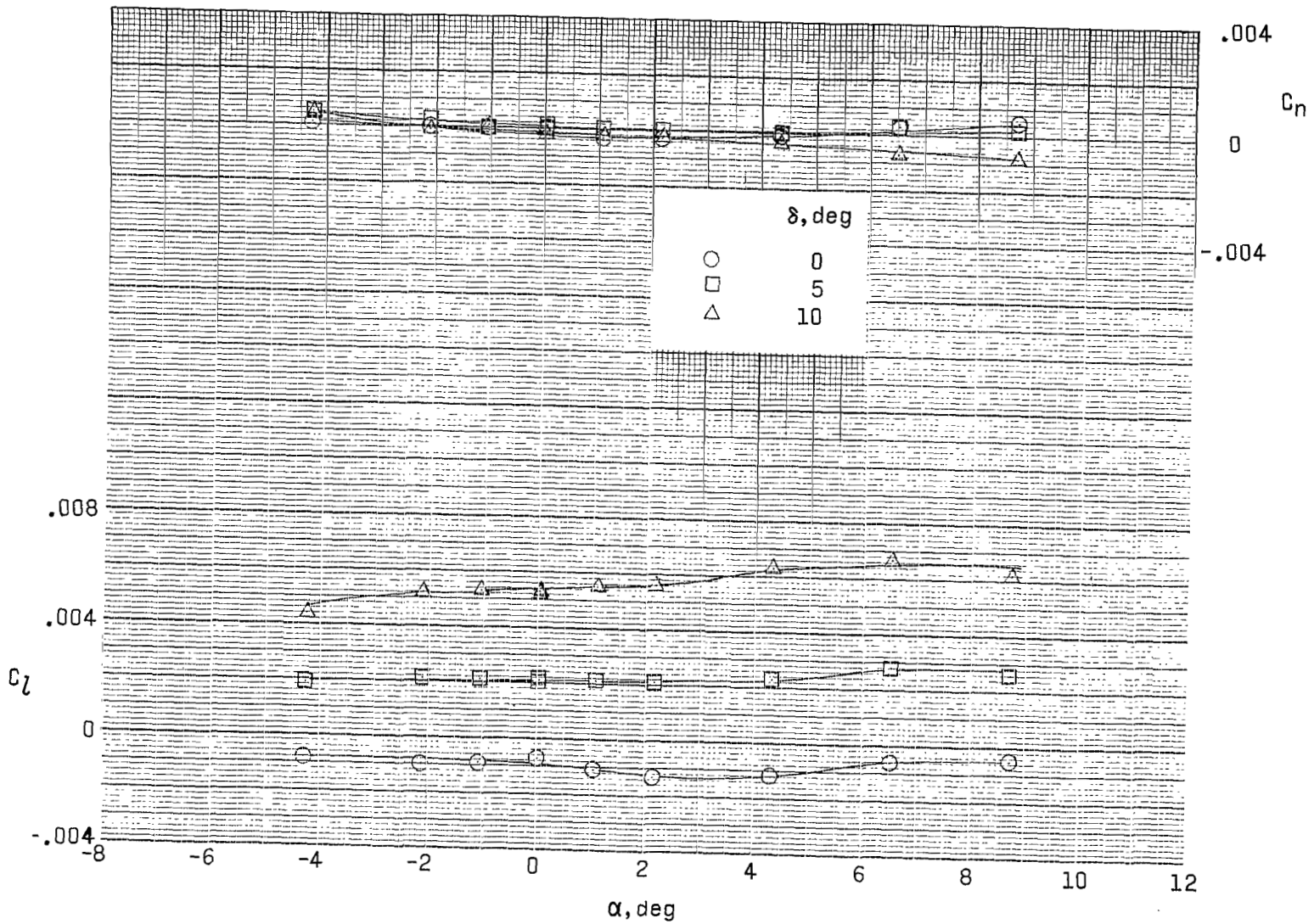

(c) Control C. $\gamma = 90^{\circ}$.

Figure 16.- Concluded.

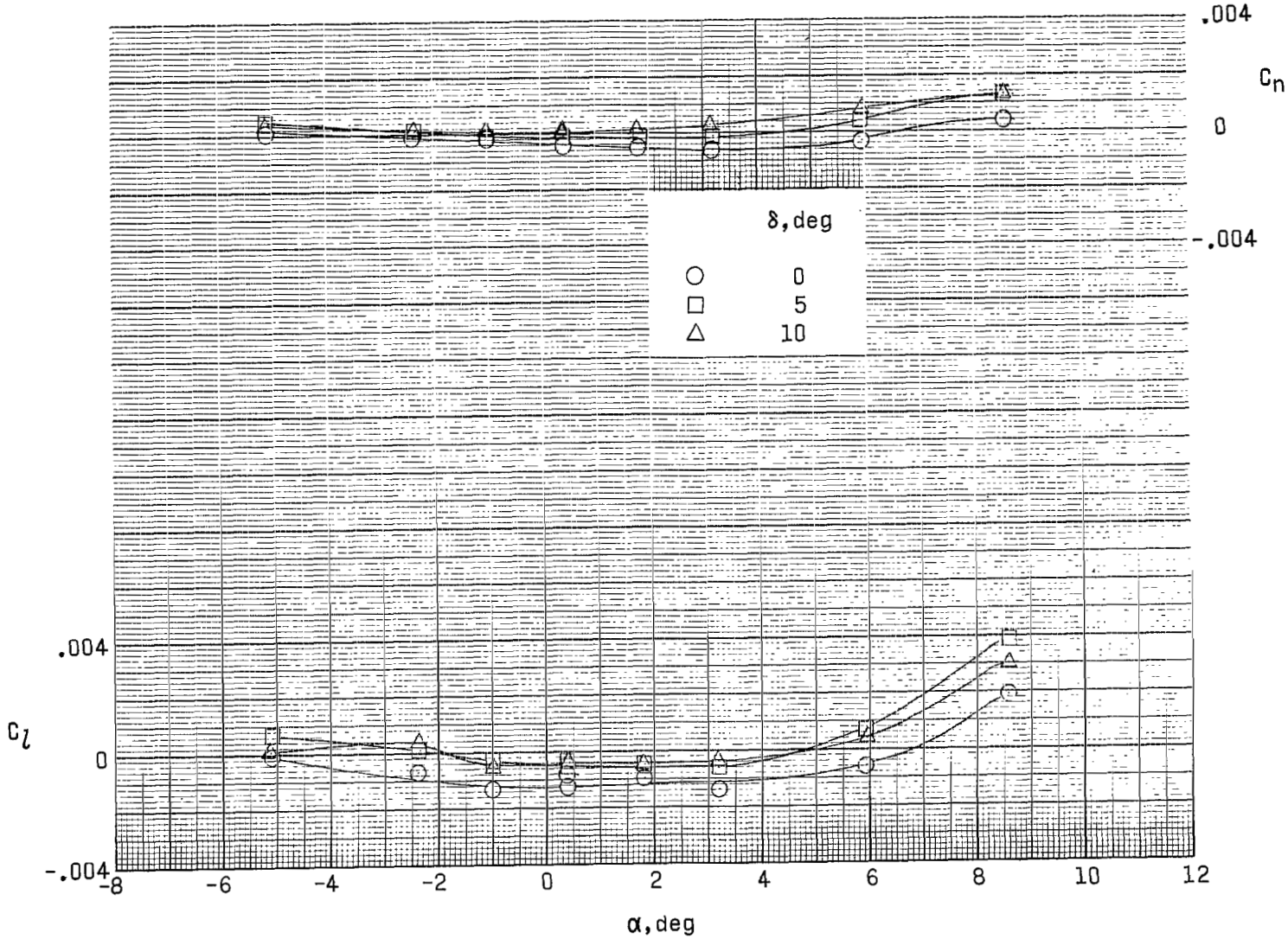

(a) Control A. $\gamma = 5^{o}$.

Figure 17.- Effect of control deflection on lateral aerodynamic characteristics. $\Lambda = 30^{o}$; $\beta = 0^{o}$; $M = 0.80$.

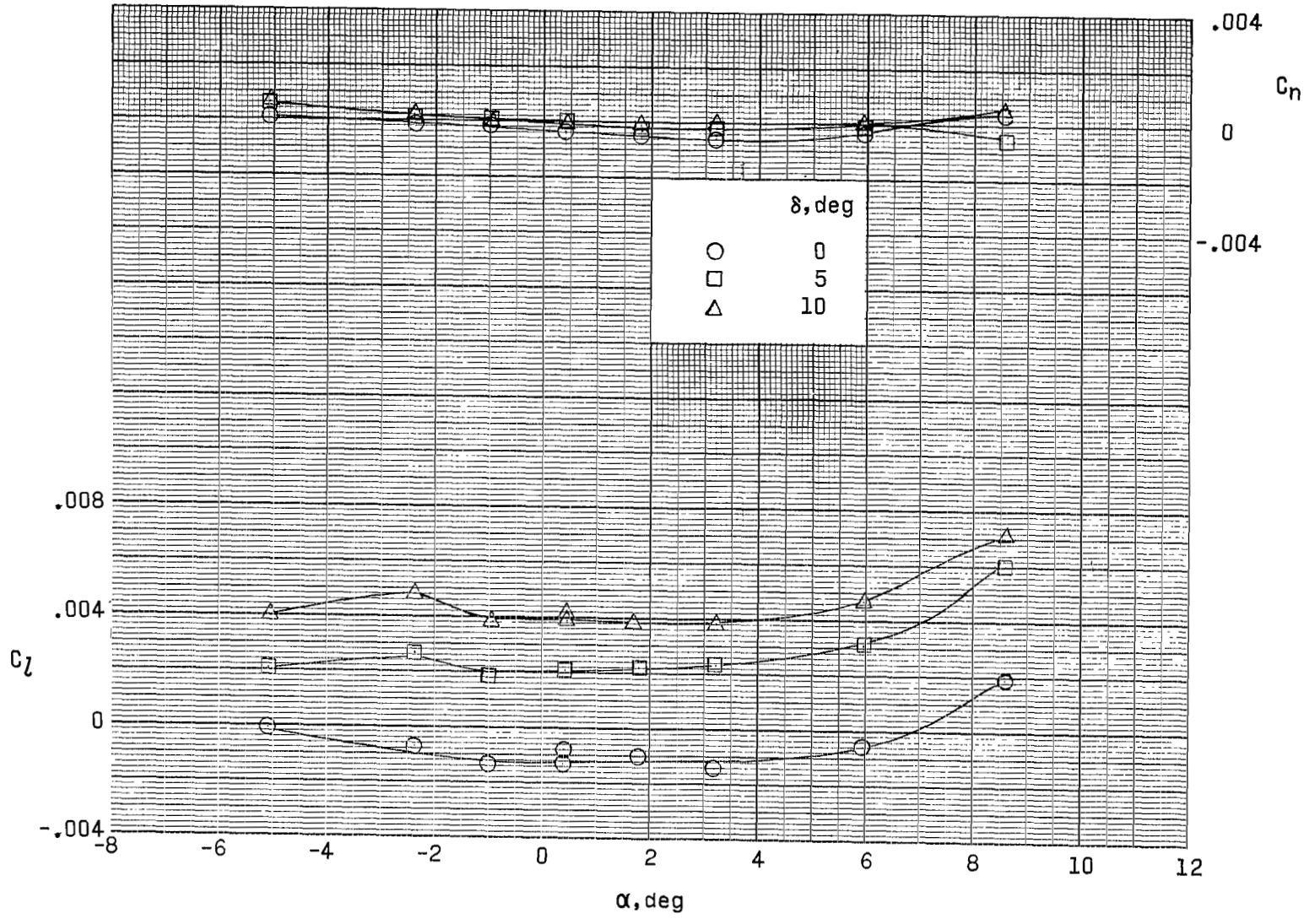

(b) Control B. $\gamma = 25^0$.

Figure 17.- Continued.

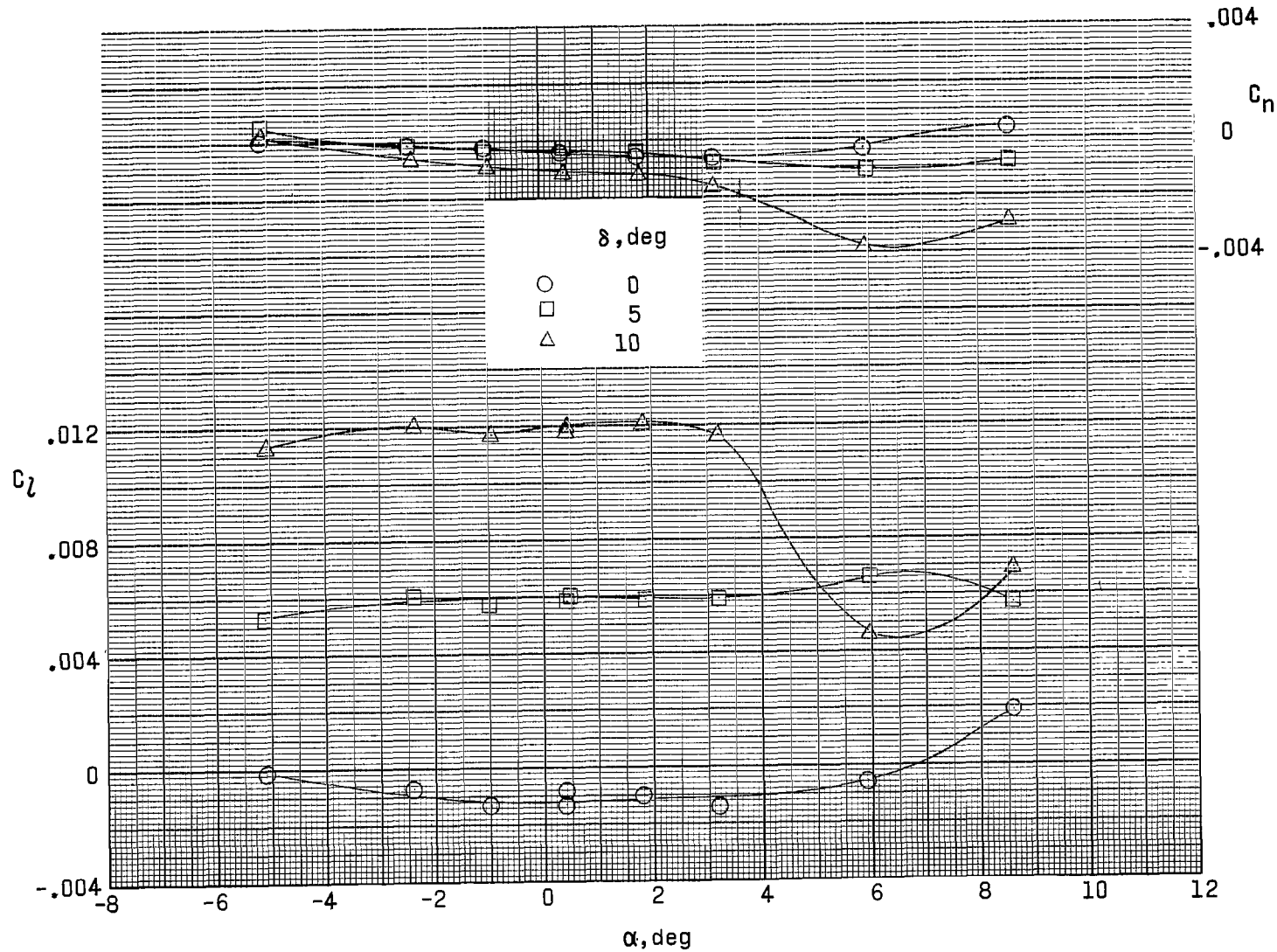

(c) Control C. $\gamma = 45^{\circ}$.

Figure 17.- Concluded.

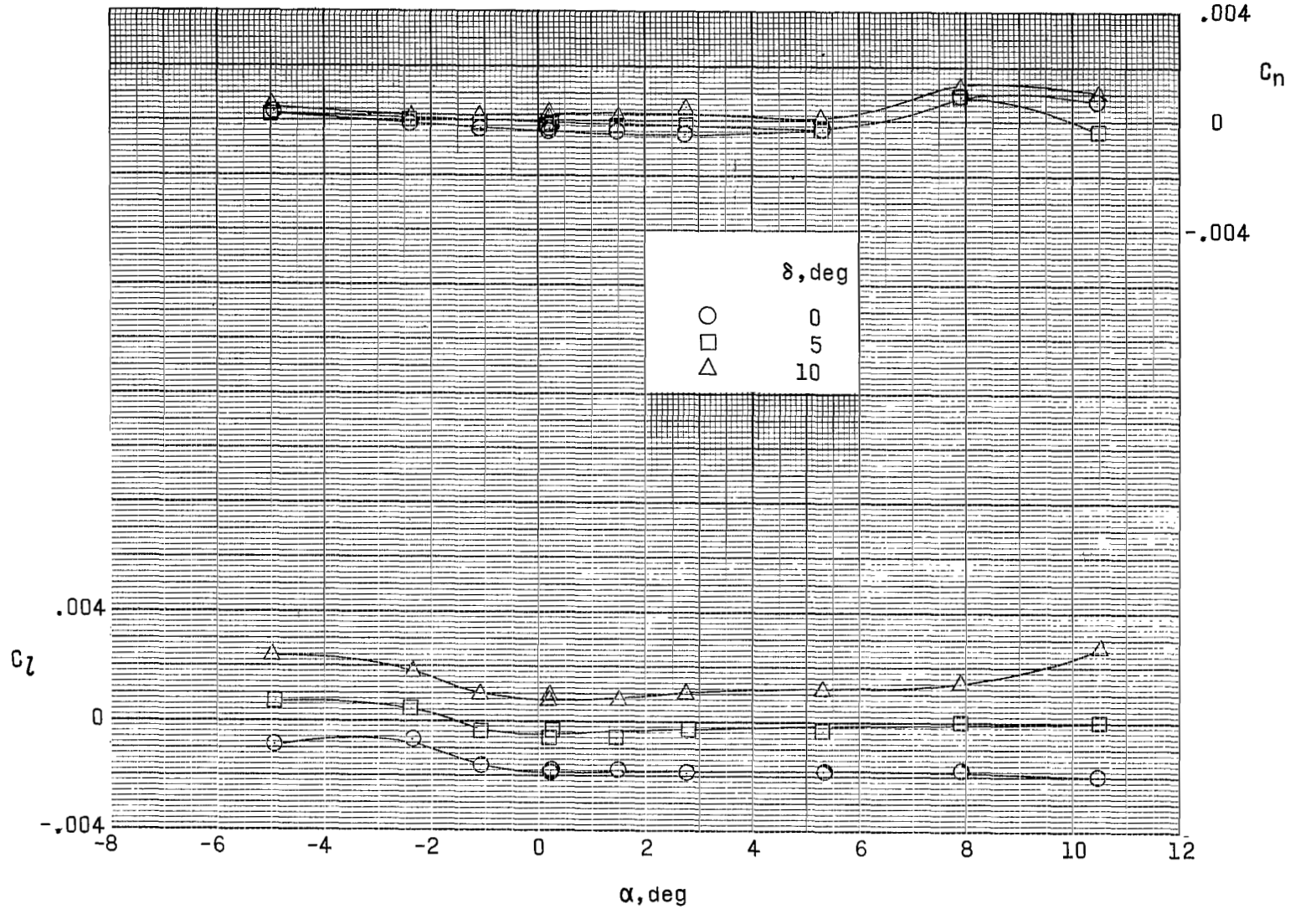

(a) Control A. $\gamma = 20^0$.

Figure 18.- Effect of control deflection on lateral aerodynamic characteristics. $\Lambda = 45^0$; $\beta = 0^0$; $M = 0.80$.

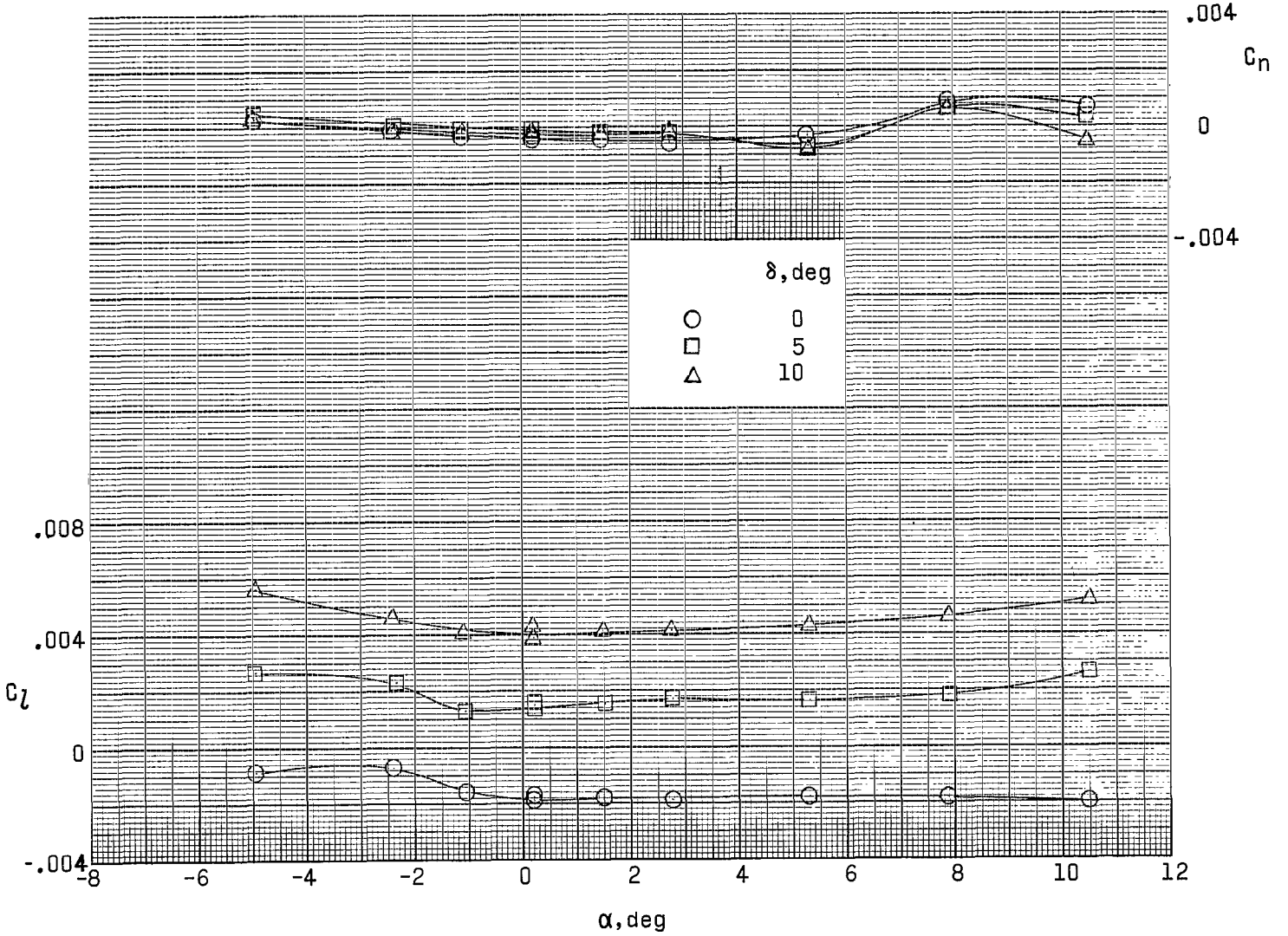

(b) Control B. $\gamma = 40^0$.

Figure 18.- Continued.

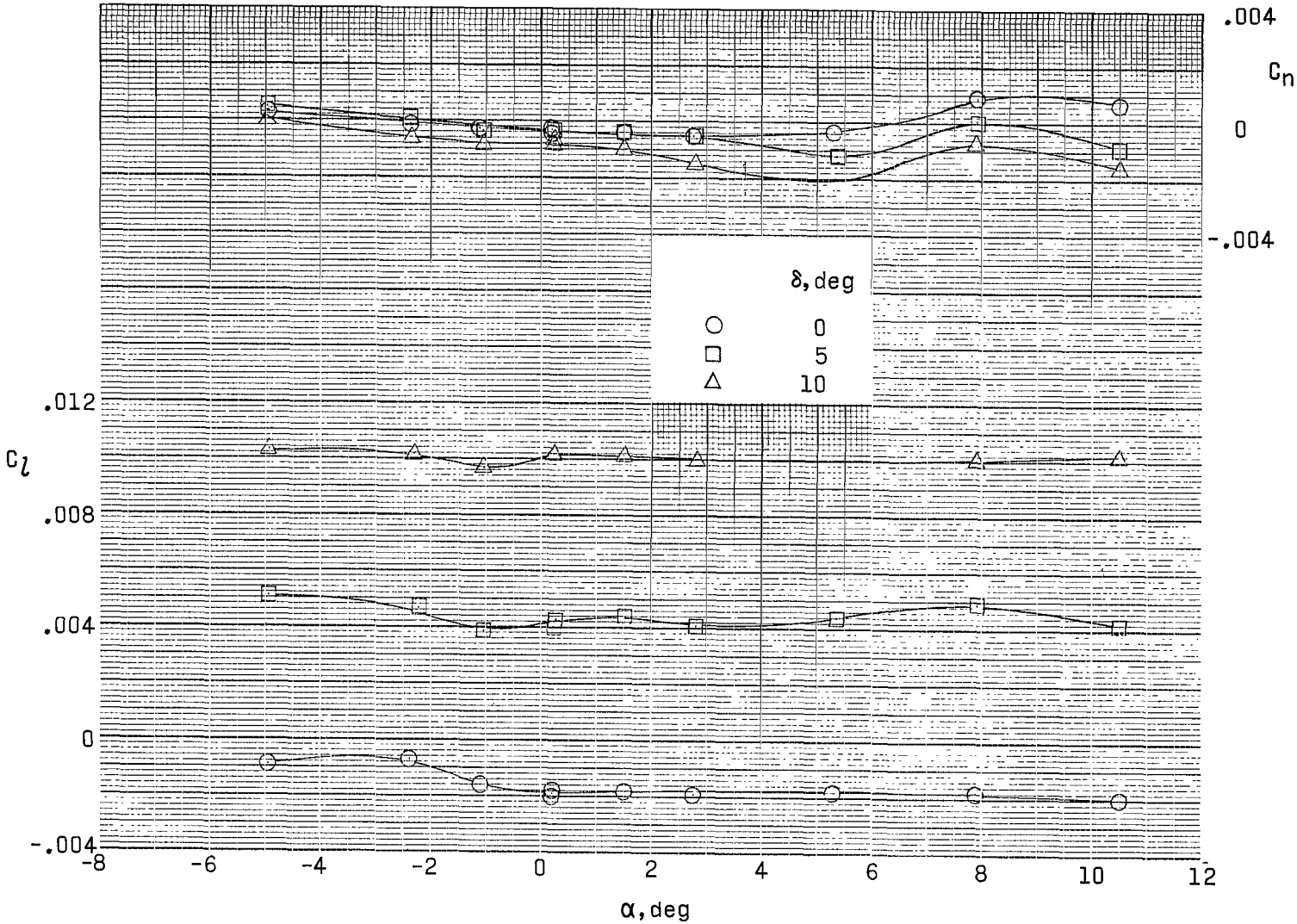

(c) Control C. $\gamma = 60^0$.

Figure 18.- Concluded.

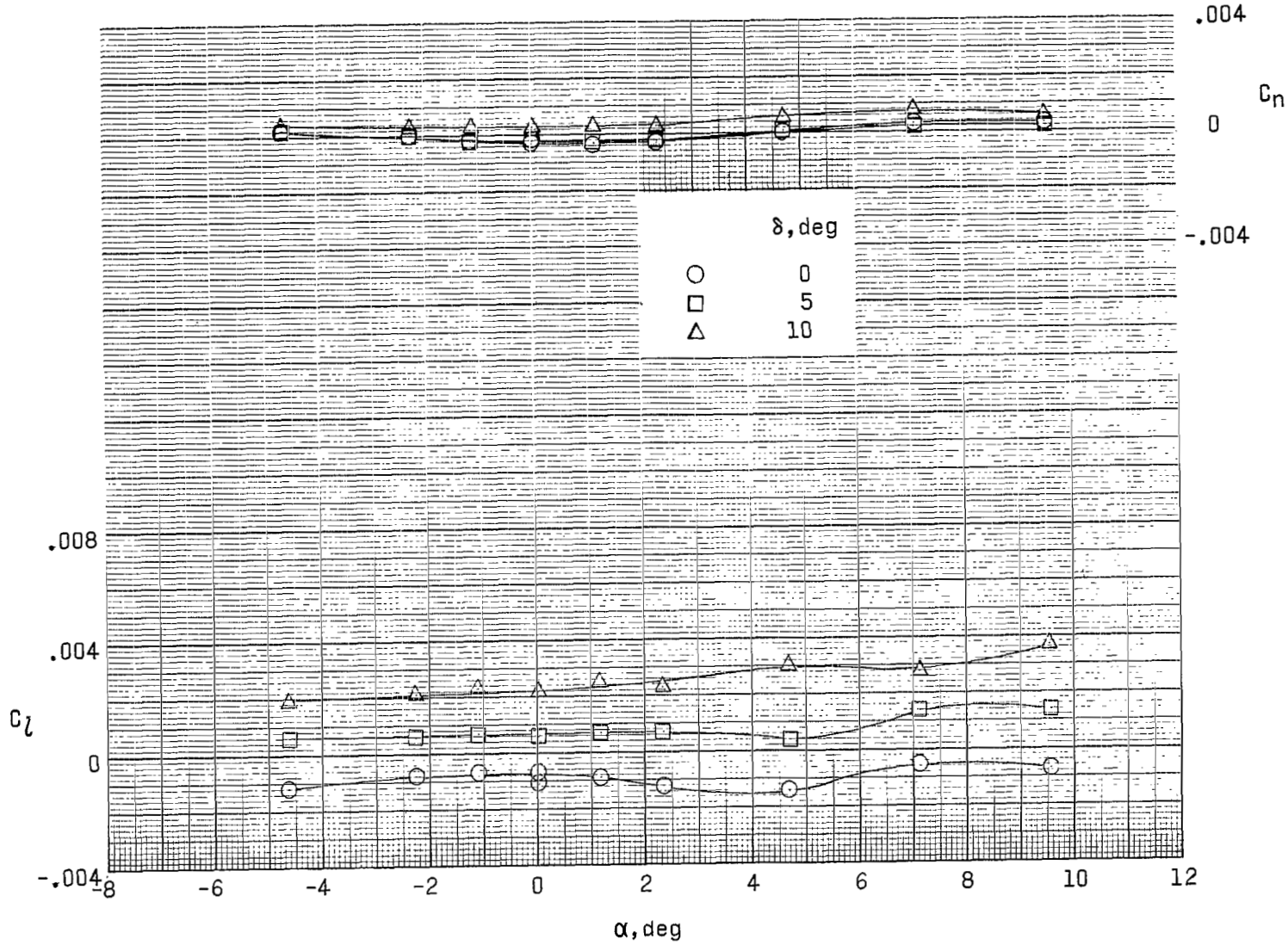

(a) Control A. $\gamma = 50^{\circ}$.

Figure 19.- Effect of control deflection on lateral aerodynamic characteristics. $\Lambda = 75^{\circ}$; $\beta = 0^{\circ}$; $M = 0.80$.

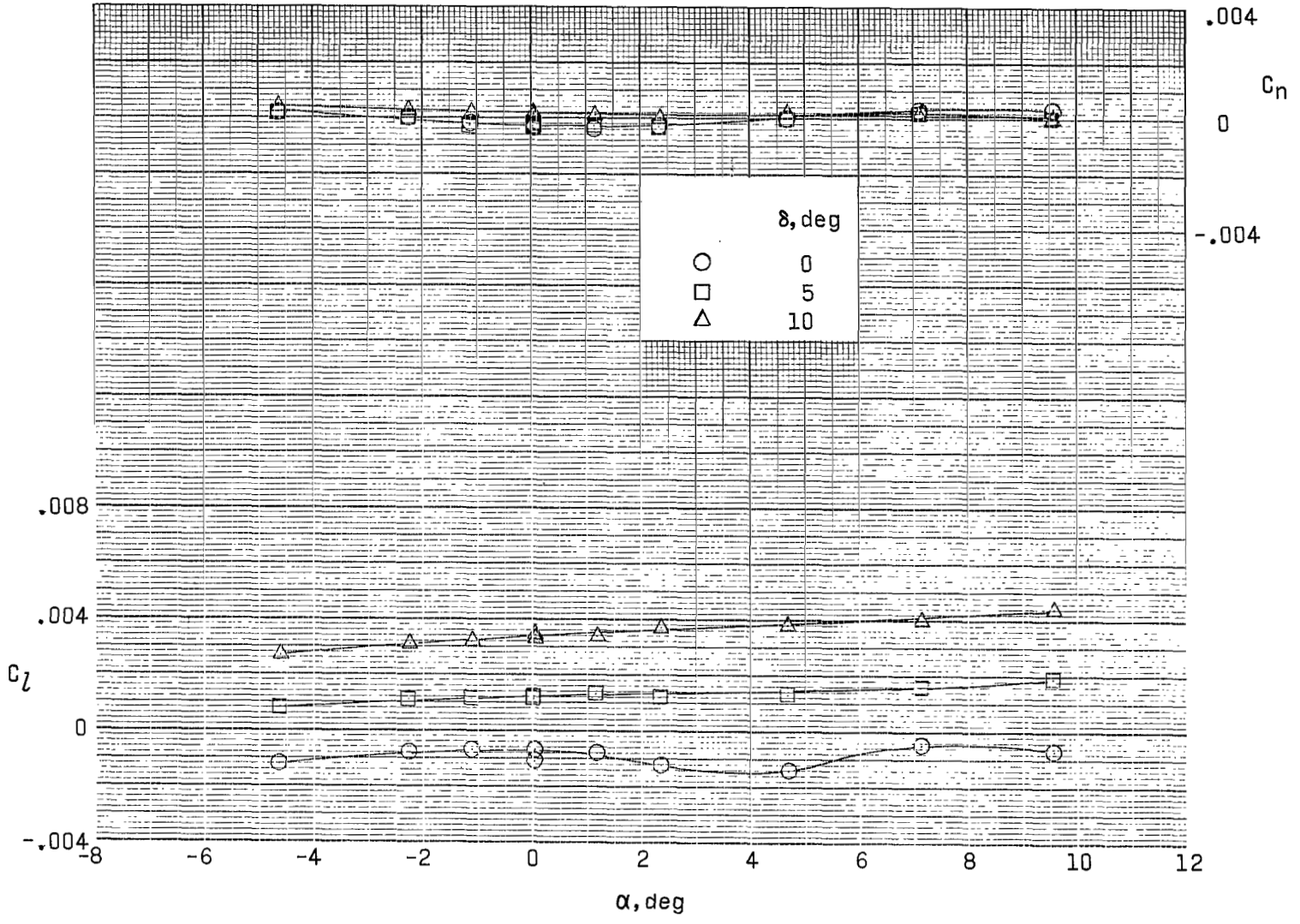

(b) Control B. $\gamma = 70^{o}$.

Figure 19.- Continued.

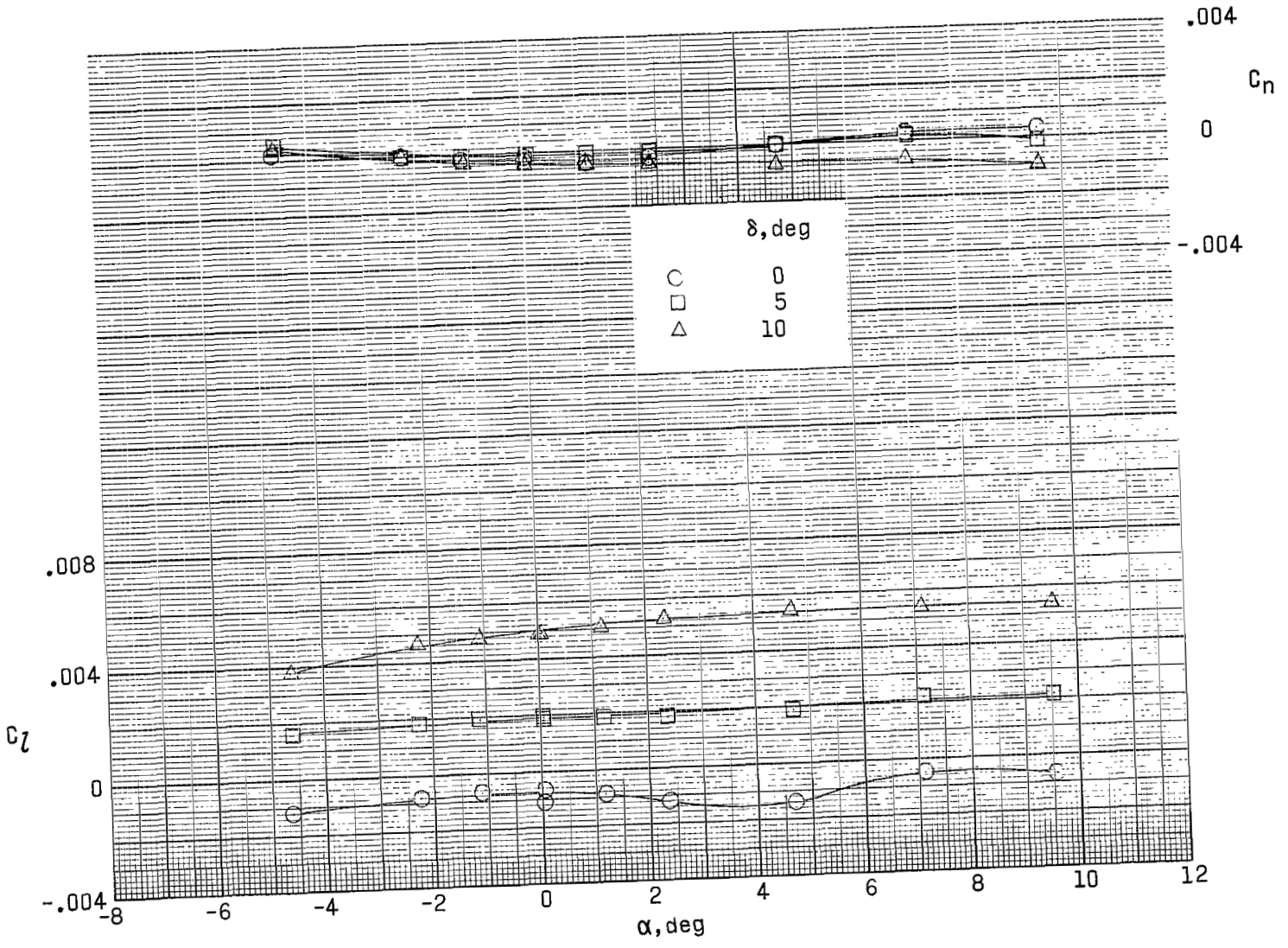

(c) Control C. $\gamma = 90^{o}$.

Figure 19.- Concluded.

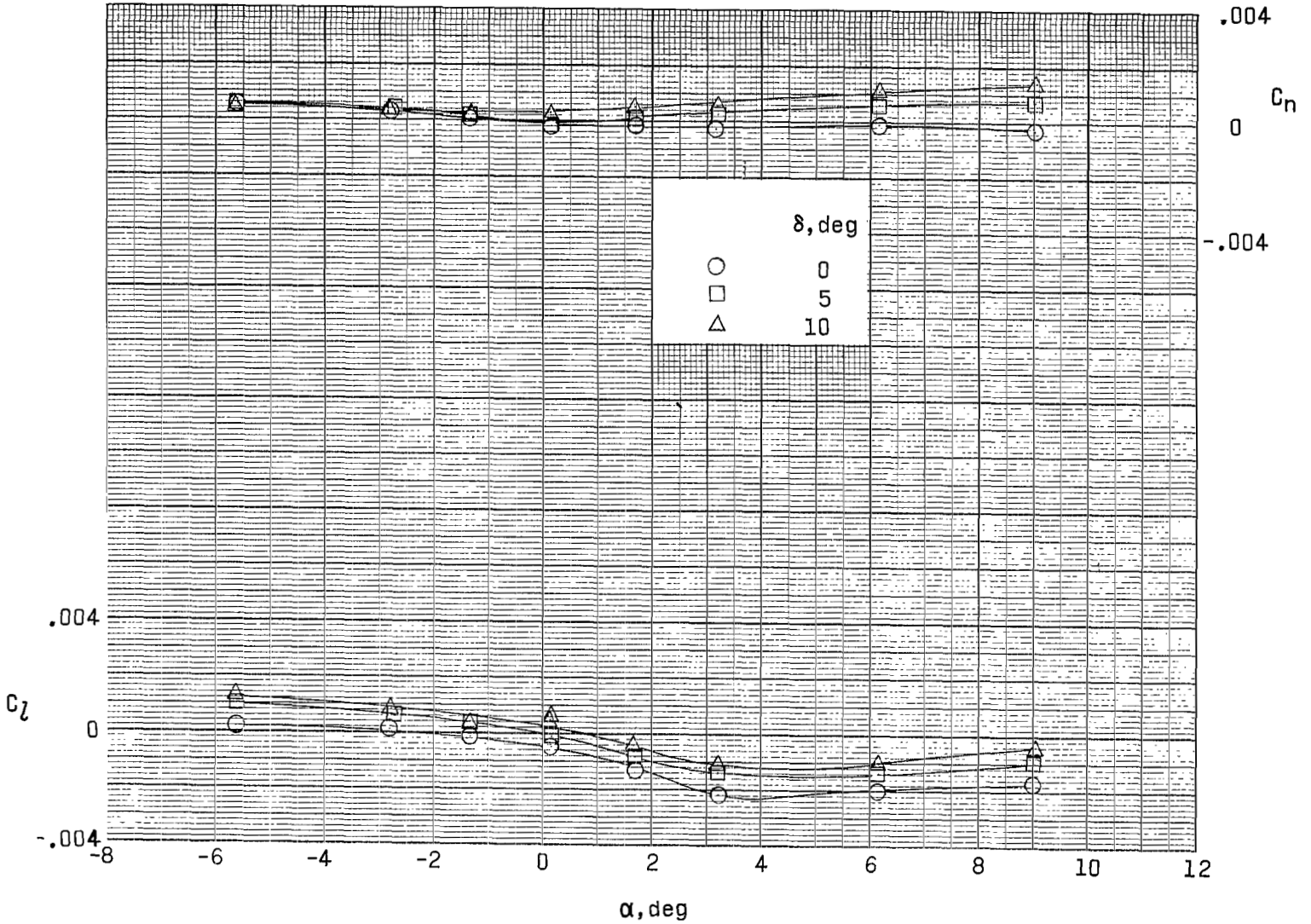

(a) Control A. $\gamma = 5^0$.

Figure 20.- Effect of control deflection on lateral aerodynamic characteristics. $\Lambda = 30^0$; $\beta = 0^0$; $M = 0.97$.

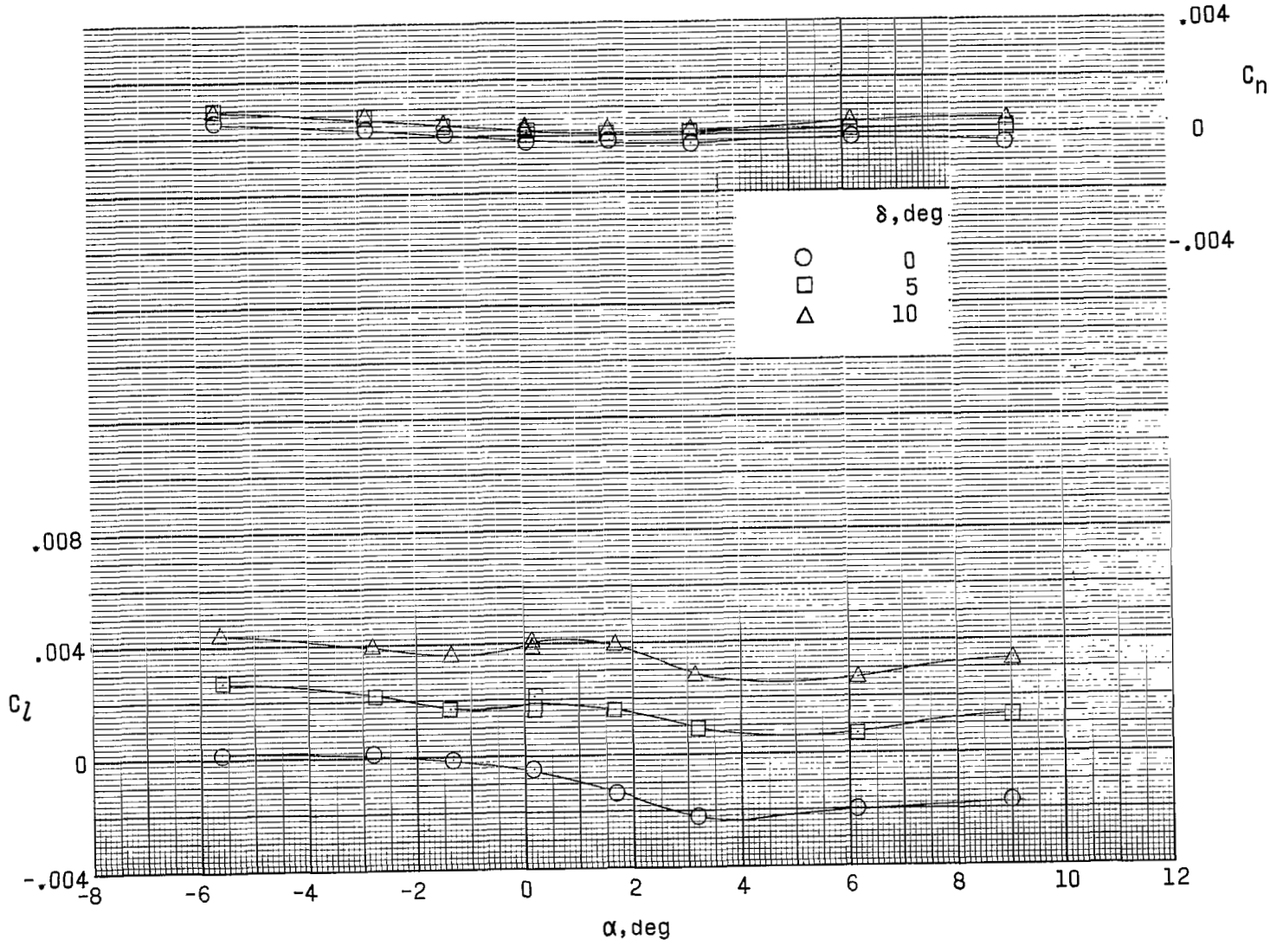

(b) Control B. $\gamma = 25^0$.

Figure 20.- Continued.

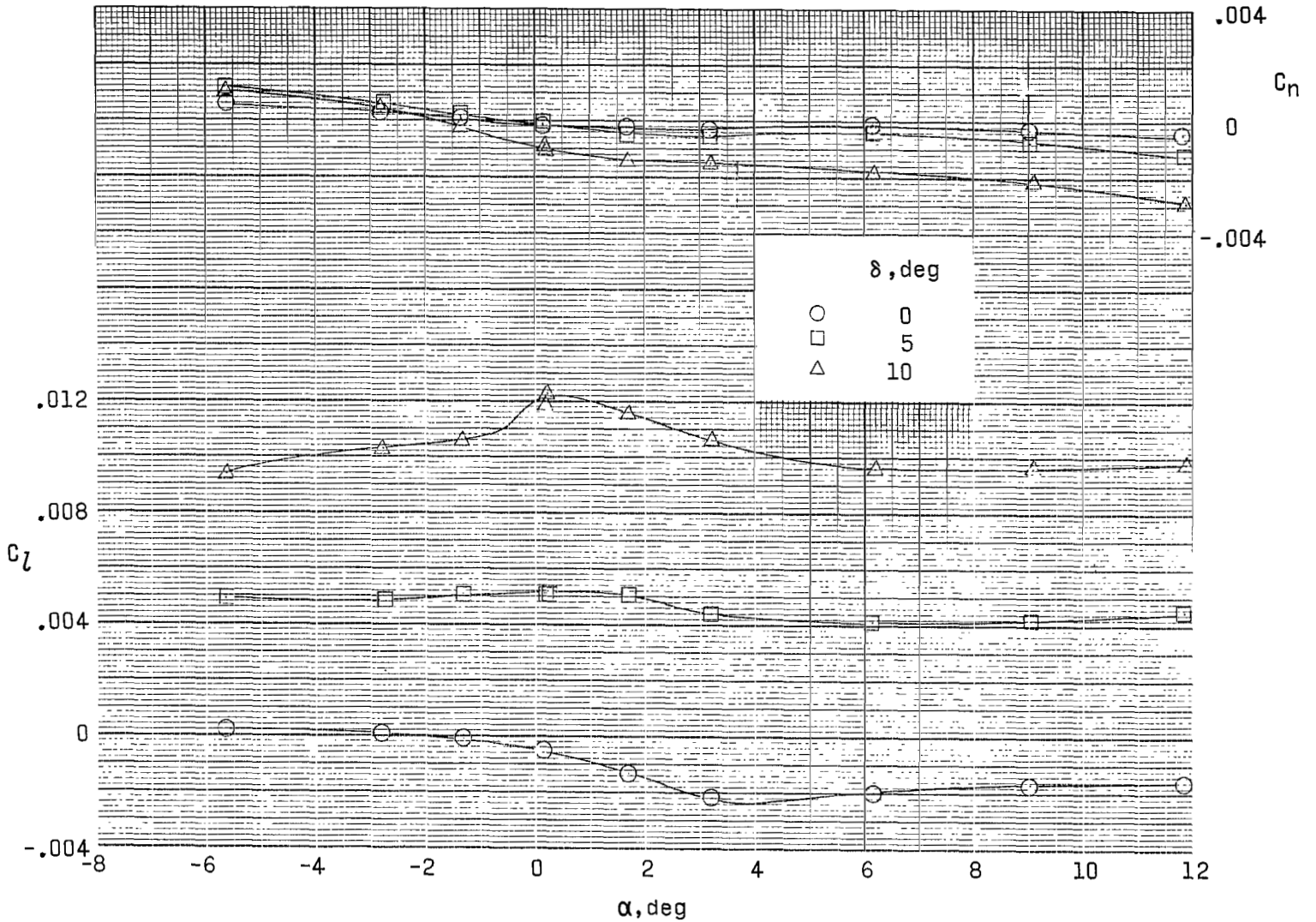

(c) Control C. $\gamma = 45^{\circ}$.

Figure 20.- Concluded.

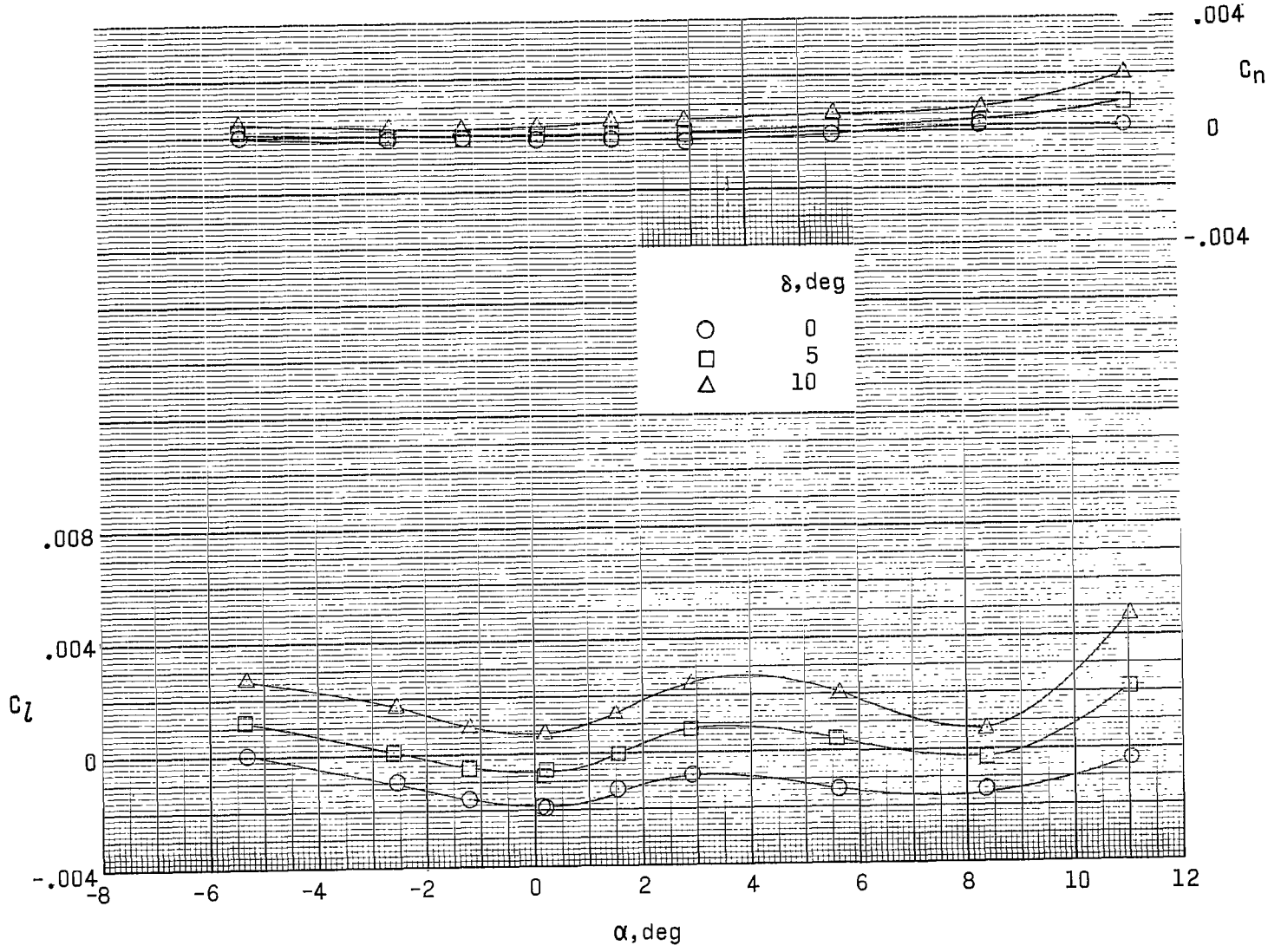

(a) Control A. $\gamma = 20^{\circ}$.

Figure 21.- Effect of control deflection on lateral aerodynamic characteristics. $\Lambda = 45^{\circ}$; $\beta = 0^{\circ}$; $M = 0.97$.

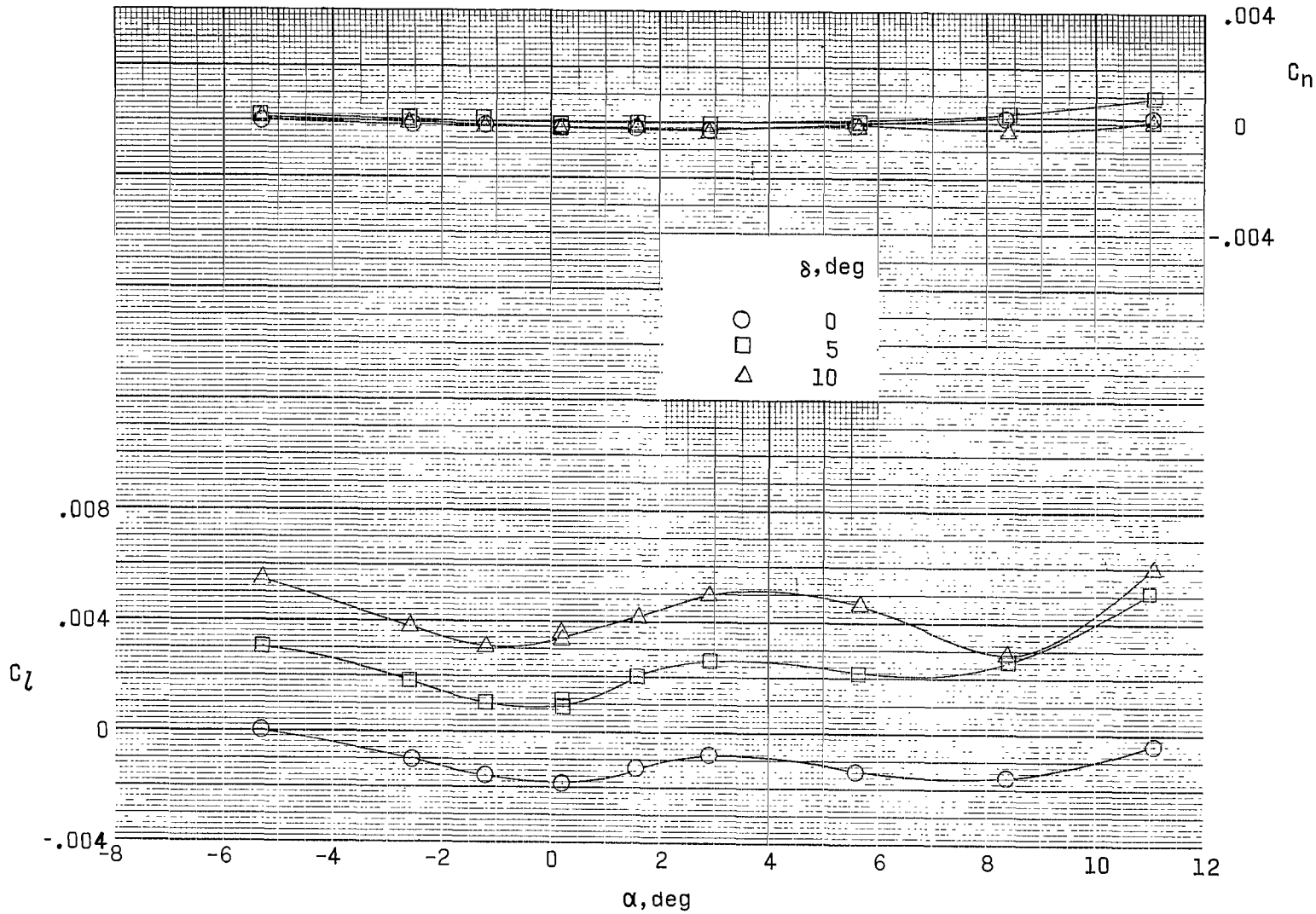

(b) Control B. $\gamma = 40^{\circ}$.

Figure 21.- Continued.

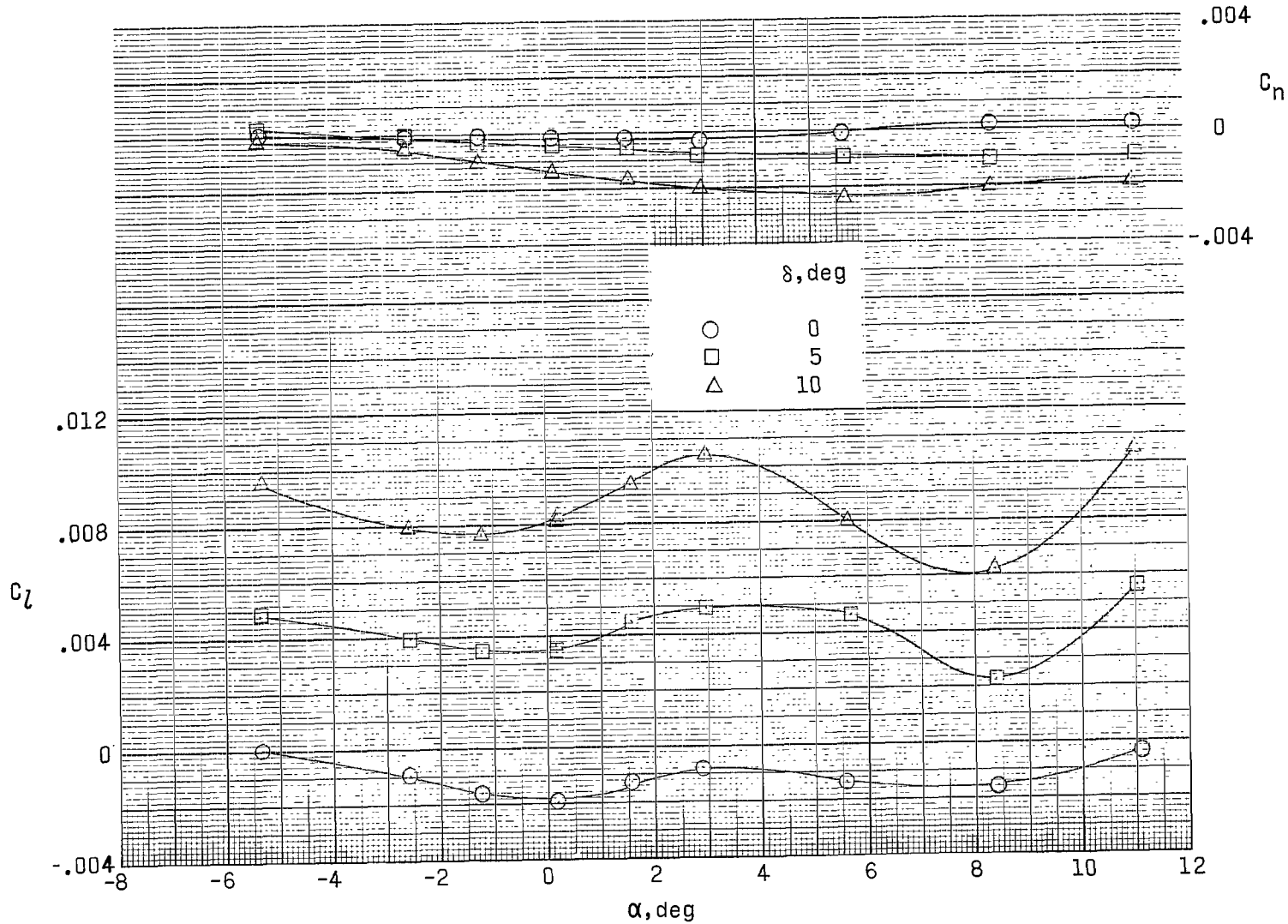

(c) Control C. $\gamma = 60^{0}$.

Figure 21.- Concluded.

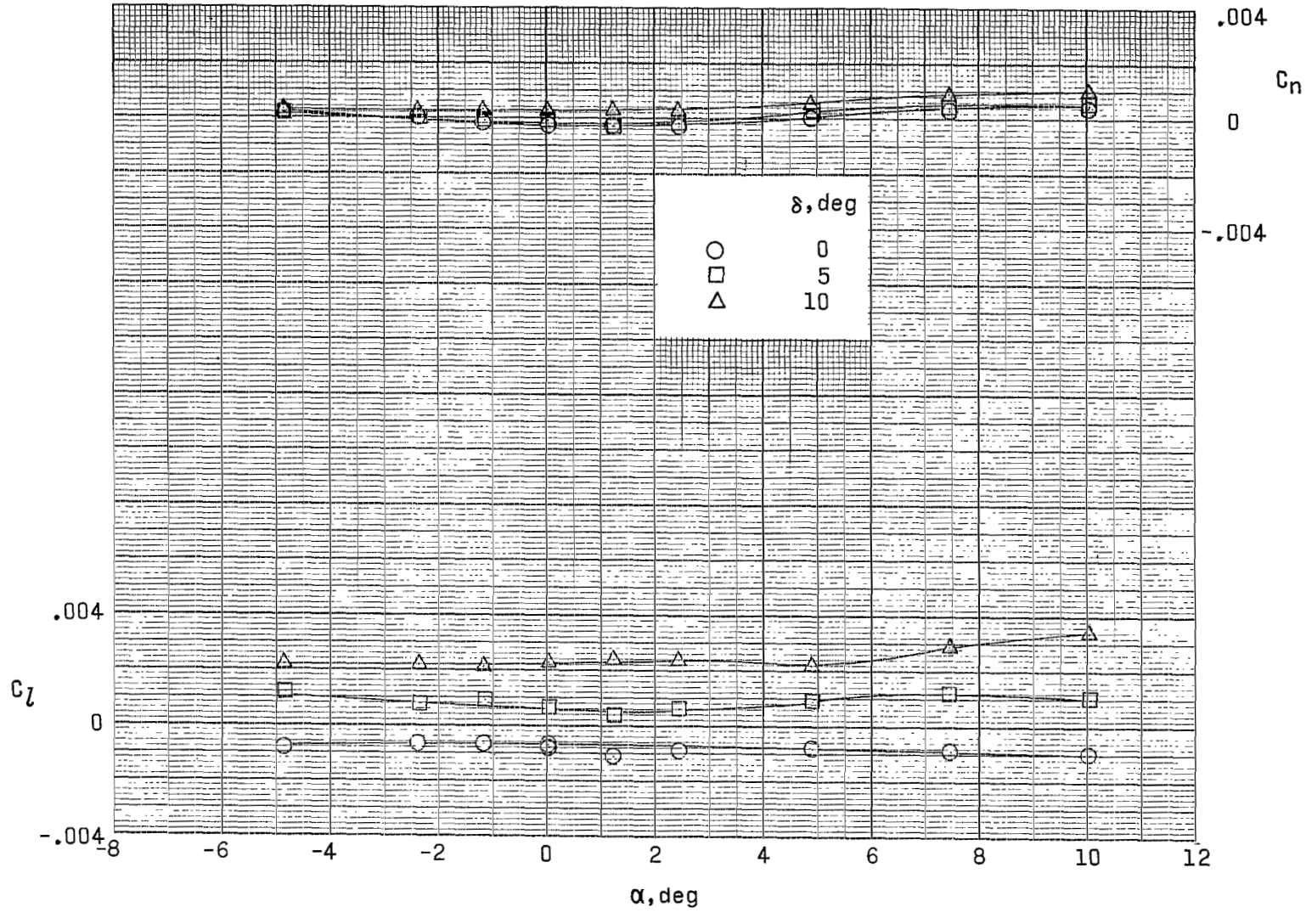

(a) Control A. $\gamma = 50^{o}$.

Figure 22.- Effect of control deflection on lateral aerodynamic characteristics. $\Lambda = 75^{o}$; $\beta = 0^{o}$; $M = 0.97$.

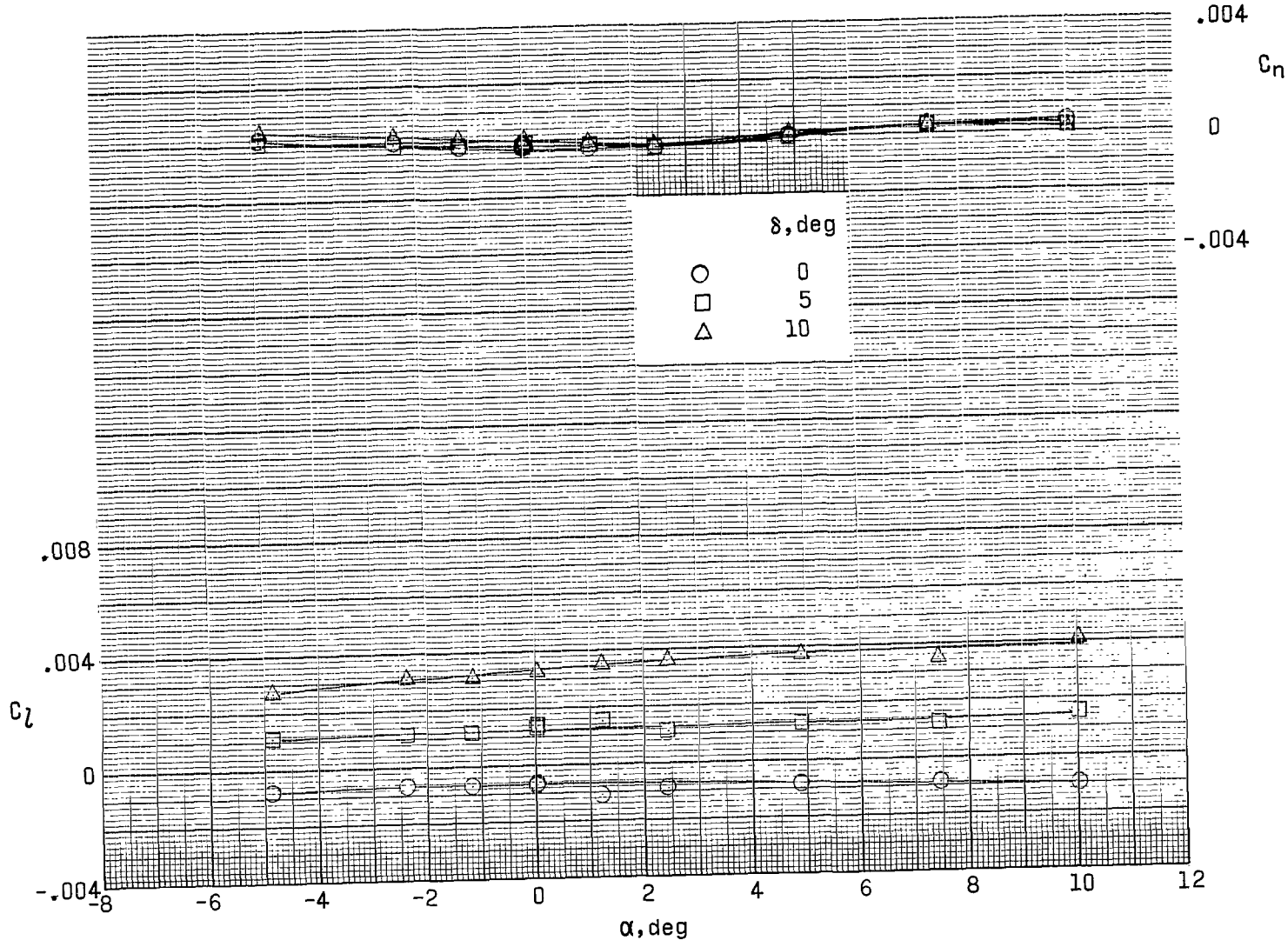

(b) Control B. $\gamma = 70^{0}$.

Figure 22.- Continued.

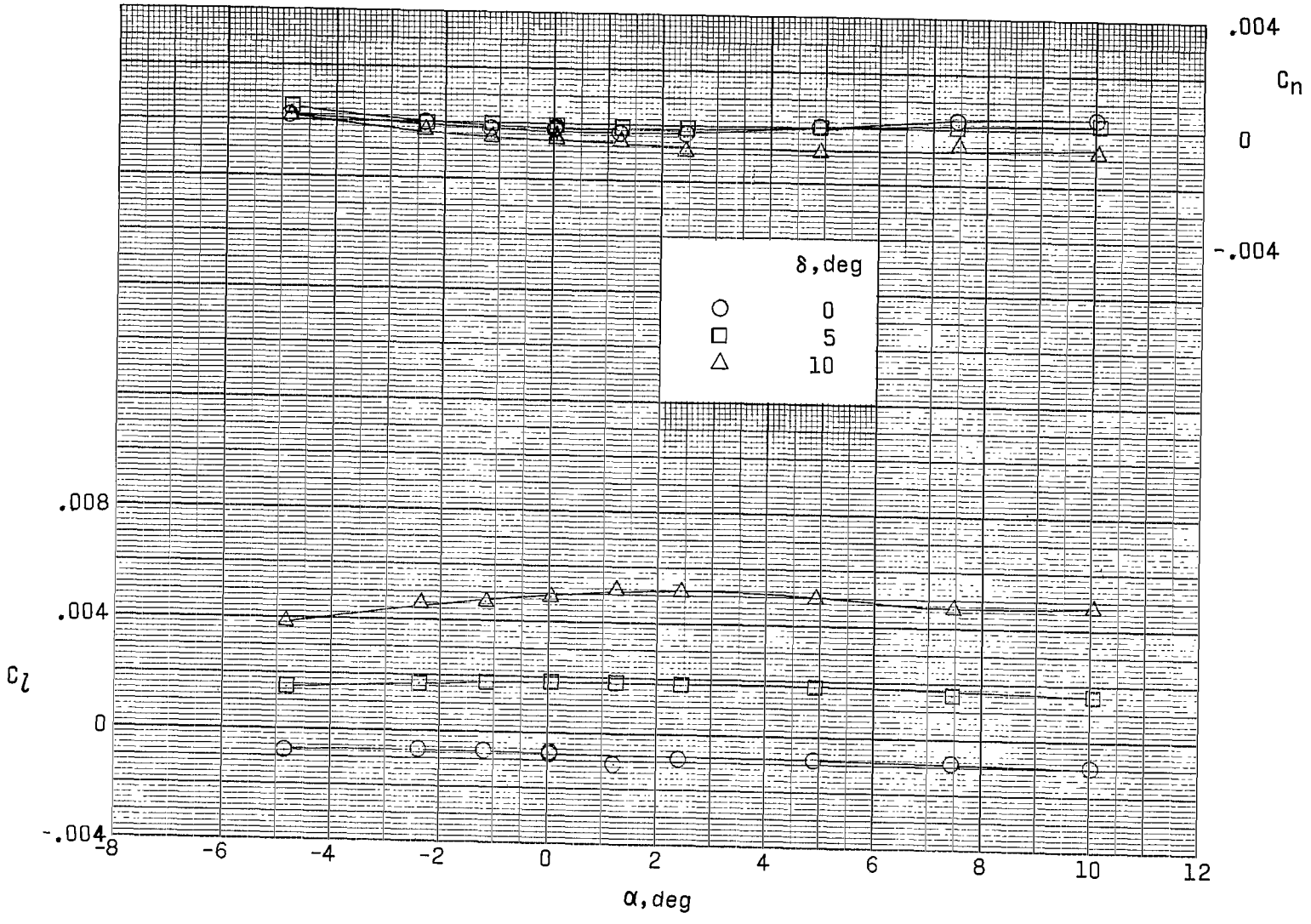

(c) Control C. $\gamma = 90^{0}$.

Figure 22.- Concluded.

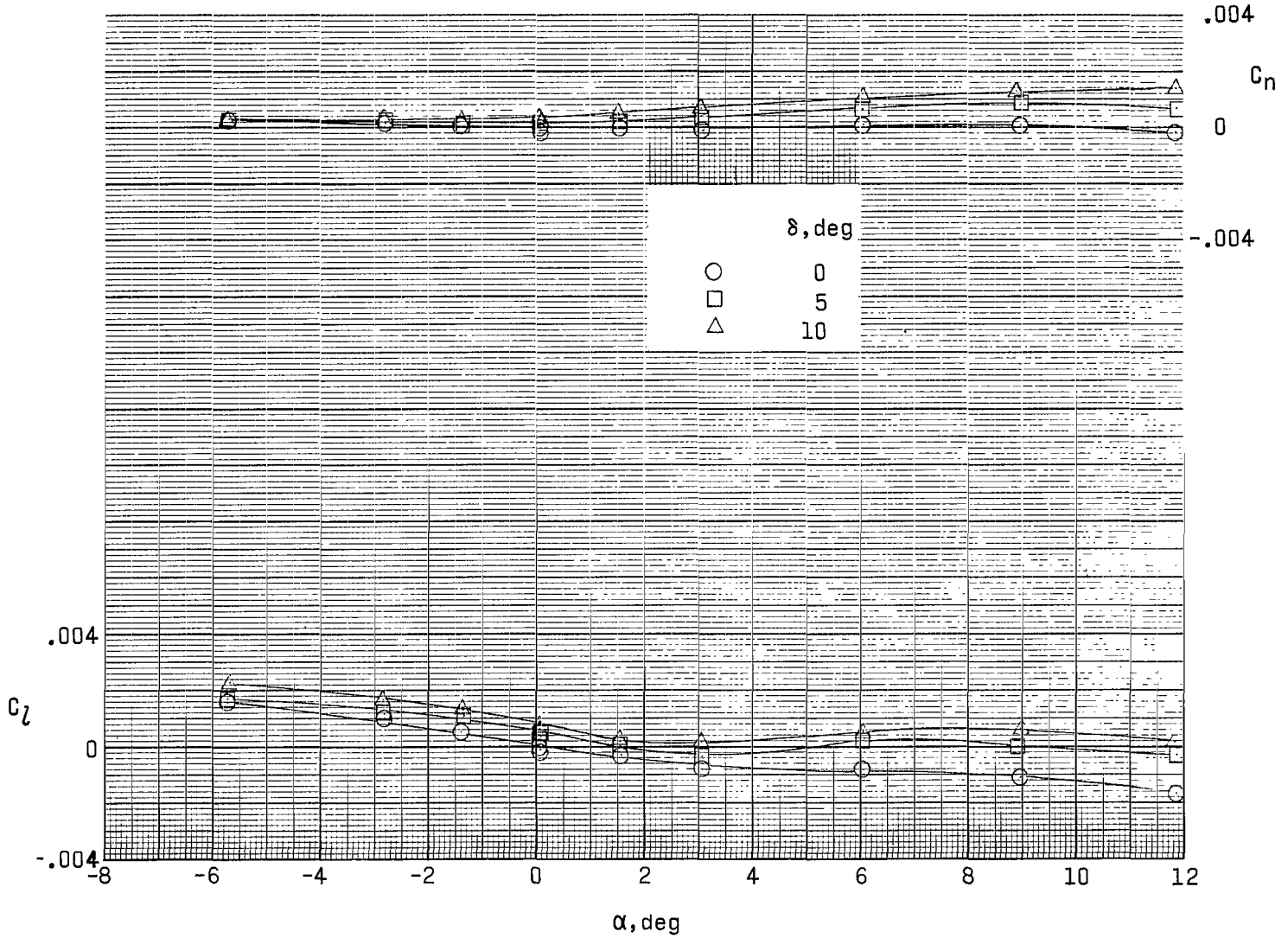

(a) Control A. $\gamma = 5^0$.

Figure 23.- Effect of control deflection on lateral aerodynamic characteristics. $\Lambda = 30^0$; $\beta = 0^0$; $M = 1.20$.

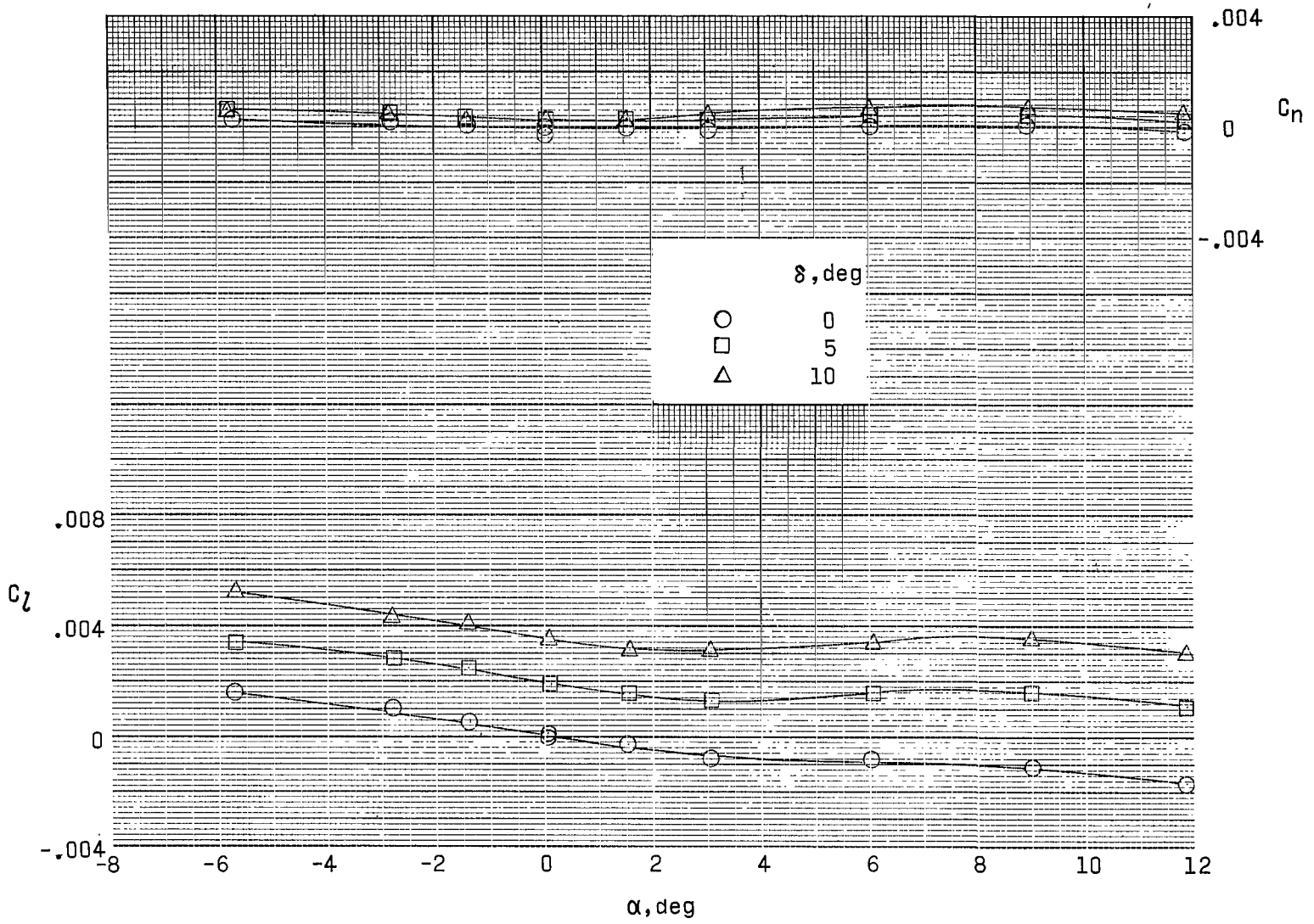

(b) Control B. $\gamma = 25^0$.

Figure 23.- Continued.

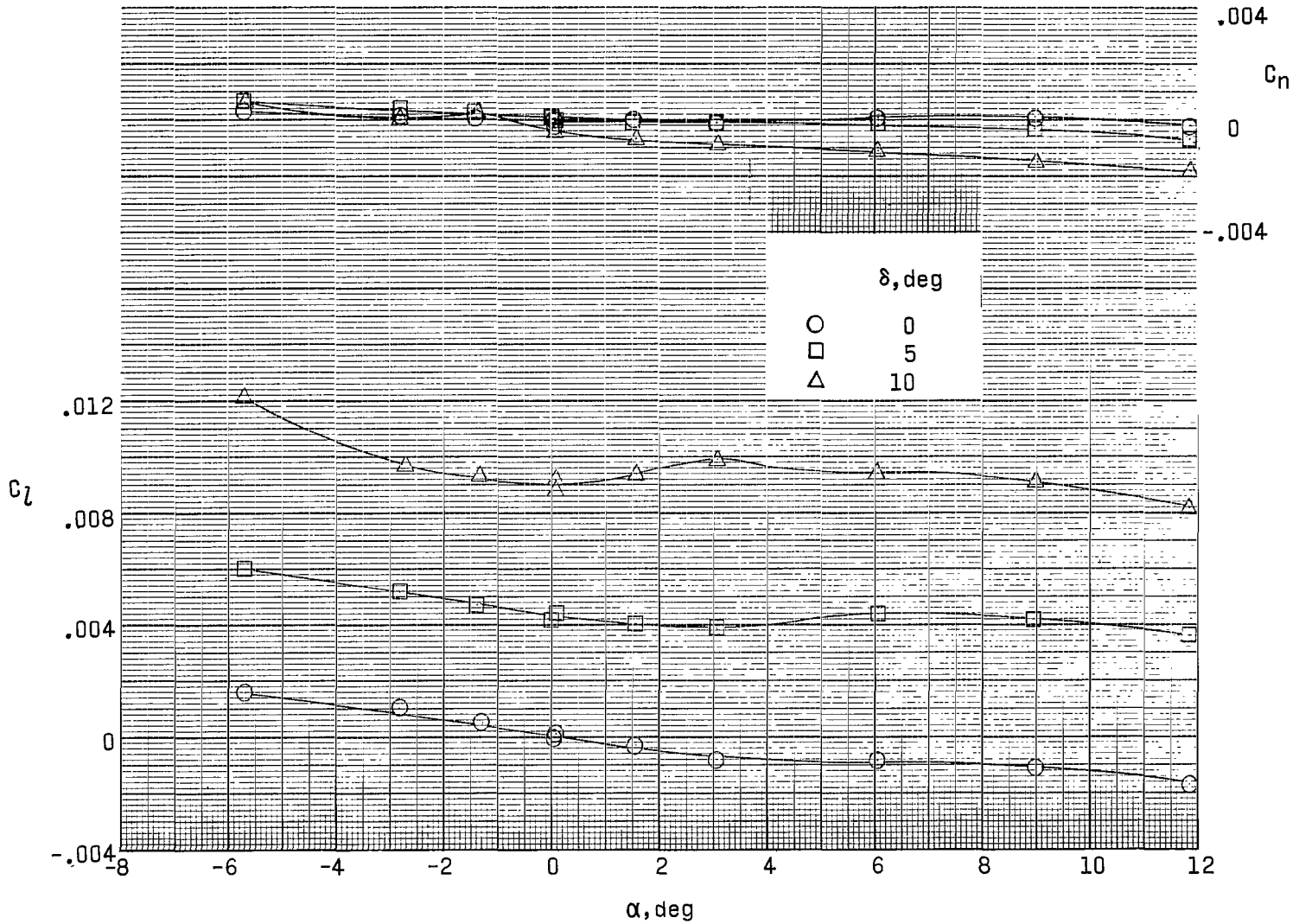

(c) Control C. $\gamma = 45^0$.

Figure 23.- Concluded.

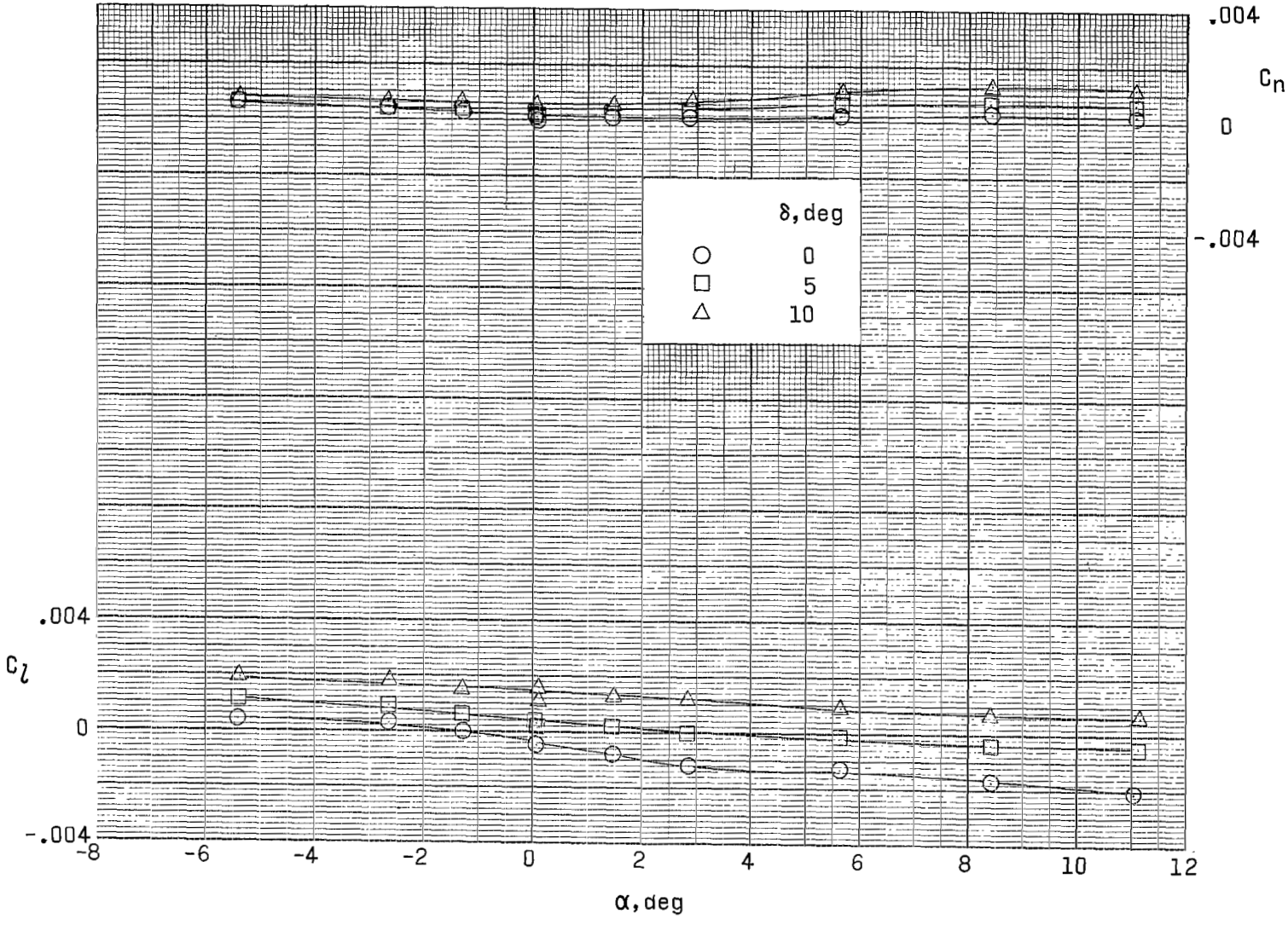

(a) Control A. $\gamma = 20^0$.

Figure 24.- Effect of control deflection on lateral aerodynamic characteristics. $\Lambda = 45^0$; $\beta = 0^0$; $M = 1.20$.

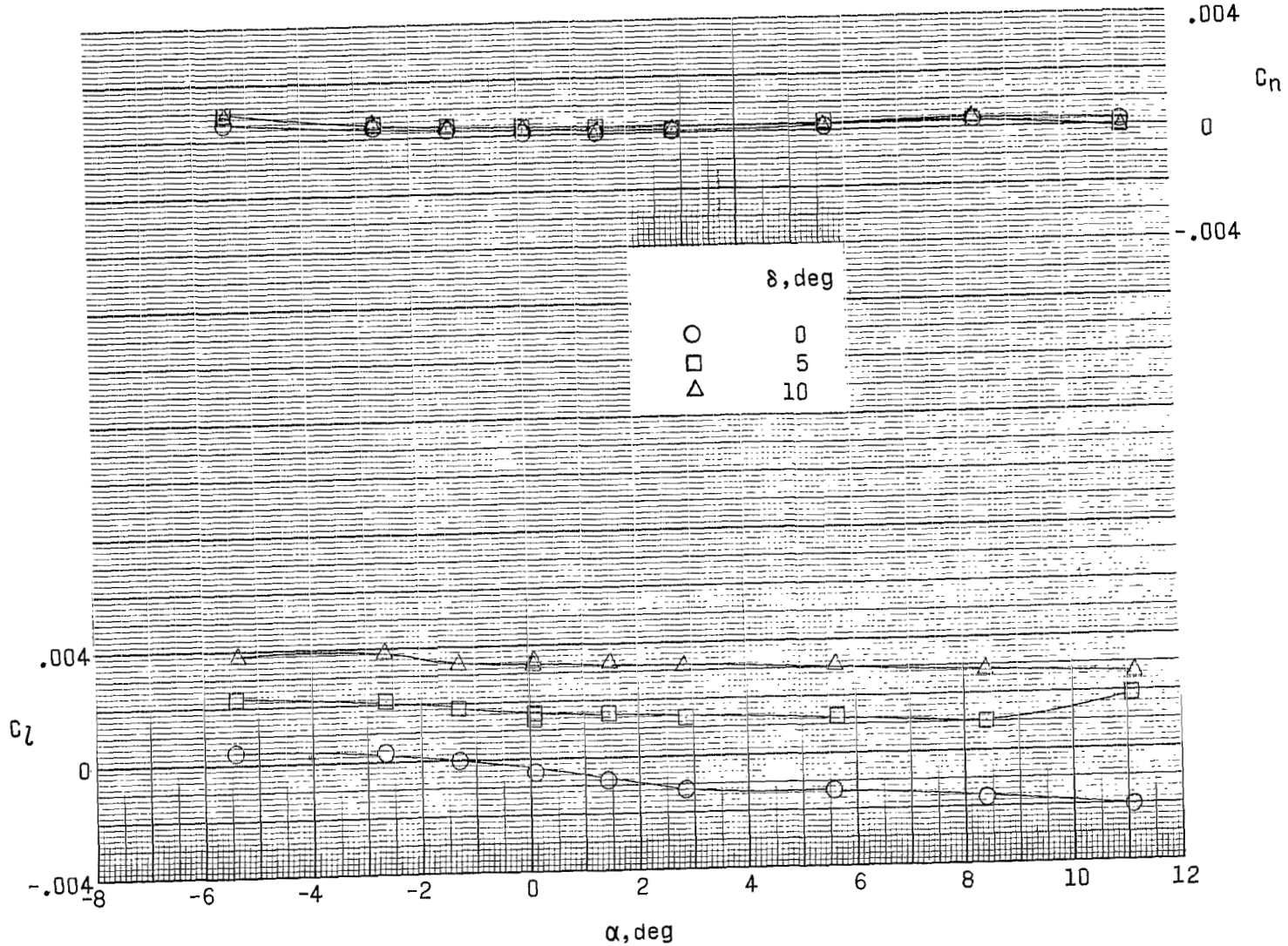

(b) Control B. $\gamma = 40^{o}$.

Figure 24.- Continued.

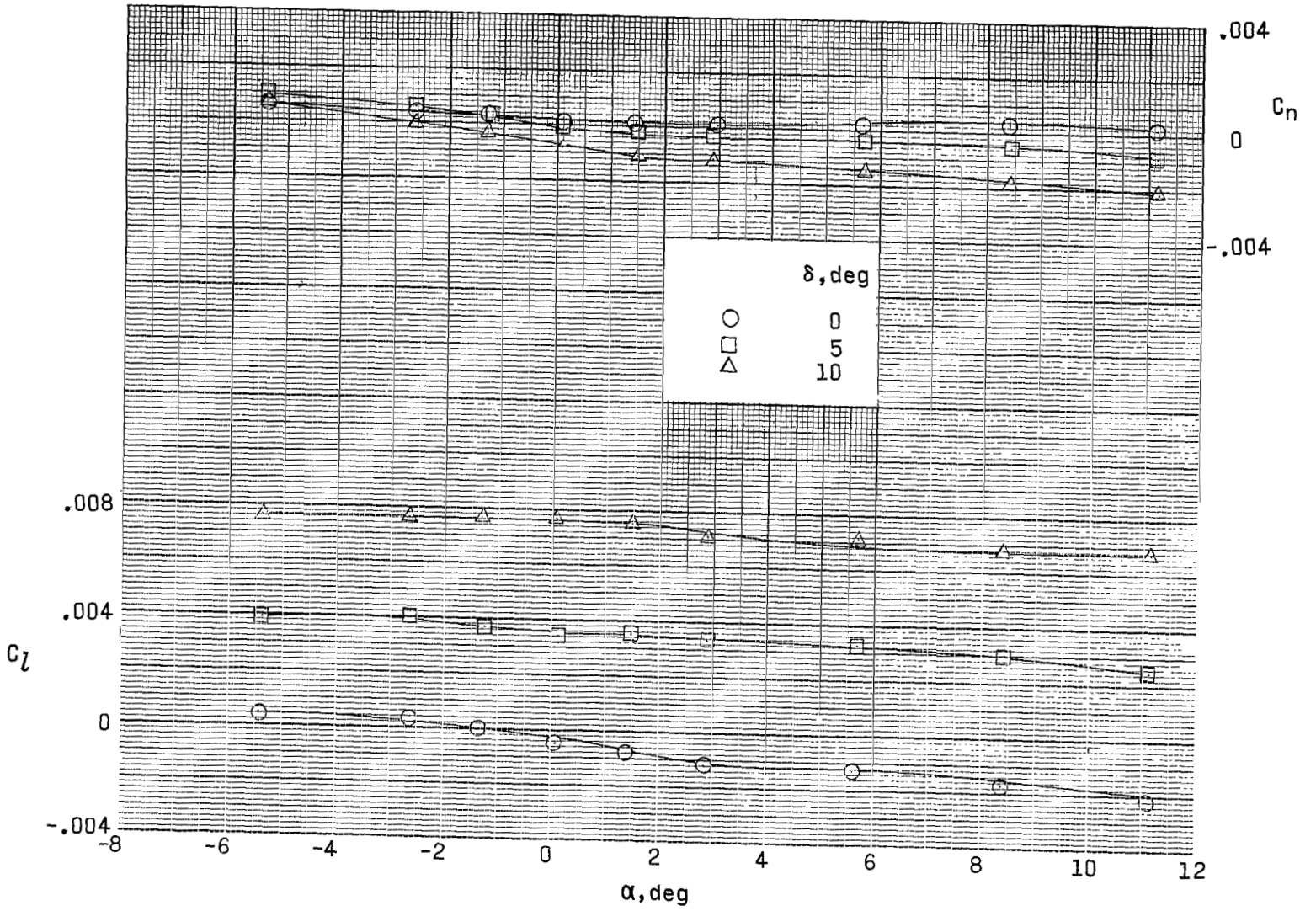

(c) Control C. $\gamma = 60^{\circ}$.

Figure 24.- Concluded.

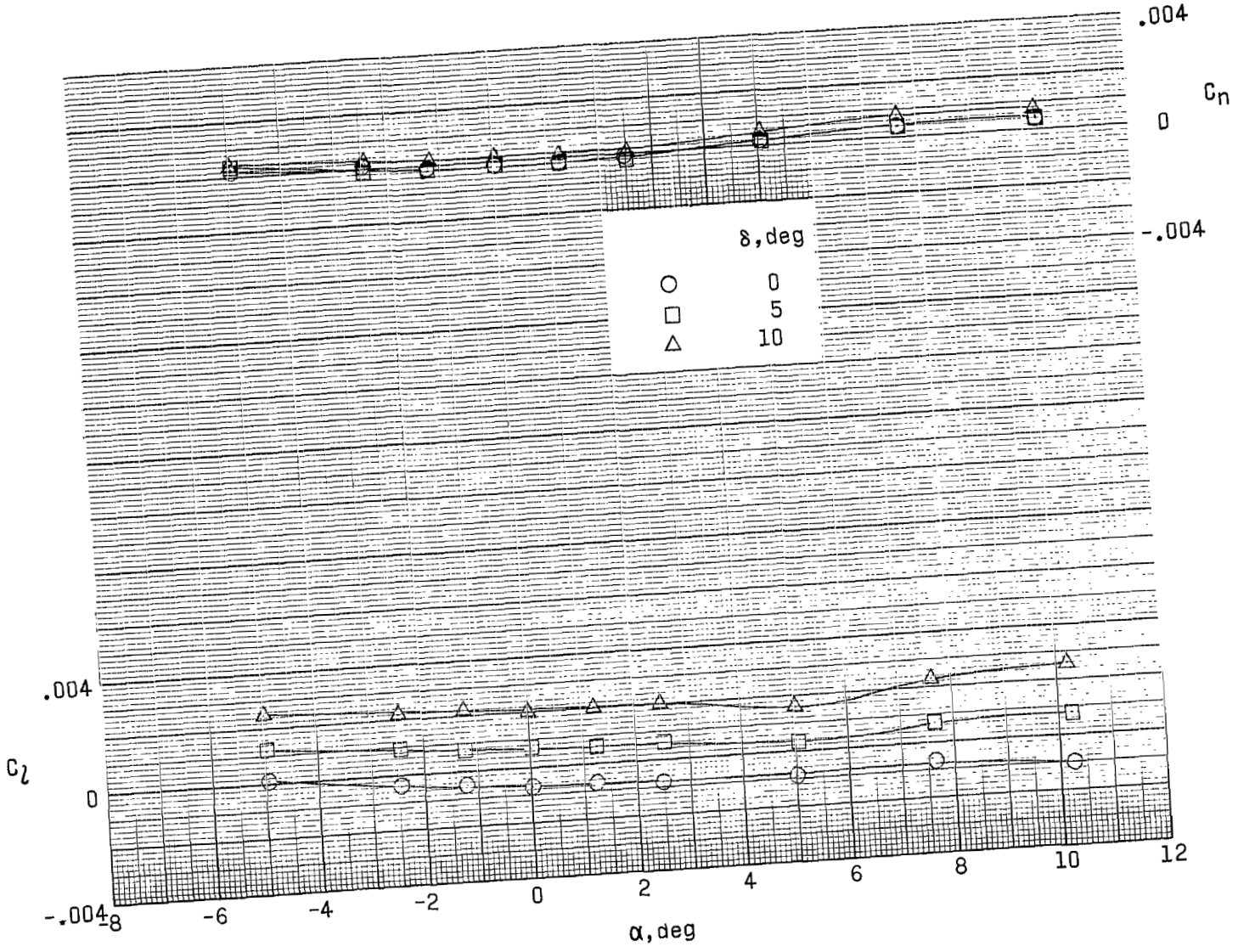

(a) Control A. $\gamma = 50^{0}$.

Figure 25.- Effect of control deflection on lateral aerodynamic characteristics. $\Lambda = 75^{0}$; $\beta = 0^{0}$; $M = 1.20$.

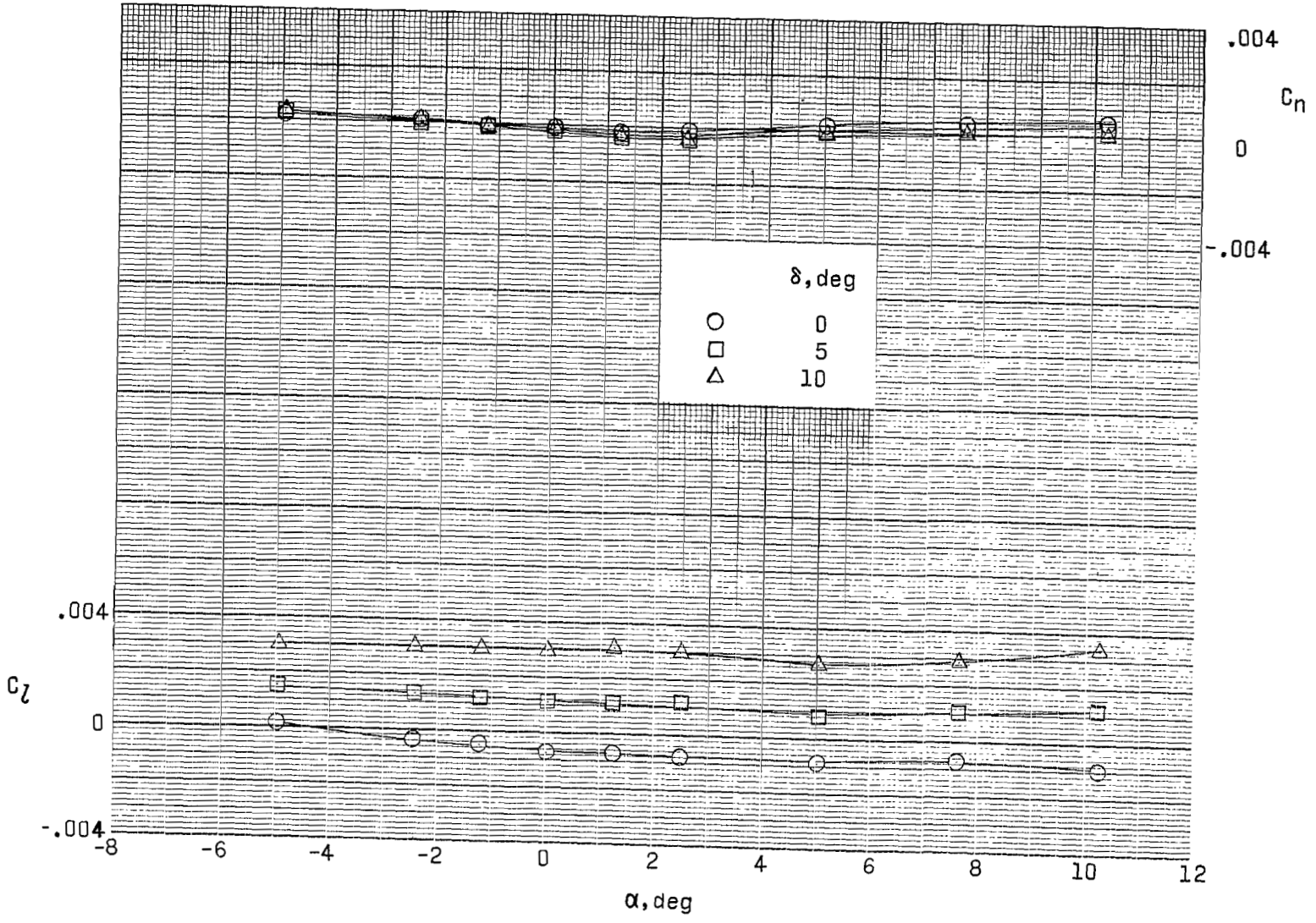

(b) Control B. $\gamma = 70^{o}$.

Figure 25.- Continued.

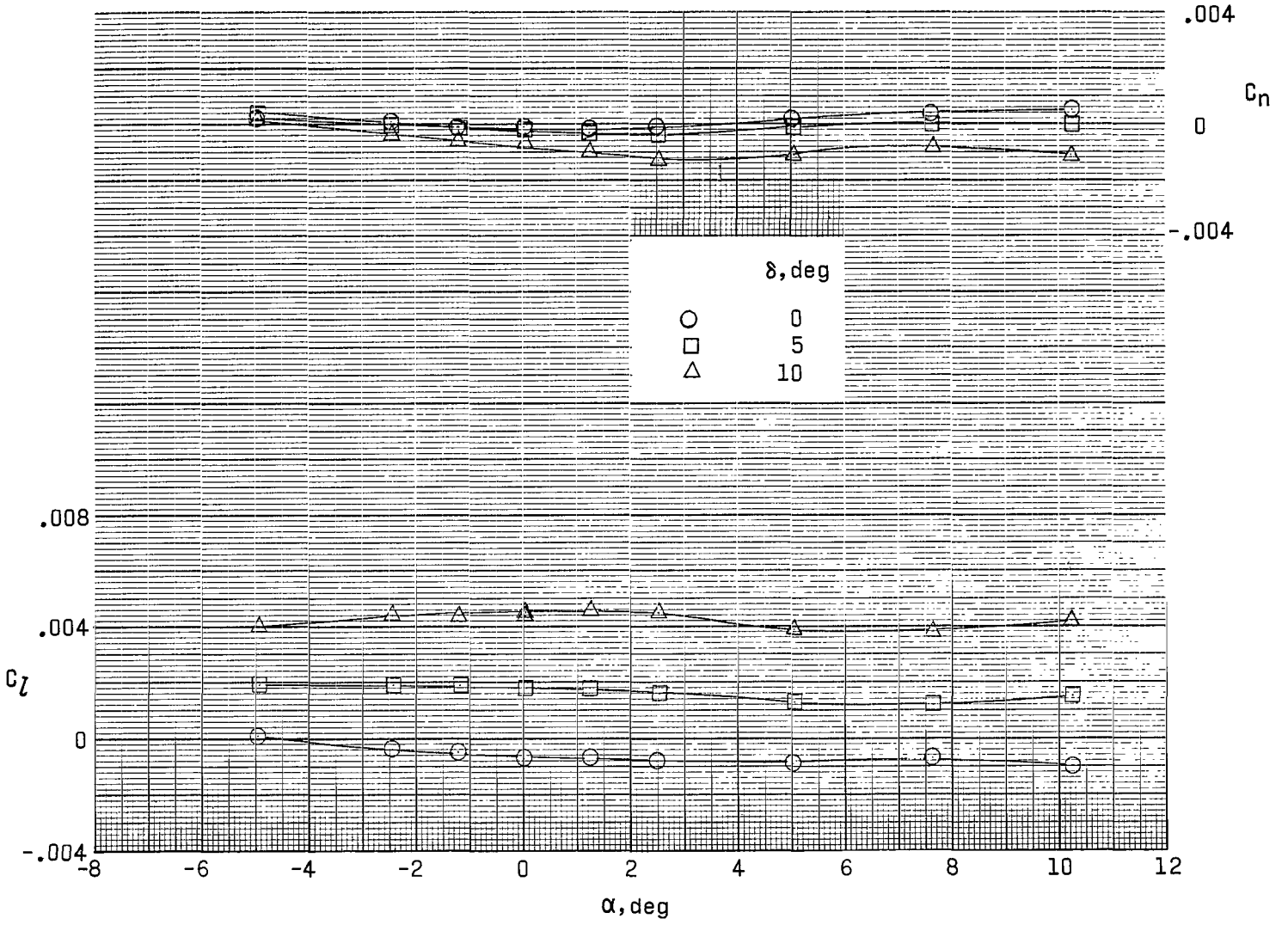

(c) Control C. $\gamma = 90^0$.

Figure 25.- Concluded.

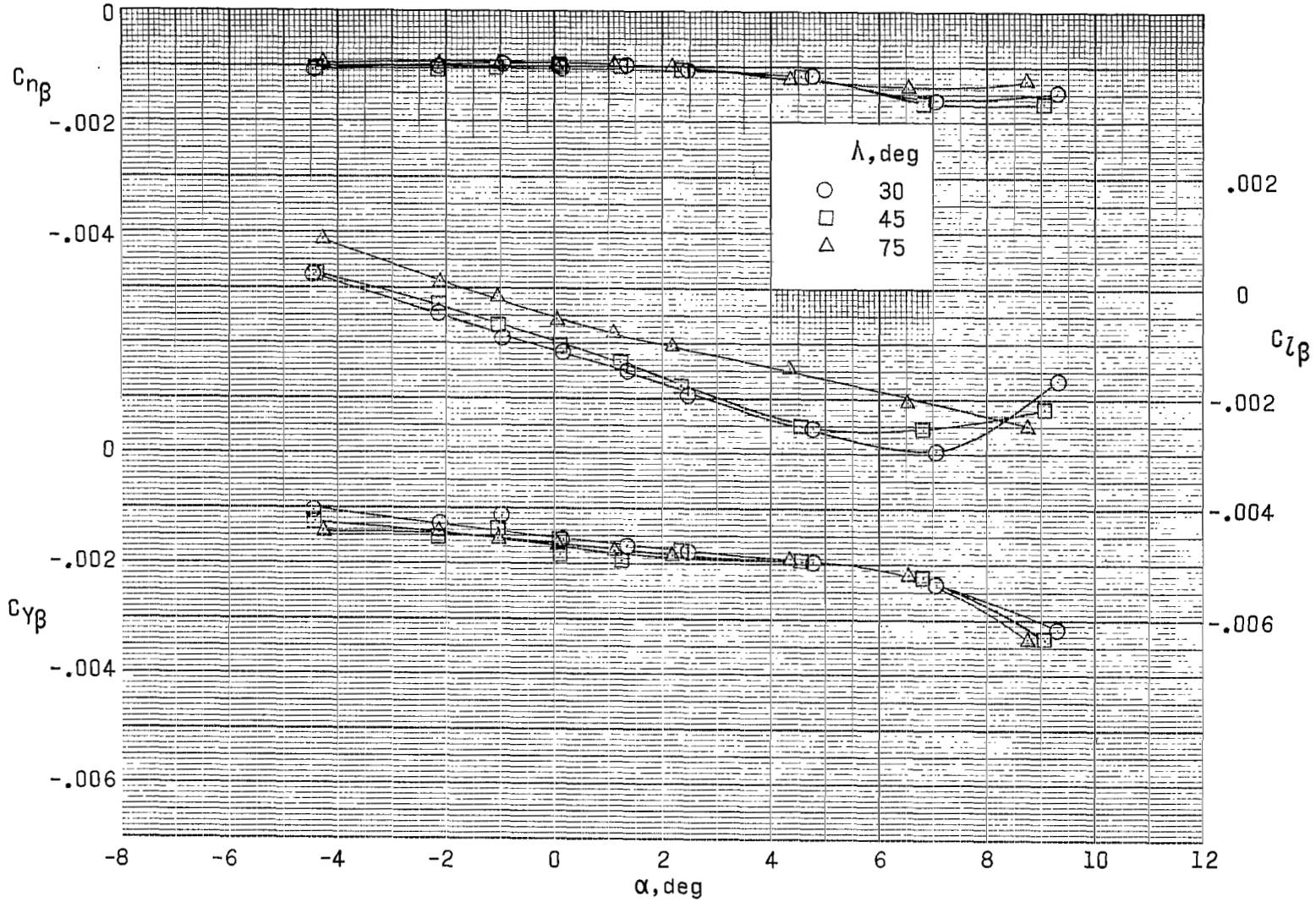

(a) M = 0.50.

Figure 26.- Variation of static lateral stability derivatives with angle of attack. $\delta = 0^0$.

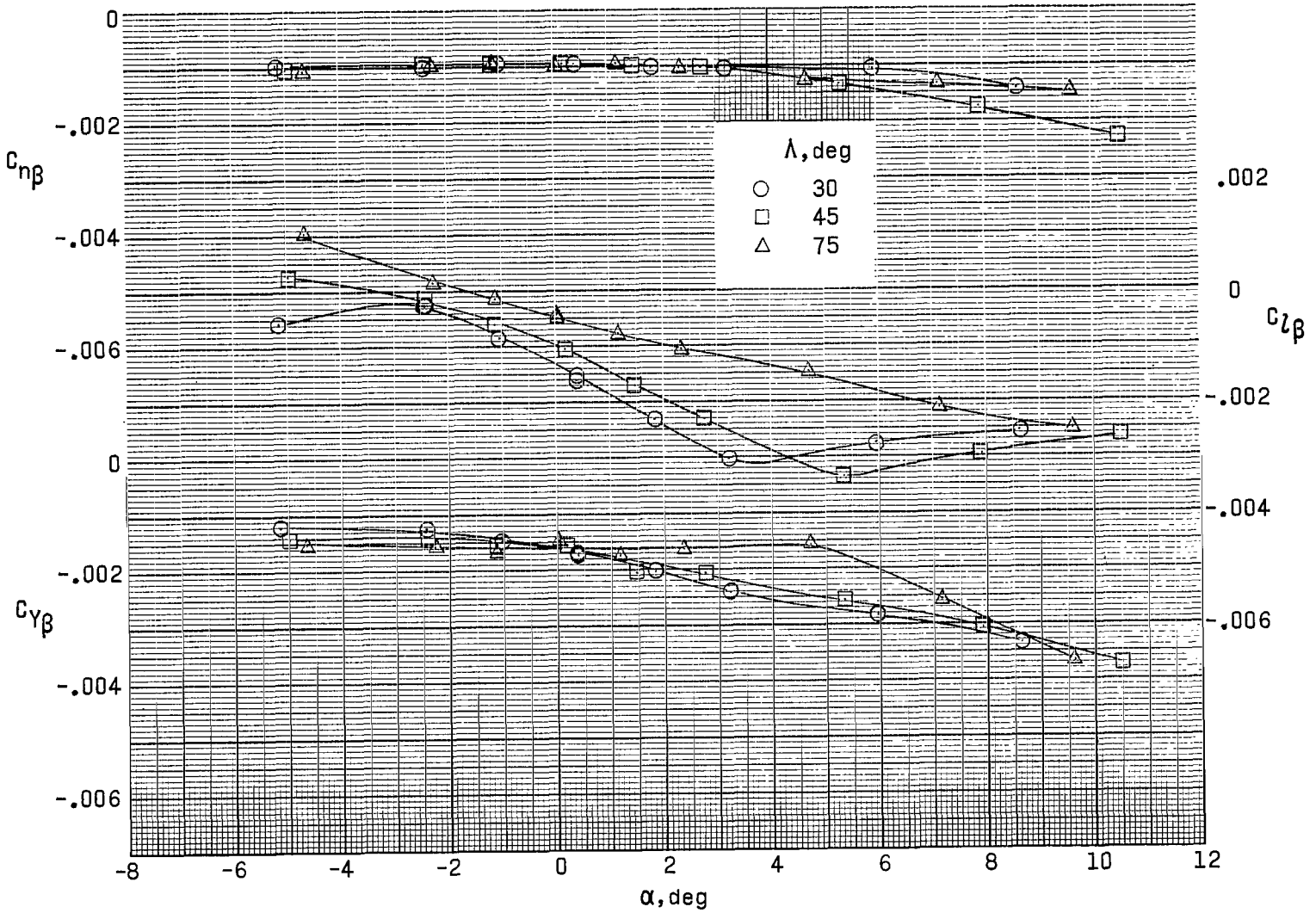

(b) M = 0.80.

Figure 26.- Continued.

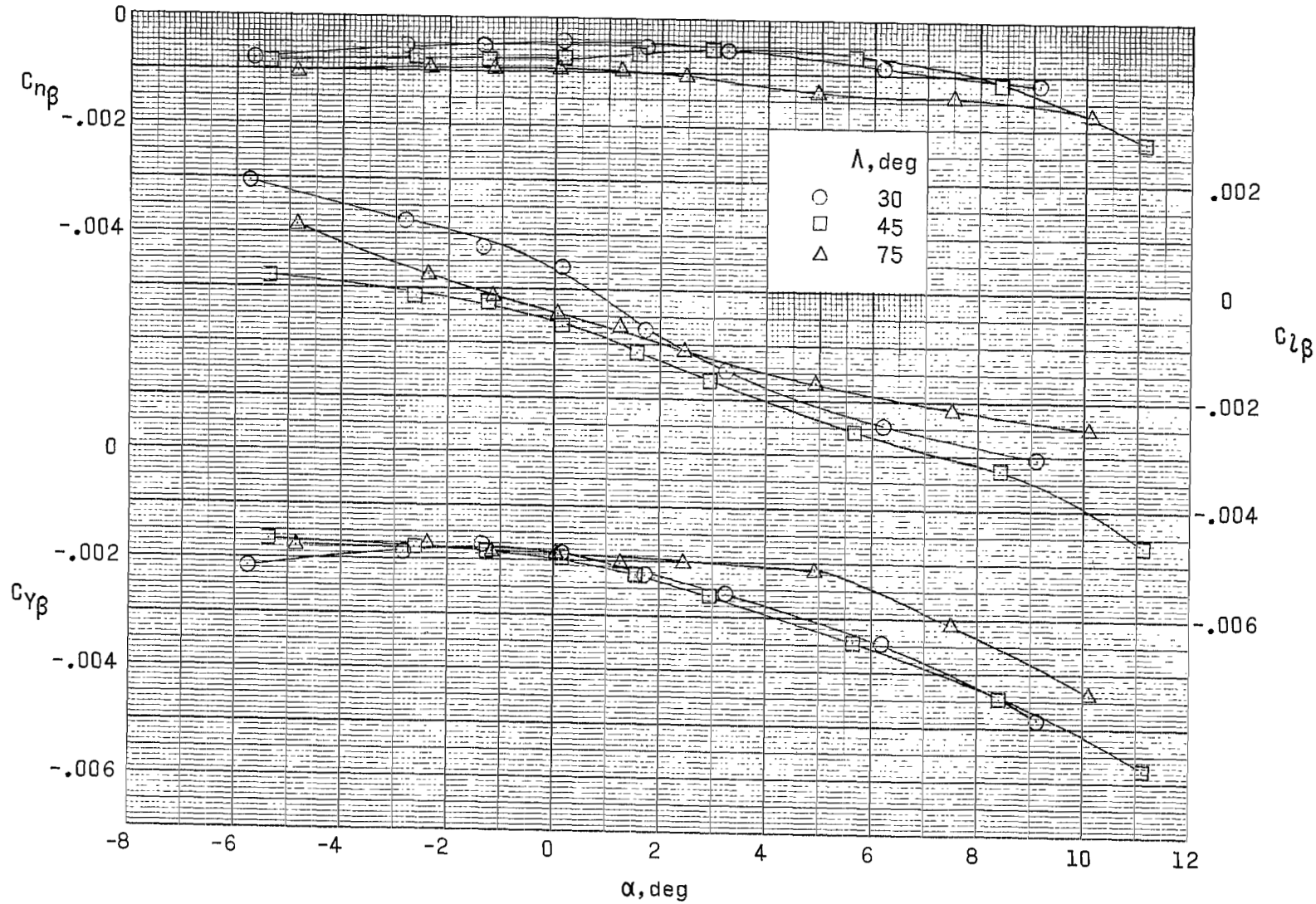

(c) M = 0.97.

Figure 26.- Continued.

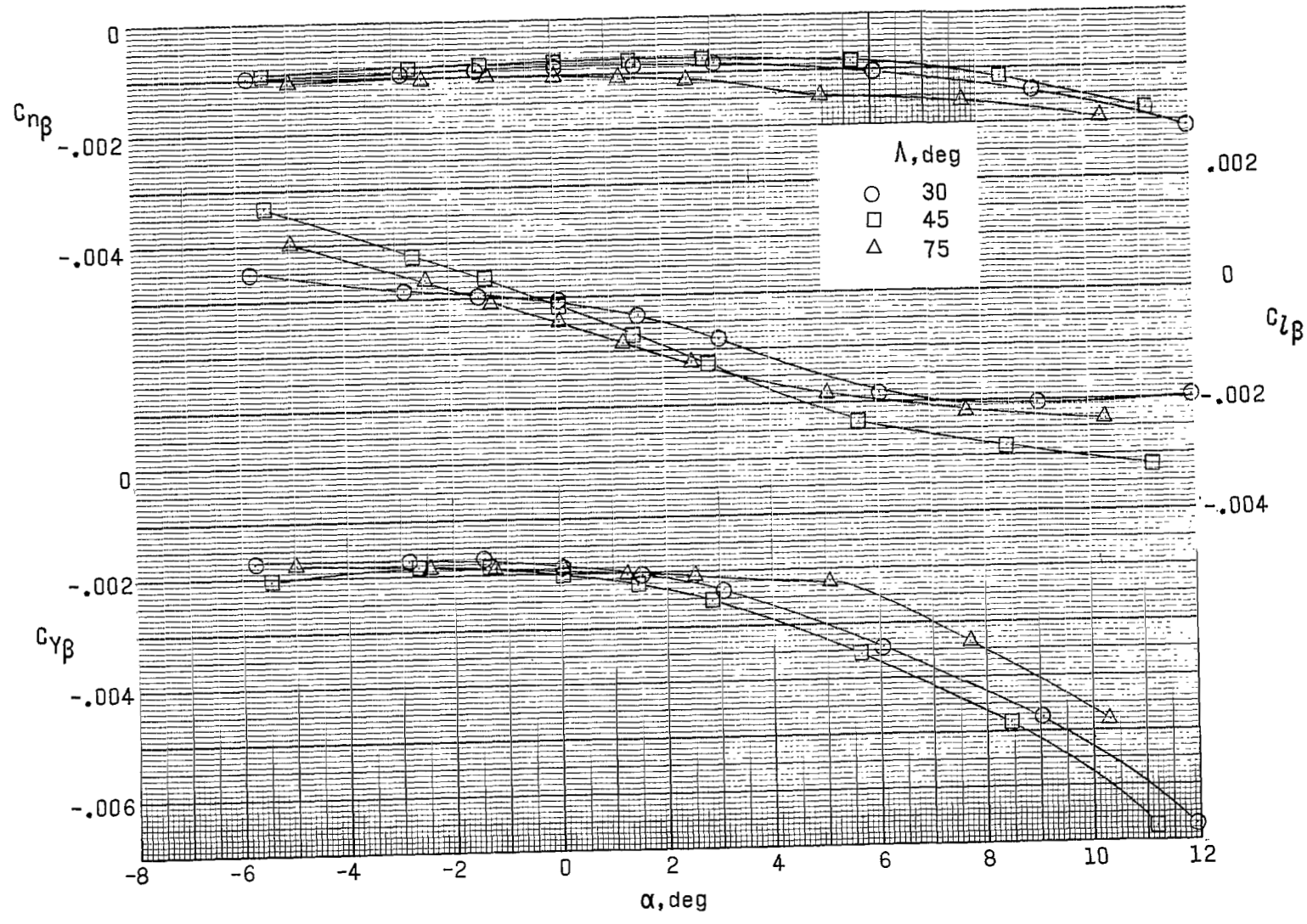

(d) M = 1.20.

Figure 26.- Concluded.

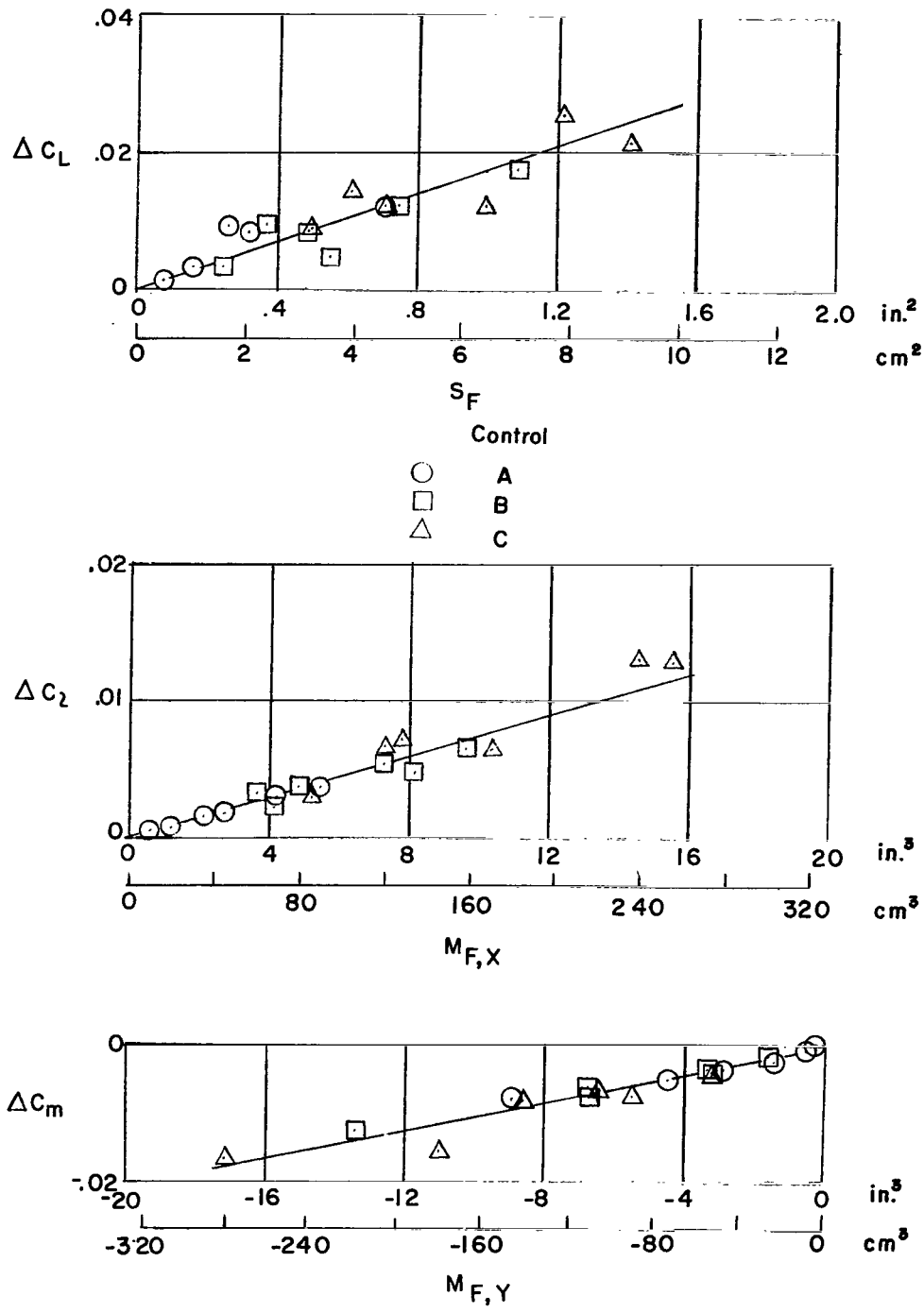

(a) M = 0.50.

Figure 27.- Control effectiveness correlations.

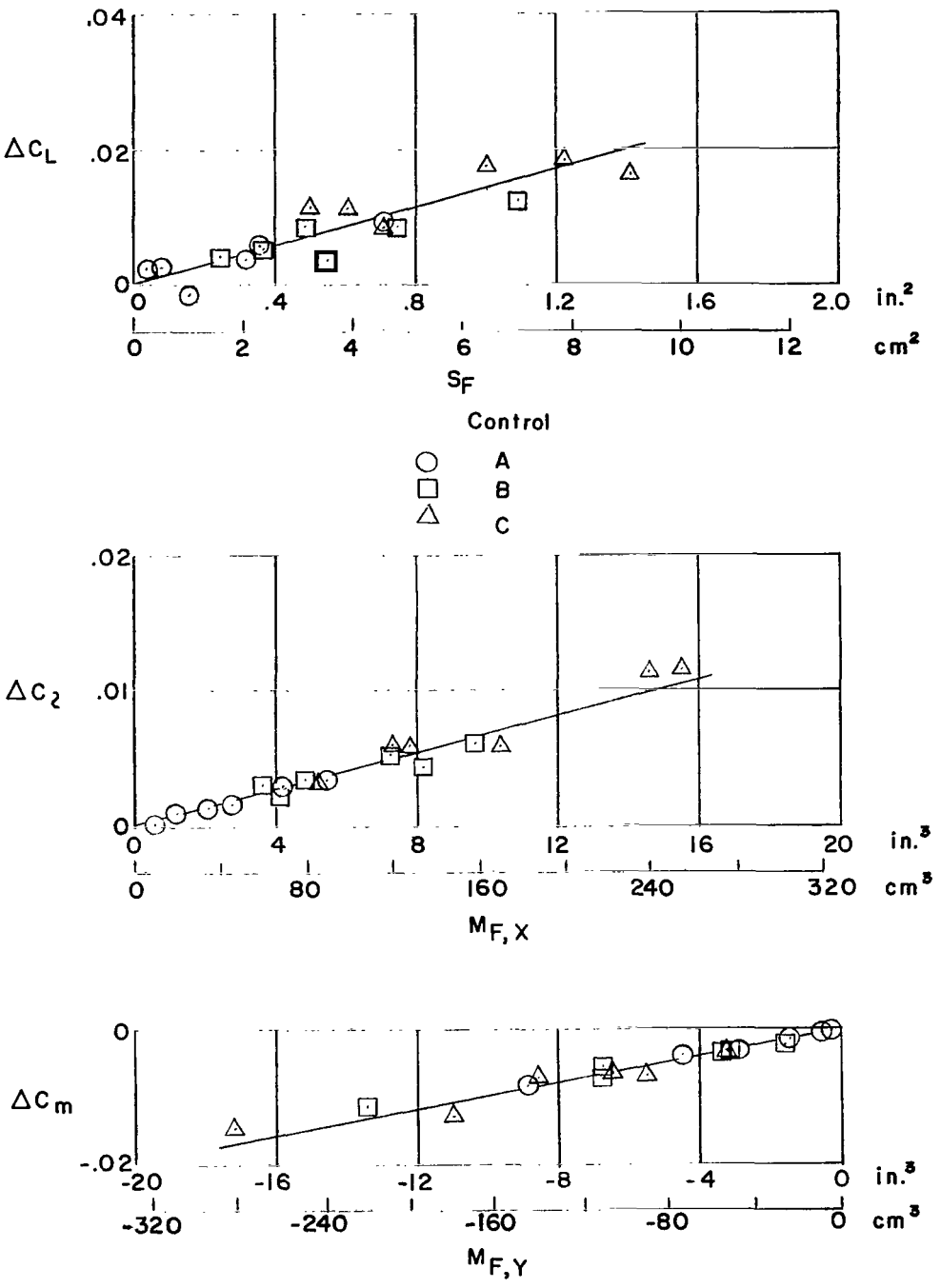

(b) M = 0.80.

Figure 27.- Continued.

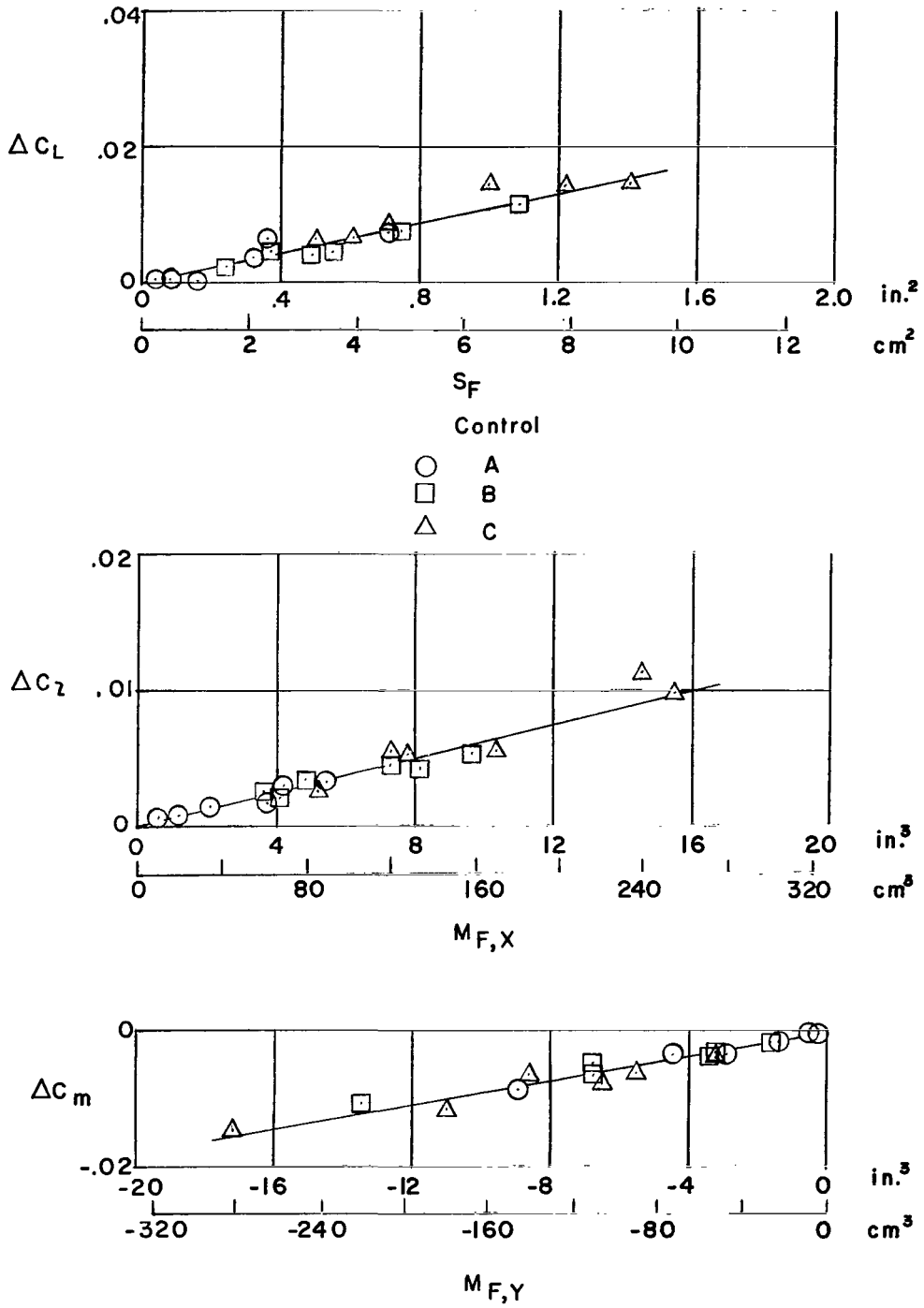

(c) M = 0.97.

Figure 27.- Continued.

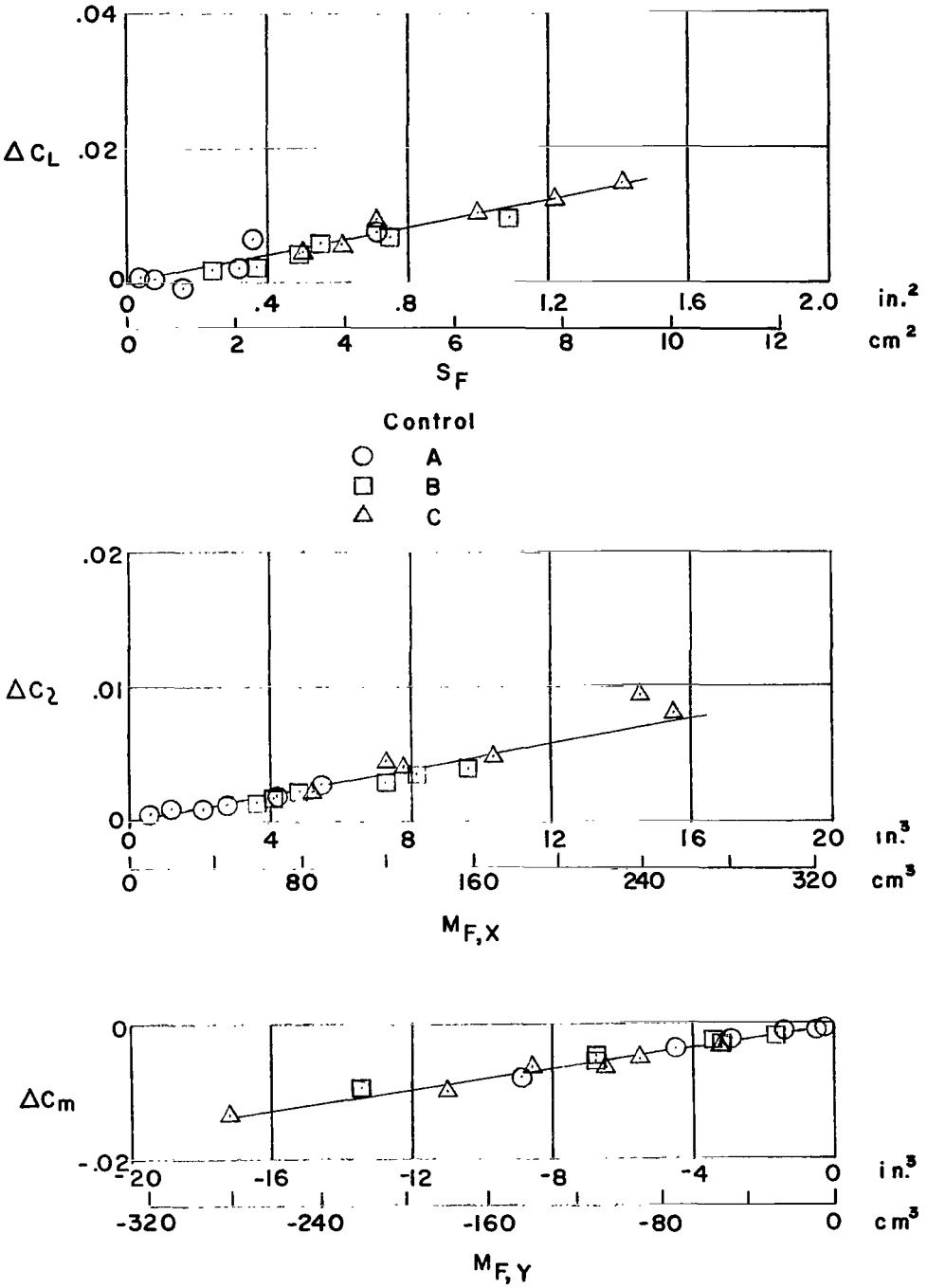

(d) M = 1.20.

Figure 27.- Concluded.

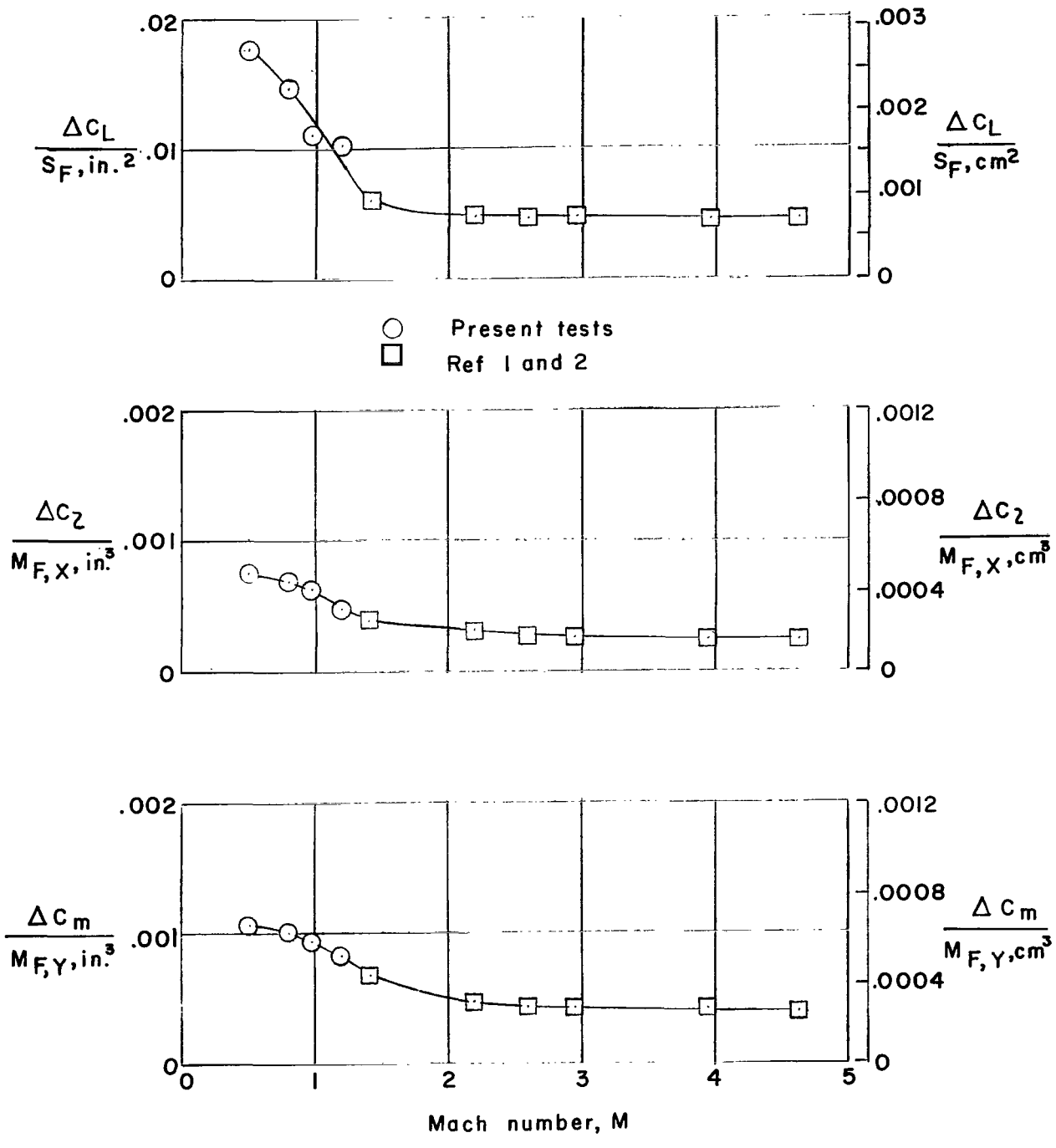

Figure 28.- Effect of Mach number on control-effectiveness correlations.

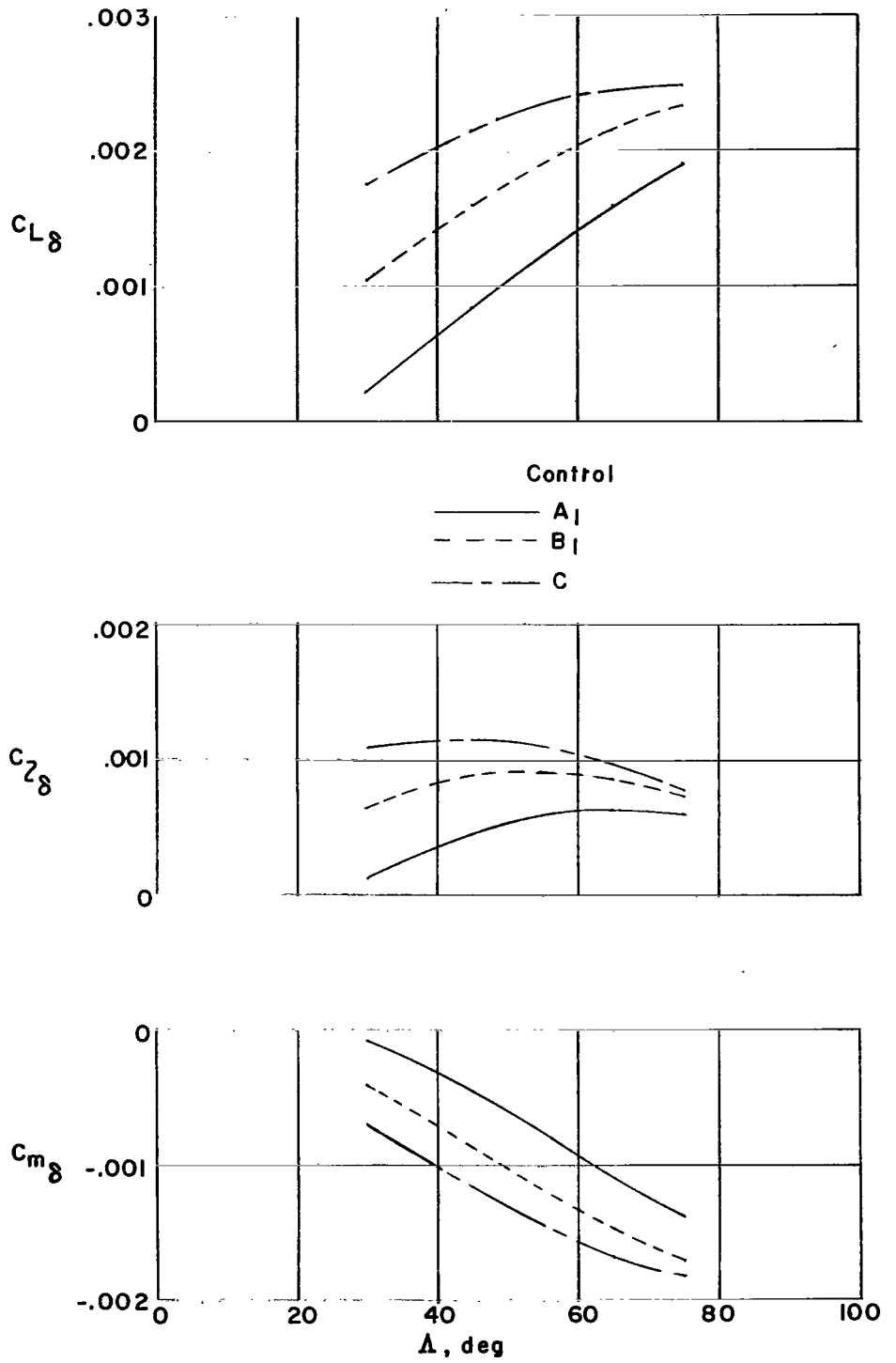

Figure 29.- Control effectiveness for constant area controls. M = 0.5.

"The aeronautical and space activities of the United States shall be conducted so as to contribute . . . to the expansion of human knowledge of phenomena in the atmosphere and space. The Administration shall provide for the widest practicable and appropriate dissemination of information concerning its activities and the results thereof."

—NATIONAL AERONAUTICS AND SPACE ACT OF 1958

NASA SCIENTIFIC AND TECHNICAL PUBLICATIONS

TECHNICAL REPORTS: Scientific and technical information considered important, complete, and a lasting contribution to existing knowledge.

TECHNICAL NOTES: Information less broad in scope but nevertheless of importance as a contribution to existing knowledge.

TECHNICAL MEMORANDUMS: Information receiving limited distribution because of preliminary data, security classification, or other reasons.

CONTRACTOR REPORTS: Technical information generated in connection with a NASA contract or grant and released under NASA auspices.

TECHNICAL TRANSLATIONS: Information published in a foreign language considered to merit NASA distribution in English.

TECHNICAL REPRINTS: Information derived from NASA activities and initially published in the form of journal articles.

SPECIAL PUBLICATIONS: Information derived from or of value to NASA activities but not necessarily reporting the results of individual NASA-programmed scientific efforts. Publications include conference proceedings, monographs, data compilations, handbooks, sourcebooks, and special bibliographies.

Details on the availability of these publications may be obtained from:

SCIENTIFIC AND TECHNICAL INFORMATION DIVISION

NATIONAL AERONAUTICS AND SPACE ADMINISTRATION

Washington, D.C. 20546